

**Improvement of Olefin Metathesis Efficiency
through Understanding Catalyst Stability**

Thesis by

Soon Hyeok Hong

In Partial Fulfillment of the Requirements
for the Degree of
Doctor of Philosophy

California Institute of Technology
Pasadena, California

2007

(Defended March 22, 2007)

© 2007

Soon Hyeok Hong

All Rights Reserved

For My Family

Acknowledgements

I deeply appreciate many people for their assistance and contributions to the work in this dissertation and for helping me enjoy life as a graduate student.

I want to begin by acknowledging Professor Bob Grubbs for being a wonderful advisor. He has been very patient with me and provided a unique environment to do chemistry. The freedom which Bob provided allowed me to pursue some interesting challenges for myself and participate in research projects beyond a mere student. Yet at the same time, he guided me to approach problems in the right direction at some critical points. I am very honored to have had the great opportunity to work in his group.

I thank my committee member, Professors John Bercaw, David Tirrell, Brian Stoltz, and David MacMillan for their support in my career development as well as for their helpful suggestions on my research and proposals.

All the members of the Grubbs group are wonderful. I appreciate Jen Love, JP Morgan, Professor So-Yeop Han, Tae-Lim Choi, and James Tsai for the kind help when I first joined the group and embarked on a journey here. I thank Professor Han especially for introducing the Grubbs group to me and strongly recommending that I join the group. It did not take me so long to realize that she was right.

I have had excellent collaborators for this thesis research. Dan Sanders and Choon Woo Lee at Materia worked together in developing a method to prevent undesirable olefin isomerization. Dan was a hard-working guy who frequently stays in 217 Lab until midnight. I thank him for letting me take over the project when he graduated. I appreciate Choon Woo Lee at Materia for kindly answering my silly questions related to industrial problems on metathesis and engaging in helpful discussions regarding my research. With Jason Jordan,

Professor Louis Kuo, and Pawel Sledz, we have challenged aqueous metathesis and applications. I thank Jason for letting me get involved in the PEG project and helping me work on aqueous metathesis. I am grateful to Professor Louis Kuo at Lewis & Clark College for participating in my career development with good advice and collaboration in aqueous projects. I thank Pawel Sledz for working with me as a SURF student. It was good to see his improvements and build our friendship. I hope he will be a great chemist in the near future as he wishes. I thank Anatoly Chlenov for letting me get involved in the interesting C–H activation project with his catalyst. The independent research from Anna Wenzel and Tina Salguero made my decomposition work look beautiful with cool, novel organometallic complexes. I deeply thank all of my collaborators for their great contributions to my research and for their helpful suggestions.

I also have had a great time with people in Grubbs group. As a new father, I enjoyed talking about kids with Erin Guidry, Donde Anderson, Professor Louis Kuo, Cheol Keun Chung, Joseph Samec, Mike Page, and Connie Hou. I thank Donde for her helpful discussions on organometallic research projects and for helping me understand the American culture. Cultural diversity is another merit in the Grubbs group. With Georgios Vougiokalakakis, Joseph, James Tsai, Pawel, Erin, Jason, Anatoly, Masao, and Takashi, I have enjoyed talking about their unique cultures and religions. Donde, Ron Walker, Anatoly, and Andy Hejl were all Korean-food lovers. I regret that I could not hang out with them more frequently. I hope I can invite them some day to Korea for authentic Korean foods. I also enjoyed talking with Cheol, who took over my bench, about everything including career, chemistry, and life. He showed me how a true synthetic organic chemist organizes the bench.

I am very grateful to people who have critiqued my proposals and manuscripts and proofread my English writings—Donde, Jen, Jason, Chris Douglas, Anna, Tina, Louis, Dan, Katie Campbell, Georgios, Cheol, Paula Diaconescu, Anatoly, Greg Beutner, Erin, Daryl Allen, and Mike Page. Their invaluable help and suggestions have reflected on all of my publications including this dissertation.

I appreciate Caltech staff for their kind support. I especially thank Linda Syme, a wonderful manager of the Grubbs group, Dian Buchness, Tom Dunn, Laura Howe, Steve Gould, and Rick Gerhard. I also thank Larry Henling and Dr. Mike Day for X-ray crystallography, Dr. Mona Shahgholi for mass spectroscopy, Dr. Scott Ross, Dr. Sonjong Hwang and Jon Owen for their helpful suggestions on NMR experiments.

I want to thank people at Smyrna Church and the Caltech Korean Association. I deeply appreciate Pastor Seong-Soo Kim for his sermons and help. I have never met such a pastor who clearly knows and teaches the Gospel, the meaning of life in this world for Christians, and how and for what we should live, solely based on the Bible. I appreciate all Smyrna church members who have shown true love to my family. There are too many people to whom I owe the debt of love at church. All I can say is I truly thank and love you with the love of Jesus Christ. I also appreciate Korean school teachers who voluntarily teach lovely children every Saturday morning. I also have had a great time talking about politics, science policies, sciences, and news with Caltech Korean folks. Thank you all!

I am very grateful to my family in Korea. I deeply respect my parents for their endless support, sacrifice, and love for me. My lovely sister, Jee-Hyun, and brother, Soon-Hwa, always cheer me up whenever I am in a bad condition with crazy chemistries. I miss

them all, and hope to get together with them more frequently in the future with my pretty nephew and nieces.

Most of all, I want to thank my wife, Jamie (Ja-Young) and my son, David (Joon-Pyo). Meeting Jamie and David have been the most fortunate and wonderful events during my graduate study and during my whole life. I deeply thank Jamie for her bottomless support and love. I hope she will become a good dentist who truly cares about her patients. With David, my lifestyle has been totally changed. Sometimes, it was difficult to balance out family life and study, but David's million-dollar smile was more than enough to get me going.

Lastly, I would like to thank God. It is impossible to express all of my gratitude with the limited languages of this world, but I would like to say that I am very happy and grateful for being in your Grace.

Abstract

The recent development of ruthenium olefin metathesis catalysts, which show high activity and functional group tolerance, has expanded the scope of olefin metathesis. To improve efficiency of the ruthenium-catalyzed olefin metathesis, this dissertation describes: (1) mechanistic study to understand decomposition pathways of ruthenium olefin metathesis catalysts for the development of more stable and efficient catalysts, (2) a method to prevent an undesirable side reaction for the improvement of selectivity of ruthenium-catalyzed olefin metathesis, and (3) a novel ruthenium catalyst to increase olefin metathesis efficiency in aqueous media for potential biological applications and environmentally friendly approaches to this chemistry.

Chapter 2 describes the first well-characterized decomposition products, dinuclear ruthenium hydride complex and methylphosphonium salt, from an *N*-heterocyclic carbene-based ruthenium catalyst under typical metathesis conditions. In Chapter 3, the decomposition study was expanded to other widely used ruthenium olefin metathesis catalysts. Phosphine-involvement in the decomposition was consistently observed whether or not an olefin was present. The presence of other decomposition modes for phosphine-free ruthenium catalysts was also described. Chapter 4 addresses another decomposition pathway of an *N,N'*-diphenylbenzimidazol-2-ylidene-based catalyst via C–H activation. Chapter 6 describes the development of a novel poly(ethylene glycol)-supported water-soluble catalyst, which is active and stable in aqueous media. Chapter 7 describes an efficient, practical, and environmentally friendly method to remove residual ruthenium-containing byproducts by simple aqueous workup from olefin metathesis products using the poly(ethylene glycol)-supported catalyst.

Table of Contents

Chapter 1. Introduction	1
References and Notes	5
Chapter 2. Decomposition of $(\text{H}_2\text{IMes})(\text{PCy}_3)(\text{Cl})_2\text{Ru}=\text{CH}_2$, A Key Intermediate in Ruthenium Catalyzed Olefin Metathesis	
Abstract	6
Introduction	6
Results and Discussion	9
Conclusion	15
Experimental	15
References and Notes	18
Chapter 3. Decomposition of Ruthenium Olefin Metathesis Catalysts	
Abstract	21
Introduction	22
Results and Discussion	23
Conclusion	36
Experimental	37
References and Notes	51
Chapter 4. Double C–H Activation of an N-Heterocyclic Carbene Ligand in a Ruthenium Olefin Metathesis Catalyst	
Abstract	55
Introduction	55
Results and Discussion	56
Conclusion	61
Experimental	61

	x
References and Notes	65
Chapter 5. Prevention of Undesirable Olefin Isomerization during Olefin Metathesis	
Abstract	67
Introduction	67
Results and Discussion	68
Conclusion	74
Experimental	75
References and Notes	83
Chapter 6. Highly Active Water-Soluble Olefin Metathesis Catalyst	
Abstract	86
Introduction	86
Results and Discussion	88
Conclusion	93
Experimental	93
References and Notes	98
Chapter 7. Efficient Removal of Ruthenium Byproducts from Olefin Metathesis Products by Simple Aqueous Extraction	
Abstract	101
Introduction	101
Results and Discussion	102
Conclusion	106
Experimental	106
References and Notes	108

Chapter 1

Introduction

Olefin metathesis is a powerful carbon-carbon bond formation reaction in both polymer and small molecule synthesis.^{1,2} This reaction is a unique process of carbon-carbon double bond rearrangement mediated by transition-metal catalysts. This reaction has an enormous variety of applications, including ring-closing metathesis (RCM), cross metathesis (CM), acyclic diene metathesis polymerization (ADMET), ring-opening metathesis polymerization (ROMP), and ring-opening cross metathesis (ROCM) (Figure 1). The generally accepted mechanism, originally proposed by Chauvin in 1971, involves the formation and subsequent cleavage of a metallacyclobutane intermediate (Scheme 1).³

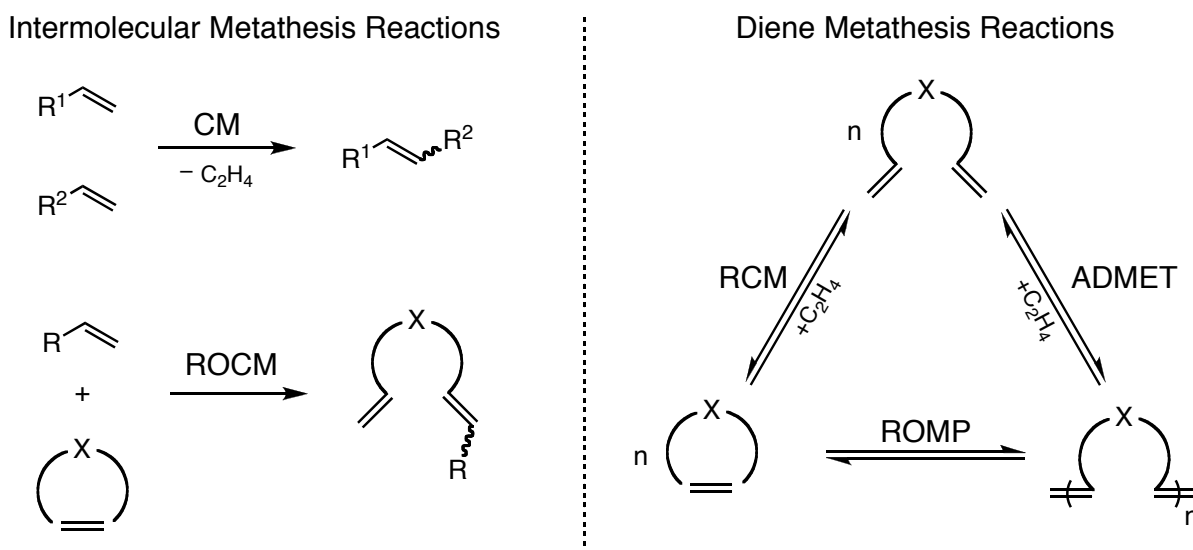
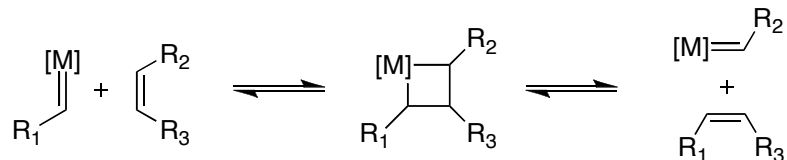


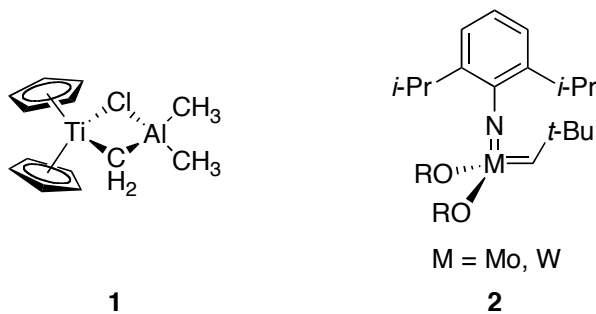
Figure 1. Olefin metathesis reactions.

Scheme 1

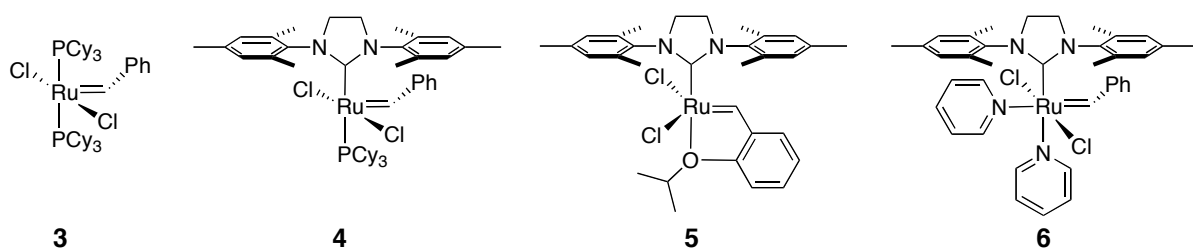


Olefin metathesis was discovered in the mid-1950s independently by workers at DuPont, Standard Oil of Indiana, and Phillips Petroleum as a reaction catalyzed either homo- or heterogeneously usually by multicomponent systems that consisted of early transition metal salts and alkylating agents.⁴ In 1966, the Trioлеfin Process, conversion of propene to ethylene and butanes, was commercialized, but later discontinued by other less expensive processes.⁴

However, there were only a few advances made in catalyst design until the isolation of the first well-defined metal carbene complexes in the late 1970s. In particular, the titanium-based “Tebbe” complex **1** provided many of the mechanism insights on olefin metathesis.⁵ Schrock introduced tungsten and molybdenum alkylidene catalysts that opened a new era of olefin metathesis.⁶⁻⁸ A variety of Mo and W catalysts **2** were developed by Schrock in the late 1980s and early 1990s. These complexes enabled living ROMP reactions and RCM applications.⁹⁻¹¹



In spite of these advances, low thermal stability and oxophilicity of early transition metals limited the scope of substrates in Mo- and W-catalyzed olefin metathesis. In 1992, Grubbs and co-workers reported the first well-defined ruthenium-carbene olefin metathesis catalyst.¹² Since then, a wide variety of ruthenium-based catalysts have been developed. In particular, ruthenium olefin metathesis catalysts **3–6** have been used extensively due to their high activity and functional group tolerance. Over the last decade, the applications of ruthenium-based olefin metathesis catalysts have expanded to include the synthesis of molecules in organic, inorganic, biochemical, polymer, and materials chemistry.¹³⁻¹⁶



However, there are still many challenges in olefin metathesis that include catalyst stability, substrate specificity, stereoselectivity, enantioselectivity, use of large amount of solvent for RCM, metathesis in aqueous media, and residual metal removal.¹⁷

This thesis describes recent approaches to solve some of these problems in ruthenium catalyzed olefin metathesis. The objectives of the work described in this dissertation were (1) to understand decomposition pathways of ruthenium olefin metathesis catalysts for the development of more stable and efficient catalysts, (2) to prevent an undesirable side reaction for the improvement of selectivity of ruthenium catalyzed olefin metathesis, and (3) to increase olefin metathesis efficiency in aqueous media for biological applications and environmentally friendly approaches to this chemistry.

Decomposition and stability of various ruthenium olefin metathesis catalysts is addressed in Chapters 2–4. These works were carried out in collaboration with Dr. Anatoly Chlenov, Dr. Anna G. Wenzel and Dr. Tina T. Salguero. Decomposition mechanisms of currently widely used ruthenium olefin metathesis catalysts are proposed. Chapter 5 describes a new method for preventing an undesirable olefin isomerization during olefin metathesis, which was developed in collaboration with Dr. Daniel P. Sanders, and Dr. Choon Woo Lee of Materia. Chapter 6 focuses on the development of a poly(ethylene glycol)-supported water-soluble catalyst which is stable and active in aqueous media. Finally, Chapter 7 describes a novel, efficient and environmentally friendly method to remove ruthenium by-products from olefin metathesis products.

References and Notes

- (1) Ivin, K. J.; Mol, J. C. *Olefin Metathesis and Metathesis Polymerization*; Academic Press: San Diego, CA, 1997.
- (2) *Handbook of Metathesis*; Grubbs, R. H., Ed.; Wiley-VCH: Weinheim, Germany, 2003; Vol. 1-3.
- (3) Herisson, J. L.; Chauvin, Y. *Makromol. Chem.* **1971**, *141*, 161.
- (4) Spessard, G. O.; Miessler, G. L. *Organometallic Chemistry*; Prentice-Hall, Inc.: Upper Saddle River, New Jersey, 1997.
- (5) Tebbe, F. N.; Parshall, G. W.; Reddy, G. S. *J. Am. Chem. Soc.* **1978**, *100*, 3611–3613.
- (6) Schrock, R. R. *Angew. Chem., Int. Ed.* **2006**, *45*, 3748–3759.
- (7) Schrock, R. R. *Acc. Chem. Res.* **1990**, *23*, 158–165.
- (8) Feldman, J.; Schrock, R. R. *Prog. Inorg. Chem.* **1991**, *39*, 1–74.
- (9) Gilliom, L. R.; Grubbs, R. H. *J. Am. Chem. Soc.* **1986**, *108*, 733–742.
- (10) Schrock, R. R.; Feldman, J.; Cannizzo, L. F.; Grubbs, R. H. *Macromolecules* **1987**, *20*, 1169–1172.
- (11) Grubbs, R. H.; Miller, S. J.; Fu, G. C. *Acc. Chem. Res.* **1995**, *28*, 446–452.
- (12) Nguyen, S. T.; Johnson, L. K.; Grubbs, R. H.; Ziller, J. W. *J. Am. Chem. Soc.* **1992**, *114*, 3974–3975.
- (13) Trnka, T. M.; Grubbs, R. H. *Acc. Chem. Res.* **2001**, *34*, 18–29.
- (14) Grubbs, R. H. *Tetrahedron* **2004**, *60*, 7117–7140.
- (15) Fürstner, A. *Angew. Chem. Int. Ed.* **2000**, *39*, 3012–3043.
- (16) Frenzel, U.; Nuyken, O. *J. Polym. Sci., Part A: Polym. Chem.* **2002**, *40*, 2895–2916.
- (17) Thayer, A. M. *Chem. Eng. News* **2007**, *85*, 37–47.

Chapter 2

Decomposition of $(\text{H}_2\text{IMes})(\text{PCy}_3)(\text{Cl})_2\text{Ru}=\text{CH}_2$, A Key Intermediate in Ruthenium Catalyzed Olefin Metathesis[†]

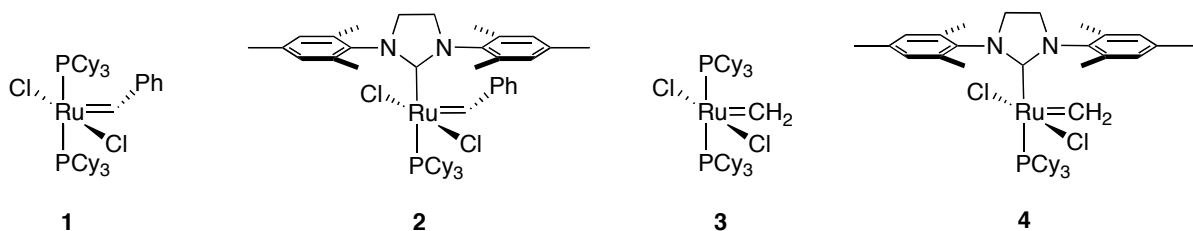
Abstract

Dinuclear ruthenium complex with a bridging carbide and a hydride ligand, and methyltricyclohexylphosphonium chloride result from thermal decomposition of olefin metathesis catalyst, $(\text{H}_2\text{IMes})(\text{PCy}_3)(\text{Cl})_2\text{Ru}=\text{CH}_2$. Involvement of dissociated phosphine in the decomposition is proposed. The dinuclear complex has catalytic olefin isomerization activity, which can be responsible for competing isomerization processes in certain olefin metathesis reactions.

Introduction

Over the past decade, olefin metathesis has emerged as a powerful method for the formation of carbon-carbon double bonds.^{1,2} In particular, ruthenium olefin metathesis catalysts, such as **1** and **2**, have been used extensively in organic and polymer chemistry due to their high activity and functional group tolerance.³⁻⁶

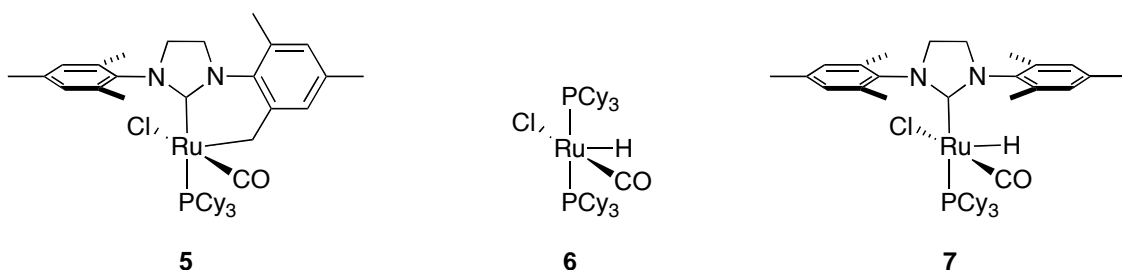
[†] Portions of this chapter have been published: Hong, S. H.; Day, M. W.; Grubbs, R. H. *J. Am. Chem. Soc.* **2004**, *126*, 7414–7415.



Despite these advances, one of the major limiting factors for the use of ruthenium carbene catalysts in many reactions is the lifetime and efficiency of these catalysts. As a result, the ring closing of large rings requires high-dilution conditions, and the metathesis of highly substituted or electron-deficient olefins still requires elevated temperatures and extended reaction times.⁷⁻¹⁰ Furthermore, catalyst decomposition sometimes leads to unwanted side reactions, such as olefin isomerizations.¹¹⁻¹⁴ As identified in previous work, the key to catalyst efficiency is the ratio of the rate of olefin metathesis relative to that of catalyst decomposition.¹⁵ Thus to rationally design a more efficient catalyst for olefin metathesis, it is essential to understand the decomposition pathways of existing catalysts.

Ruthenium methylenes such as **3** and **4** serve as critical intermediates in most metathesis reactions, such as ring-closing metathesis (RCM), cross-metathesis (CM), and acyclic diene metathesis (ADMET) reactions. However, these intermediates also rank amongst the least stable isolable species.¹⁵ A thorough understanding of methyldiene decomposition and stability is crucial to the design of more stable catalyst systems.¹⁵⁻¹⁷ Previous studies from our group showed that **4** decomposes by a unimolecular pathway similar to **3**, and exhibits a longer half-life than complex **3** (5 h 40 min vs. 40 min).^{15,18} Notably, the decomposition of **3** and **4** is not inhibited by added phosphines, while the decomposition of benzylidenes **1** and **2** is slower and is suppressed by the addition of phosphines.¹⁷

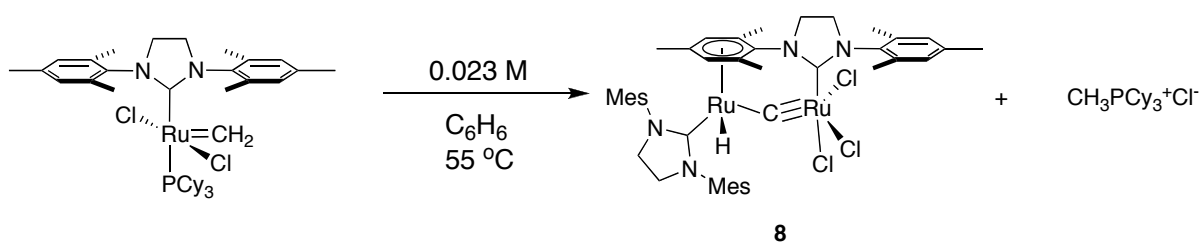
In spite of the information obtained from kinetic studies, it has been difficult to understand the decomposition pathway of the ruthenium olefin metathesis catalysts since there has been no report of well-characterized decomposition products generated under typical metathesis conditions. Fortunately, during the synthesis of **2**, we observed a decomposition product **5**.¹⁹ In complex **5**, the Ru center has inserted into a C–H bond of one of the mesityl groups. It has also been observed that complexes **1** and **2** decompose into hydrido-carbonyl-chloride complexes **6** and **7** upon treatment with methanol.¹⁹⁻²² Diver and co-workers reported carbon monoxide-promoted benzylidene or methylidene insertion into a mesityl group of complex **2** or **4**.²³ Van Rensburg and co-workers have suggested a substrate-induced decomposition mechanism for these catalysts based on DFT calculations involving a β -hydride transfer from a ruthenacyclobutane intermediate.²⁴ However, the lack of well-characterized decomposition products under typical metathesis conditions has limited the understanding of the decomposition mechanism overall. In this chapter, the first well-characterized decomposition products of the *N*-heterocyclic based ruthenium olefin metathesis catalyst **4** in benzene is reported.



Results and Discussion

Thermal decomposition of complex **4** was studied. When complex **4** was monitored at 55 °C in C₆D₆ by ³¹P NMR spectroscopy, a new peak at δ34.5 ppm was observed. This peak increased over time while the peak corresponding to methyldene **4** (δ38.6 ppm) decreased. An orange-yellow crystalline solid precipitated from the solution as decomposition proceeded, and it was isolated as **8** in 46% yield after 72 h. Formation of complex **8** is reproducible in benzene solution (Scheme 1).

Scheme 1



As shown by X-ray crystallography (Figure 1), **8** is a dinuclear ruthenium compound with a bridging carbide between the ruthenium centers and a hydride ligand on Ru2. Also, η⁶-binding of Ru2 to one of the mesityl rings in the *N*-heterocyclic carbene on Ru1 is observed along with complete loss of phosphine ligands. The hydride ligand has a chemical shift of δ-8.6 ppm in the ¹H NMR spectrum and was located on the electronic density map from crystallographic data. The location of the hydride on Ru2 was unambiguously confirmed by an NOE experiment, which shows an NOE between the hydride ligand and a proton of the η⁶-coordinated mesityl ring (Figure 2). The proton of the mesityl ring has a characteristic ¹H chemical shift of δ5.6 ppm which is shifted upfield by the η⁶-binding of Ru2.

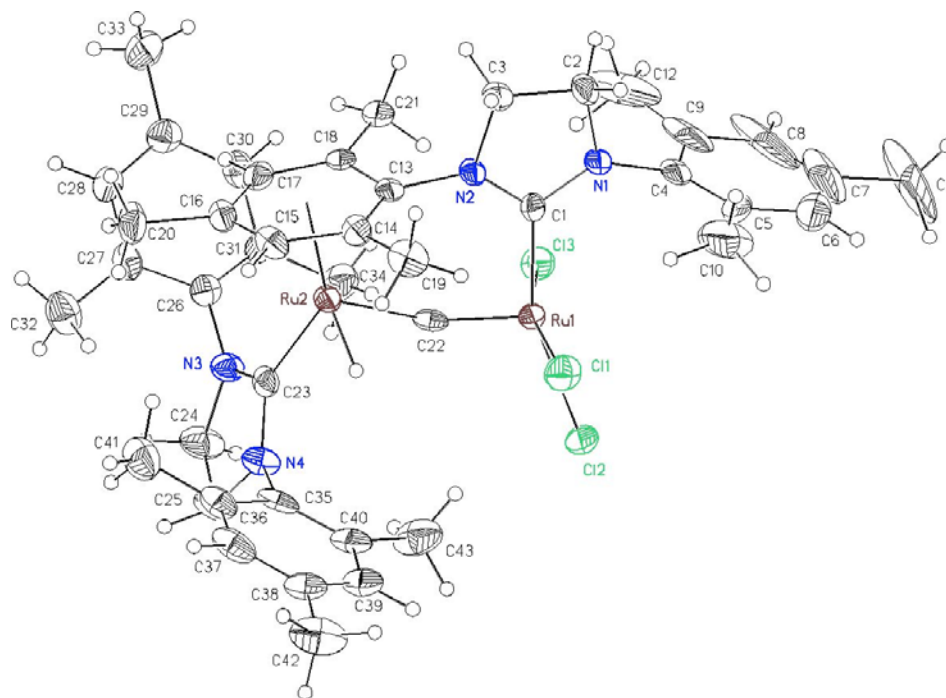


Figure 1. ORTEP drawing of **8** with thermal ellipsoids at 50% probability.

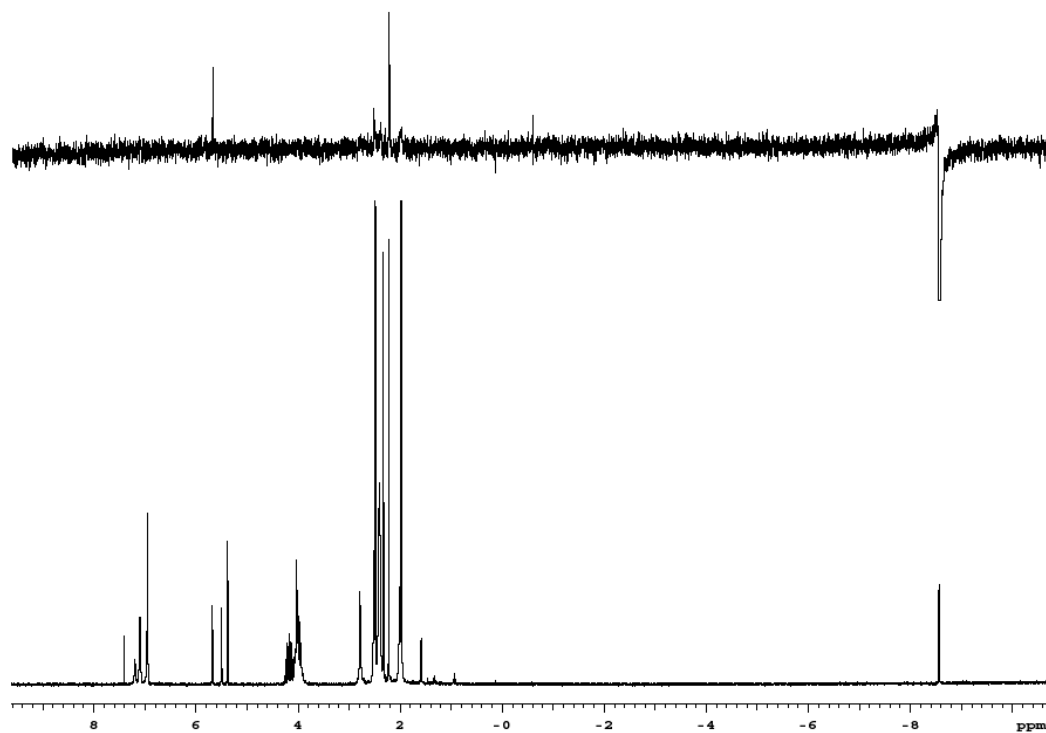


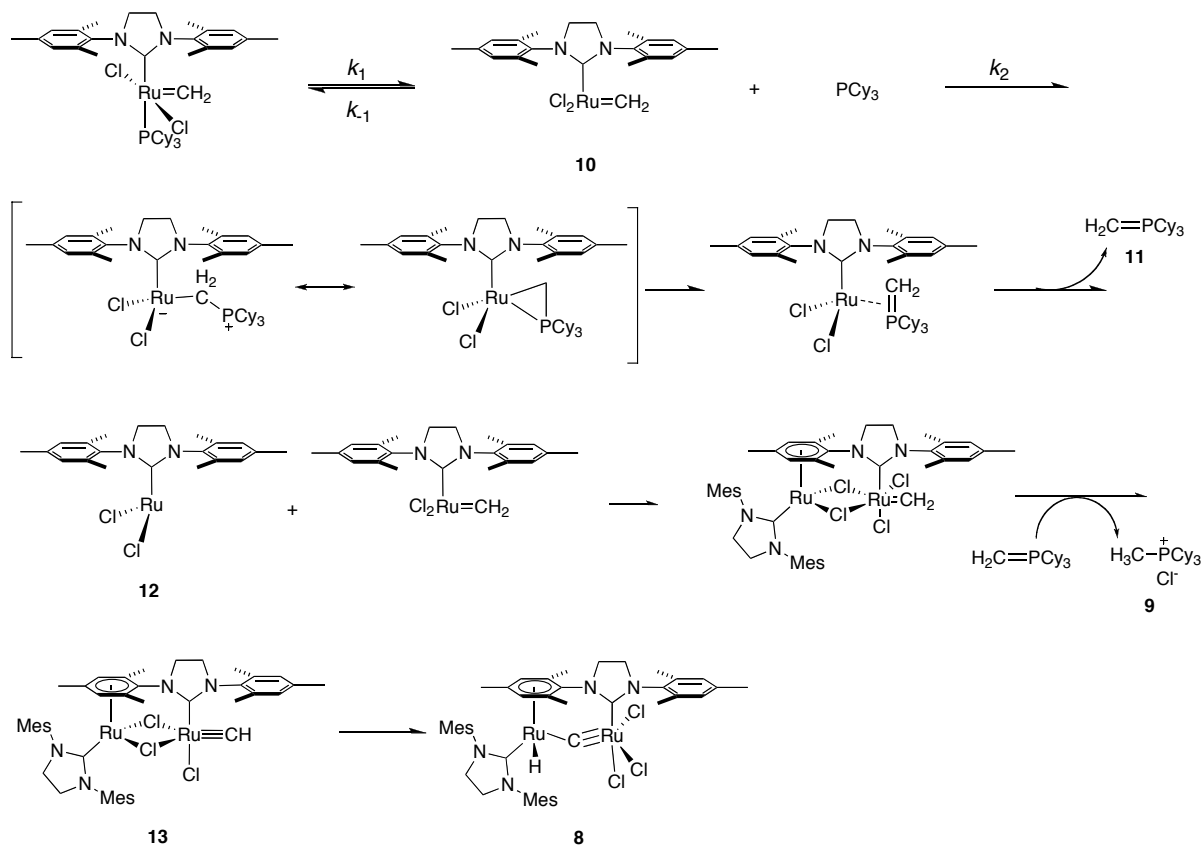
Figure 2. NOE and ^1H NMR spectra of **8**.

The carbide between the ruthenium centers has a distinctive ^{13}C chemical shift of 414.0 ppm, coupled with the hydride ($J_{\text{HC}} = 10.4$ Hz); this falls within the range of 211–446.3 ppm known for other μ -carbide complexes.²⁵⁻²⁸ The single carbon bridge between two ruthenium centers is slightly bent with a Ru1–C22–Ru2 angle of $160.3(2)^\circ$. The Ru1–C22 distance in **8** is $1.698(4)$ Å and is slightly longer than in other reported μ -carbide ruthenium complex such as in $(\text{PCy}_3)_2(\text{Cl})_2\text{Ru}\equiv\text{C}-\text{Pd}(\text{Cl})_2(\text{SMe}_2)$ ($1.662(2)$ Å)²⁵ and $[(\text{PPr}^i_3)_2(\text{Cl})(\text{CF}_3\text{CO}_2)\text{Ru}\equiv\text{CCH}_2\text{Ph}][\text{BAr}_4]$ ($1.660(4)$ Å).²⁹ The Ru2–C22 distance of $1.875(4)$ Å is much shorter than the usual Ru–C single bonds in ruthenium complexes with carbide ligands that generally range from 2.00 to 2.09 Å³⁰⁻³² such as in $[(\text{Me}_3\text{CO})_3\text{W}\equiv\text{C}-\text{Ru}(\text{CO})_2(\text{Cp})]$ ($2.09(2)$ Å).³² Although the allylidene alternative $[\text{Ru}=\text{C}=\text{Ru}]$ is possible on the basis of bond lengths, we assign the Ru1–C22 interaction as a triple bond and the Ru2–C22 interaction as a single bond based on the electron distribution on the ruthenium atoms. If considering the allylidene alternative, the Ru1 and Ru2 would be 15- and 19-electron species, respectively.

Characterization of the major phosphine by-product with a ^{31}P chemical shift of $\delta 34.5$ ppm was also attempted. Since complex **8** has one less carbon atom than expected, we speculated that the phosphine by-product might be methyltricyclohexylphosphonium chloride, **9**, or a phosphine ylide, $\text{CH}_2=\text{PCy}_3$. Upon treatment of decomposition mixture with pentane, we isolated the phosphine product along with some unidentified decomposed ruthenium species. The ^1H , ^{13}C , ^{31}P NMR spectra and HRMS data of the product match exactly those of an independently prepared sample of the methyltricyclohexylphosphonium salt.³³ The formation of **9** from complex **4** occurs even at room temperature. Light gray

crystals of **9** were observed with yellow-orange crystals of **4** from a saturated benzene solution of **4** at room temperature after two weeks under an N₂ atmosphere.

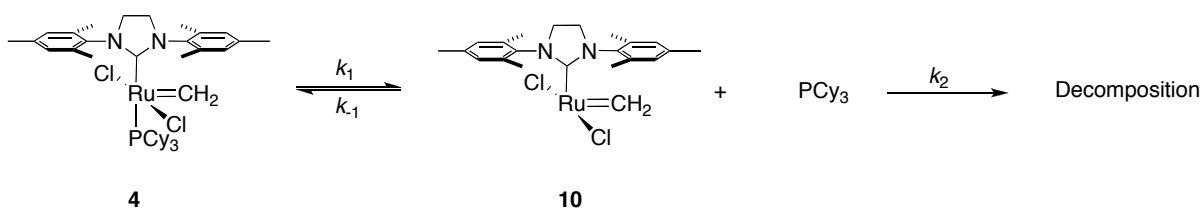
Scheme 2. A proposed mechanism.



Based on the significant formation of **9**, we propose that the decomposition of **4** occurs mainly by attack of dissociated tricyclohexylphosphine on the methyldiene of **10** (Scheme 2). This type of phosphine attack on the carbene carbon atom of Ru-alkylidenes was also reported by Hofmann and co-workers.³⁴ The 12-electron species **12** formed upon elimination of phosphine ylide **11** would bind one of the mesityl rings of **10**. Through two chloride bridges between two ruthenium centers and HCl abstraction by **11**, terminal alkylidyne complex **13** could be formed with generation of **9**. Formation of **8** can be

explained by oxidative addition of the terminal alkylidyne in **13** with migration of two chlorides. However, none of these intermediates has been observed by NMR spectroscopy.

Application of the steady-state approximation to **10** affords the decomposition rate expression (equation 1), assuming the phosphine-attacking step is rate determining. This expression is consistent with the independence of phosphine concentration and the first order kinetic observation on the decomposition of **4**.¹⁷

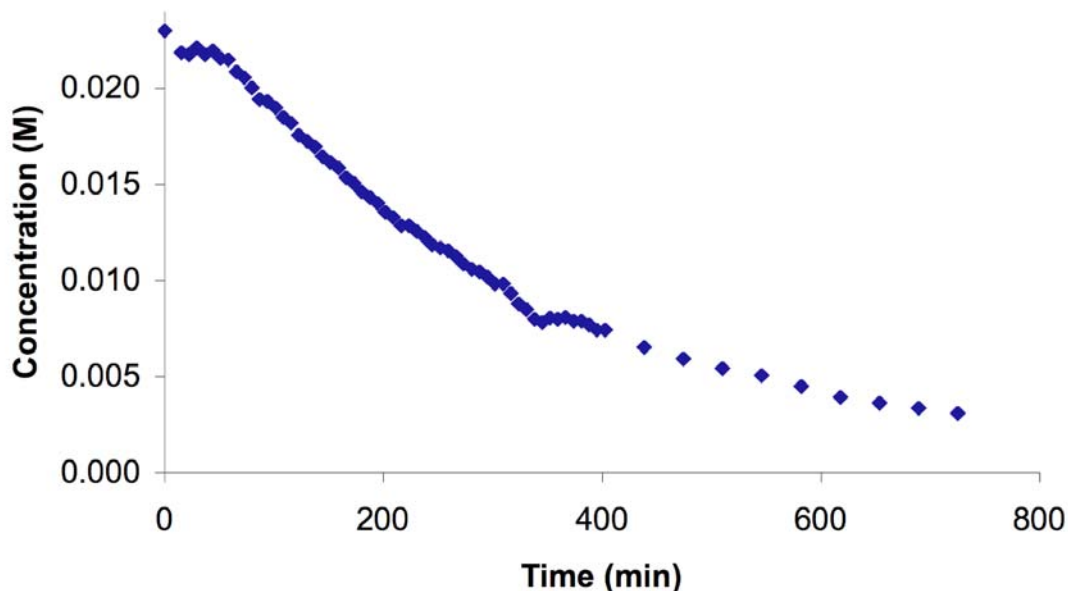


$$\text{rate of decomposition} = k_2[\mathbf{10}][\text{PCy}_3] = \frac{k_1 k_2 [\mathbf{4}][\text{PCy}_3]}{k_{-1}[\text{PCy}_3] + k_2[\text{PCy}_3]} = \frac{k_1 k_2}{k_{-1} + k_2} [\mathbf{4}] \quad (1)$$

$$\left([\mathbf{10}] = \frac{k_1[\mathbf{4}]}{k_{-1}[\text{PCy}_3] + k_2[\text{PCy}_3]} \right)$$

steady state approximation

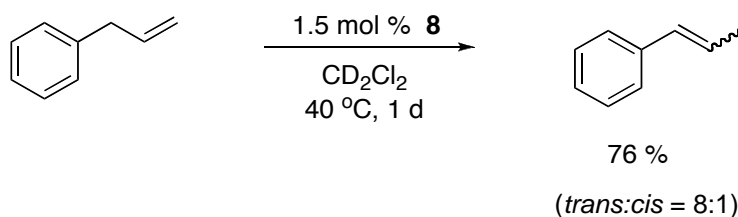
To prevent the phosphine attack on the methylidene, hydrochloric acid was added in the benzene solution of **4**. The half-life of **4** in 2.5 equiv. of HCl at 55 °C is shorter than that of **4** without HCl (4 h 35 min vs. 5 h 40 min, Chart 1). The methyltricyclohexylphosphonium salt **9** and complex **8** were not observed. Instead, unidentified phosphorous peaks around $\delta 37.8$ ppm were observed. One of these species is not $\text{HPCy}_3^+\text{Cl}^-$ which has a ^{31}P chemical shift of $\delta 22.94$ ppm in C_6D_6 and $\delta 26.12$ ppm in CD_2Cl_2 .³⁵ The presence of other decomposition modes expedited by HCl is suggested.

Chart 1. Decomposition of **4** in the presence of HCl.

The formation of a hydride species has important implications for olefin metathesis processes. Olefin isomerization is one of the side-reactions observed during olefin metathesis.¹ While not common, olefin isomerization can significantly alter the product distribution in certain metathesis reactions. Suppressing this side reaction is thus an important goal. There have been some reports on olefin isomerization with catalyst **2**, although it is generally highly selective for olefin metathesis.^{36,37} We believe that this process is catalyzed by either a hydride decomposition species, observable by ¹H NMR spectroscopy, or by impurities remaining from catalyst synthesis, as reported by Snapper and co-workers.³⁸ We have found that complex **8** catalyzes isomerization under metathesis conditions (Scheme 3). This observation implies that decomposition of catalyst **2** via methyldene **4** could be

responsible for the undesirable isomerization reaction during difficult olefin metathesis reactions.

Scheme 3



Conclusion

The dinuclear ruthenium complex **8**, and methyltricyclohexylphosphonium chloride **9** result from thermal decomposition of olefin metathesis catalyst **4** in benzene. It is proposed that dissociated phosphine is involved in the decomposition of **4**. In addition, complex **8** has catalytic olefin isomerization activity, which can be responsible for competing isomerization processes in certain olefin metathesis reactions.

Experimental

General considerations. Manipulation of organometallic compounds was performed using standard Schlenk techniques under an atmosphere of dry argon or in a nitrogen-filled Vacuum Atmospheres drybox ($\text{O}_2 < 2\text{ ppm}$). NMR spectra were recorded on a Varian Inova (499.85 MHz for ^1H ; 202.34 MHz for ^{31}P ; 125.69 MHz for ^{13}C) or on a Varian Mercury 300 (299.817 MHz for ^1H ; 121.39 MHz for ^{31}P ; 74.45 MHz for ^{13}C). ^{31}P NMR spectra were referenced using H_3PO_4 ($\delta = 0\text{ ppm}$) as an external standard. Elemental analyses were performed at Desert Analytics (Tucson, AZ). Mass spectra were recorded on JEOL JMS

600H spectrophotometer. GC spectra were recorded on Hewlett-Packard 5970B MSD with 5890 GC. Benzene, benzene- d_6 , pentane, and methylene chloride were dried by passage through solvent purification columns. CD_2Cl_2 was dried by vacuum transfer from CaH_2 . All solvents are degassed by standard procedure. Allylbenzene was obtained from Aldrich and used as received. $(IMesH_2)(PCy_3)(Cl)_2Ru=CH_2$ was prepared according to literature procedure.¹⁷

Decomposition of complex 4. Complex **4** (48.3 mg, 0.06 mmol) was dissolved in benzene (2.7 mL) in a sealed tube. The reaction mixture was heated to 55 °C. Precipitation of orange-yellow crystalline solid was observed after 7 h. After 72 h, the precipitates were filtered, washed with benzene and dried under vacuum to afford complex **8** (13.2 mg, 46%). Methyltricyclohexylphosphonium chloride **9** was obtained along with some unidentified decomposed ruthenium species by the addition of pentane (5 mL) to the filtered benzene solution.

Dinuclear ruthenium complex 8. 1H NMR (CD_2Cl_2): δ 7.14 (s, 1H), 7.05 (s, 1H), 7.04 (s, 1H), 6.90 (s, 3H), 5.62 (s, 1H), 5.44 (s, 1H), 4.19-4.06 (m, 2H), 3.99-3.86 (m, 6H), 2.73 (br s, 3H), 2.46 (br s, 3H), 2.45 (s, 3H), 2.43 (s, 3H), 2.4-2.3 (br, 9H), 2.27 (s, 3H), 2.17 (s, 3H), 1.96 (br s, 3H), 1.93 (s, 3H), 1.91 (s, 3H), -8.61 (s, 1H). $^{13}C\{^1H\}$ NMR (CD_2Cl_2): δ 413.98, 222.73, 207.87, 141.31, 140.11, 139.64, 139.04, 138.88, 138.86, 138.71, 138.44, 137.68, 135.13, 134.44, 133.65, 131.88, 130.60, 129.93, 129.89, 128.90, 128.68, 128.28, 120.30, 111.99, 111.85, 104.38, 100.60, 98.20, 51.63, 51.37, 48.81, 21.40, 20.99, 20.6-20.5 (br, m), 19.89, 19.25, 19.14, 18.53, 16.95. Anal. Calcd for $C_{43}H_{53}N_4Cl_3Ru_2$: C, 55.27; H,

5.72; N, 6.00. Found: C, 55.58; H, 5.64; N, 5.64. HRMS analysis (FAB) m/z : Calcd $[M^+]$: 936.1424, Found: 936.1434. Crystal data for **8**: $C_{41}H_{53}N_4Cl_3Ru_2 \cdot 1\frac{1}{2}C_6H_6$, $M=1051.55$, monoclinic, space group $P2_1/c$, $a = 12.4536(9) \text{ \AA}$, $b = 16.1001(11) \text{ \AA}$, $c = 19.7050(8) \text{ \AA}$, $\beta = 102.7980(10)^\circ$, $V = 4843.9(6) \text{ \AA}^3$, $T = 100(2) \text{ K}$, $Z = 4$, $\mu(\text{Mo-K}\alpha) = 0.828 \text{ mm}^{-1}$, 42525 measured reflections, 7073 reflections with $I > 2 \sigma(I)$, final $RI = 0.0488$, $wR2 = 0.0797803$. CCDC reference number 233170.³⁹

Methyltricyclohexylphosphonium chloride 9. ^1H NMR (C_6D_6): δ 2.61 (m, $(CHC_5H_{10})_3\text{-PCH}_3^+$, 3H), 2.42 (d, 3H, $CH_3\text{-PCy}_3^+$, $J_{HP} = 12.6\text{Hz}$), 1.85-1.00 (m, 30H). $^{13}\text{C}\{^1\text{H}\}$ NMR (C_6D_6): δ 30.43 (d, $(CHC_5H_{10})_3\text{-PCH}_3^+$, $J_{CP} = 42.6\text{Hz}$), 27.11 (d, $J_{CP} = 3.1\text{Hz}$), 26.47 (d, $J_{CP} = 12.6 \text{ Hz}$), 25.86, 1.5 (d, $CH_3\text{-PCy}_3^+$, $J_{CP} = 47.6\text{Hz}$). $^{31}\text{P}\{^1\text{H}\}$ NMR (C_6D_6): δ 34.5 ppm. HRMS analysis (FAB) m/z : Calcd for $C_{19}H_{36}P [M^+]$: 295.2555, found: 295.2557.

Isomerization reaction of allylbenzene. Allylbenzene (17.1 mg, 0.15 mmol) and complex **8** (2.0mg, 1.5 mol %) were dissolved in CD_2Cl_2 (0.6 mL) in an NMR tube fitted with a screw cap. The resulting solution was heated to 40°C and reaction was monitored by measuring the peak heights of allylic protons of allylbenzene and methyl protons of 1-phenyl-1-propene by ^1H NMR spectroscopy. After 1 day, yield of 1-phenyl-1-propene was determined by GC (76%, *trans:cis* = 8:1).

References and Notes

- (1) Ivin, K. J.; Mol, J. C. *Olefin Metathesis and Metathesis Polymerization*; Academic Press: San Diego, CA, 1997.
- (2) *Handbook of Metathesis*; Grubbs, R. H., Ed.; Wiley-VCH: Weinheim, Germany, 2003; Vol. 1-3.
- (3) Trnka, T. M.; Grubbs, R. H. *Acc. Chem. Res.* **2001**, *34*, 18-29.
- (4) Grubbs, R. H. *Tetrahedron* **2004**, *60*, 7117-7140.
- (5) Fürstner, A. *Angew. Chem. Int. Ed.* **2000**, *39*, 3012-3043.
- (6) Frenzel, U.; Nuyken, O. *J. Polym. Sci., Part A: Polym. Chem.* **2002**, *40*, 2895-2916.
- (7) Han, S.-Y.; Chang, S. In *Handbook of Metathesis*; Grubbs, R. H., Ed.; Wiley-VCH: Weinheim, 2003; Vol. 2, p 5-127.
- (8) Nicola, T.; Brenner, M.; Donsbach, K.; Kreye, P. *Org. Process Res. Dev.* **2005**, *9*, 513-515.
- (9) Vinokurov, N.; Michrowska, A.; Szmigielska, A.; Drzazga, Z.; Wojciuk, G.; Demchuk, O. M.; Grela, K.; Pietrusiewicz, K. M.; Butenschon, H. *Adv. Synth. Catal.* **2006**, *348*, 931-938.
- (10) Martin, W. H. C.; Blechert, S. *Curr. Top. Med. Chem.* **2005**, *5*, 1521-1540.
- (11) Alcaide, B.; Almendros, P. *Chem. Eur. J.* **2003**, *9*, 1259-1262.
- (12) Schmidt, B. *Eur. J. Org. Chem.* **2004**, 1865-1880.
- (13) Hong, S. H.; Sanders, D. P.; Lee, C. W.; Grubbs, R. H. *J. Am. Chem. Soc.* **2005**, *127*, 17160-17161.
- (14) Courchay, F. C.; Sworen, J. C.; Ghiviriga, I.; Abboud, K. A.; Wagener, K. B. *Organometallics* **2006**, *25*, 6074-6086.

- (15) Ulman, M.; Grubbs, R. H. *J. Org. Chem.* **1999**, *64*, 7202-7207.
- (16) Hong, S. H.; Day, M. W.; Grubbs, R. H. *J. Am. Chem. Soc.* **2004**, *126*, 7414-7415.
- (17) Sanford, M. S.; Love, J. A.; Grubbs, R. H. *J. Am. Chem. Soc.* **2001**, *123*, 6543-6554.
- (18) Ulman, M. *PhD Thesis*, California Institute of Technology, 2000.
- (19) Trnka, T. M.; Morgan, J. P.; Sanford, M. S.; Wilhelm, T. E.; Scholl, M.; Choi, T. L.; Ding, S.; Day, M. W.; Grubbs, R. H. *J. Am. Chem. Soc.* **2003**, *125*, 2546-2558.
- (20) Banti, D.; Mol, J. C. *J. Organomet. Chem.* **2004**, *689*, 3113-3116.
- (21) Dinger, M. B.; Mol, J. C. *Eur. J. Inorg. Chem.* **2003**, 2827-2833.
- (22) Dinger, M. B.; Mol, J. C. *Organometallics* **2003**, *22*, 1089-1095.
- (23) Galan, B. R.; Gembicky, M.; Dominiak, P. M.; Keister, J. B.; Diver, S. T. *J. Am. Chem. Soc.* **2005**, *127*, 15702-15703.
- (24) van Rensburg, W. J.; Steynberg, P. J.; Meyer, W. H.; Kirk, M. M.; Forman, G. S. *J. Am. Chem. Soc.* **2004**, *126*, 14332-14333.
- (25) Hejl, A.; Trnka, T. M.; Day, M. W.; Grubbs, R. H. *Chem. Commun.* **2002**, 2524-2525.
- (26) Etienne, M.; White, P. S.; Templeton, J. L. *J. Am. Chem. Soc.* **1991**, *113*, 2324-2325.
- (27) Miller, R. L.; Wolczanski, P. T.; Rheingold, A. L. *J. Am. Chem. Soc.* **1993**, *115*, 10422-10423.
- (28) Beck, W.; Knauer, W.; Robl, C. *Angew. Chem., Int. Ed. Engl.* **1990**, *29*, 318-320.
- (29) González-Herrero, P.; Weberndörfer, B.; Ilg, K.; Wolf, J.; Werner, H. *Angew. Chem., Int. Ed.* **2000**, *39*, 3266.
- (30) Griffith, C. S.; Koutsantonis, G. A.; Skelton, B. W.; White, A. H. *Chem. Commun.* **2002**, 2174-2175.

- (31) Ren, T.; Zou, G.; Alvarez, J. C. *Chem. Commun.* **2000**, 1197-1198.
- (32) Latesky, S. L.; Selegue, J. P. *J. Am. Chem. Soc.* **1987**, *109*, 4731-4733.
- (33) Bestmann, H. J.; Kratzer, O. *Chem. Ber. Recl.* **1962**, *95*, 1894.
- (34) Hansen, S. M.; Rominger, F.; Metz, M.; Hofmann, P. *Chem. Eur. J.* **1999**, *5*, 557-566.
- (35) Tan, K. L.; Vasudevan, A.; Bergman, R. G.; Ellman, J. A.; Souers, A. J. *Org. Lett.* **2003**, *5*, 2131-2134.
- (36) Lehman, S. E.; Schwendeman, J. E.; O'Donnell, P. M.; Wagener, K. B. *Inorg. Chim. Acta* **2003**, *345*, 190-198.
- (37) Schmidt, B. *J. Org. Chem.* **2004**, *69*, 7672-7687.
- (38) Sutton, A. E.; Seigal, B. A.; Finnegan, D. F.; Snapper, M. L. *J. Am. Chem. Soc.* **2002**, *124*, 13390-13391.
- (39) X-ray crystallographic data collection and refinement was carried out by Lawrence M. Henling and Dr. Michael W. Day.

Chapter 3

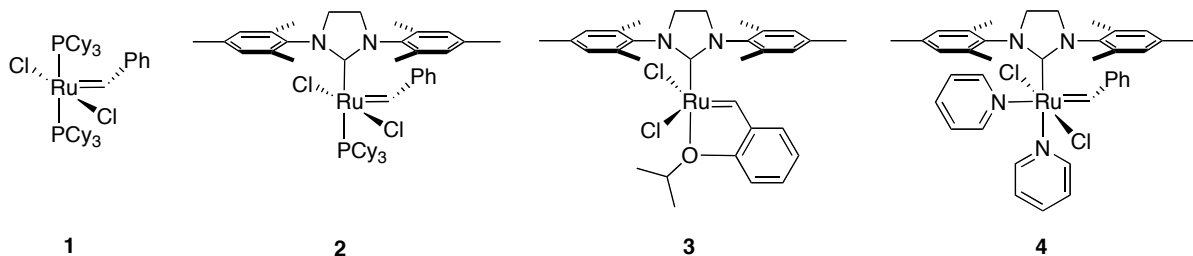
Decomposition of Ruthenium Olefin Metathesis Catalysts

Abstract

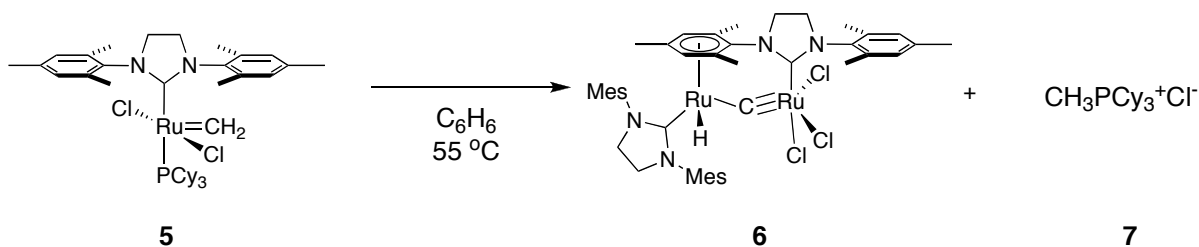
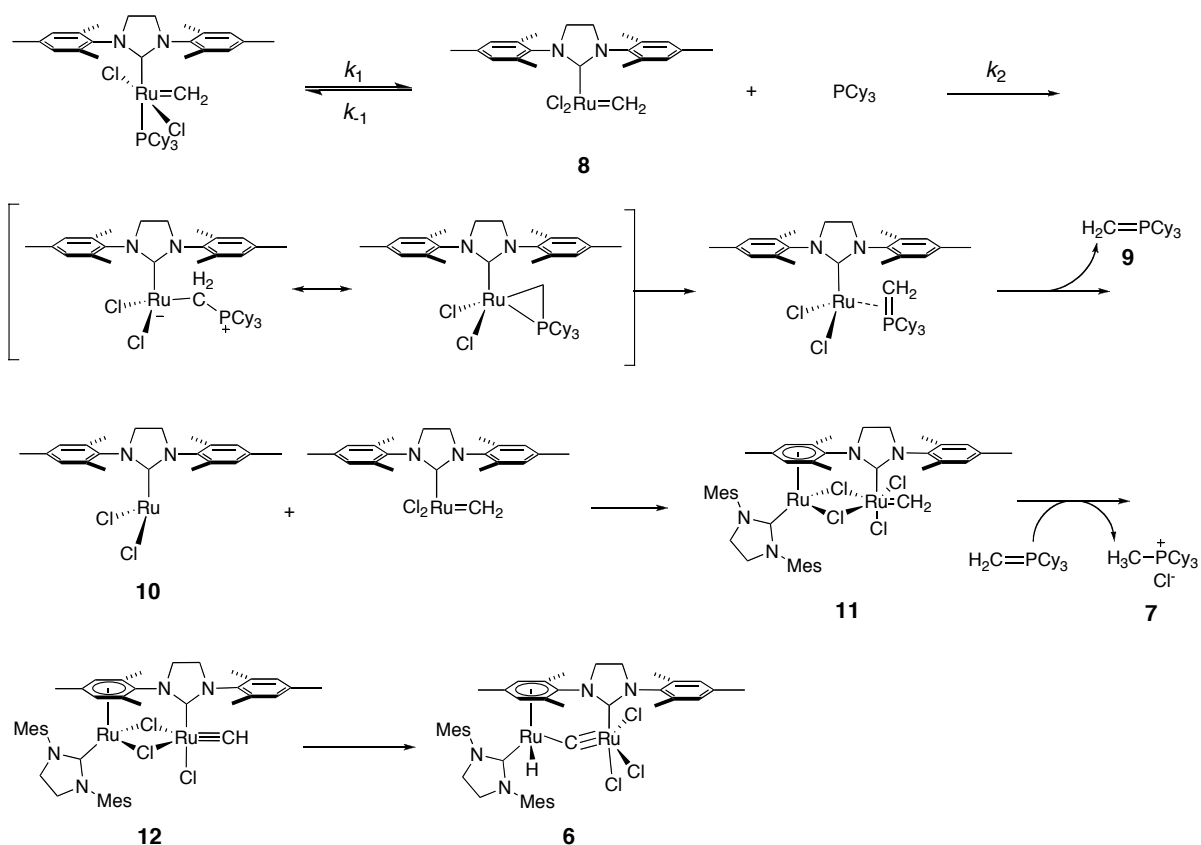
The decomposition of a series of ruthenium metathesis catalysts has been examined using methylidene species as model complexes. All of the phosphine-containing methylidene complexes decomposed to generate methylphosphonium salts, and their decomposition routes followed first order kinetics. The formation of these salts in high conversion, coupled with the observed kinetic behavior for this reaction, suggest that the major decomposition pathway involves nucleophilic attack of a dissociated phosphine on the methylidene carbon. This mechanism also is consistent with decomposition observed in the presence of ethylene as a model olefin substrate. The decomposition of phosphine-free catalyst $(\text{H}_2\text{IMes})(\text{Cl})_2\text{Ru}=\text{CH}(2\text{-C}_6\text{H}_4\text{-O-}i\text{-Pr})$ (H_2IMes = 1,3-dimesityl-4,5-dihydroimidazol-2-ylidene) with ethylene was found to generate unidentified ruthenium hydride species. The novel ruthenium complex $(\text{H}_2\text{IMes})(\text{pyridine})_3(\text{Cl})_2\text{Ru}$, which was generated during the synthetic attempts to prepare the highly unstable pyridine-based methylidene complex $(\text{H}_2\text{IMes})(\text{pyridine})_2(\text{Cl})_2\text{Ru}=\text{CH}_2$, is also described.

Introduction

The recent development of ruthenium olefin metathesis catalysts such as **1–4**, which show high activity and functional group tolerance, has expanded the scope of olefin metathesis.¹⁻⁴



As we discussed in chapter 2, it is essential to understand the decomposition pathways of existing catalysts to develop more stable and efficient catalysts. In the previous chapter, we showed that methylidene complex **5** decomposed to form the dinuclear ruthenium hydride complex **6** and methyltricyclohexylphosphonium chloride (**7**) (Scheme 1).⁵ Based on the observation of **6** and **7** and the results of kinetic experiments, we proposed that complex **5** decomposes via nucleophilic attack of a dissociated phosphine on the methylidene carbon (Scheme 2). This decomposition study has now been expanded to include other ruthenium-based olefin metathesis catalysts, including the phosphine-free catalysts **3** and **4**.

Scheme 1. Decomposition of the methylidene complex **5**.**Scheme 2.** Proposed decomposition mechanism.

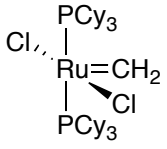
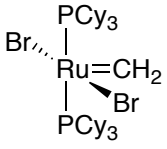
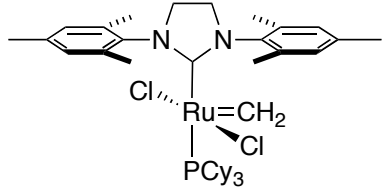
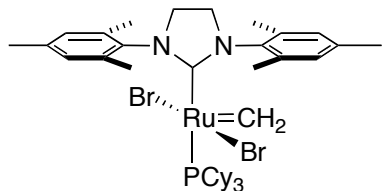
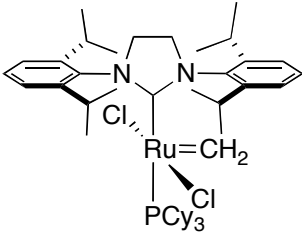
Results and Discussion

Decomposition of phosphine-based catalysts. Catalyst decomposition rates were determined with ^1H NMR spectroscopy by following the diminution of the ruthenium

methylidene resonance integral over time.⁶ Recrystallization and spectroscopic methods were used to identify and characterize decomposition products. All of the tested methylidene complexes of phosphine-based ruthenium catalysts decomposed to generate methyltricyclohexylphosphonium salts as the major phosphine species (Table 1). In our previous report, we were not able to conclusively identify the phosphine product from the decomposition of complex **13**. In this case, the phosphine activation was proposed based on the ²H-NMR study with (PCy₃)₂Cl₂Ru=CD₂ (**13-d₂**).⁶ Here, the product was characterized successfully as CH₃PCy₃⁺Cl⁻ (**7**) by comparison with an independently prepared sample of the salt (¹H, ¹³C, and HRMS). The ²H peak observed at ~2.5 ppm during the decomposition of **13-d₂** originates from the methyl protons of CD₃PCy₃⁺Cl⁻ (**7-d₃**).

The conversions to the phosphine products CH₃PCy₃⁺X⁻ were determined by comparing the ¹H NMR integration of the α-proton in the cyclohexyl rings of the phosphonium salts with an internal standard (anthracene). The conversions were high, 81% – 85%, for (PCy₃)₂Cl₂Ru=CH₂ (**13**), (PCy₃)₂Br₂Ru=CH₂ (**14**), and (H₂IPr)(PCy₃)Cl₂Ru=CH₂ (**17**) (Table 1, entries 1, 2, and 5) (H₂IPr = 1,3-bis(2,6-diisopropylphenyl)-4,5-dihydroimidazol-2-ylidene). For (H₂IMes)(PCy₃)Cl₂Ru=CH₂ (**5**) and (H₂IMes)(PCy₃)Br₂Ru=CH₂ (**16**) (entries 3 and 4) (H₂IMes = 1,3-dimesityl-4,5-dihydroimidazol-2-ylidene), the conversions could not be determined because of peak overlap, although ³¹P NMR spectra indicate methyltricyclohexylphosphonium salts are the major phosphine-containing products. These observed conversions strongly suggest that phosphine is involved in the major decomposition pathway for the ruthenium methylidene complexes listed in Table 1.

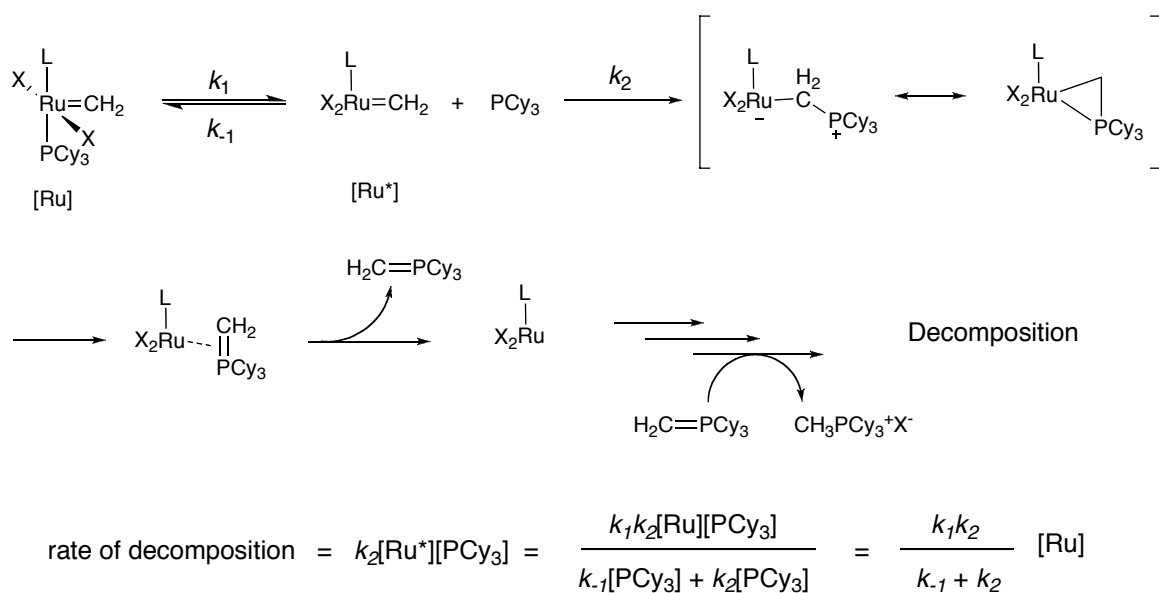
Table 1. Decomposition of ruthenium methylidene complexes^a

Entry	Methylidenes	Half-Life	k_{decomp} (s ⁻¹)	Decomposition Products (Conversion) ^b
1	 <p style="text-align: center;">13</p>	40 min	0.016	CH ₃ PCy ₃ ⁺ Cl ⁻ (82%)
2	 <p style="text-align: center;">14</p>	35 min	0.018	CH ₃ PCy ₃ ⁺ Br ⁻ (15 , 85%)
3	 <p style="text-align: center;">5</p>	5 h 40 min	0.0021	6 (46%) ^c CH ₃ PCy ₃ ⁺ Cl ^{-d}
4	 <p style="text-align: center;">16</p>	5 h 15 min	0.0024	CH ₃ PCy ₃ ⁺ Br ^{-d}
5	 <p style="text-align: center;">17</p>	1 h	0.011	CH ₃ PCy ₃ ⁺ Cl ⁻ (81%) H ₂ IPrH ⁺ Cl ^{-e}

^a Conditions: 0.023M, C₆D₆, 55 °C, anthracene as an internal standard. ^b Determined by ¹H NMR spectroscopy. ^c Isolated yield. ^d Conversions could not be determined. ^e H₂IPr = 1,3-bis(2,6-diisopropylphenyl)-4,5-dihydroimidazol-2-ylidene.

The decompositions of phosphine-based ruthenium methylidene complexes were found to follow first-order kinetics; the decomposition rates were not affected by the addition of excess phosphine.⁵⁻⁷ As anticipated, catalysts containing an *N*-heterocyclic carbene ligand had increased lifetimes compared with bis(phosphine)-based catalysts.^{5,8,9} Changing the chloride ligands to bromides was found to only slightly decrease the catalyst lifetimes. Attempts to replace the chloride ligands with iodides were unsuccessful, presumably due to even more rapid decomposition.⁷

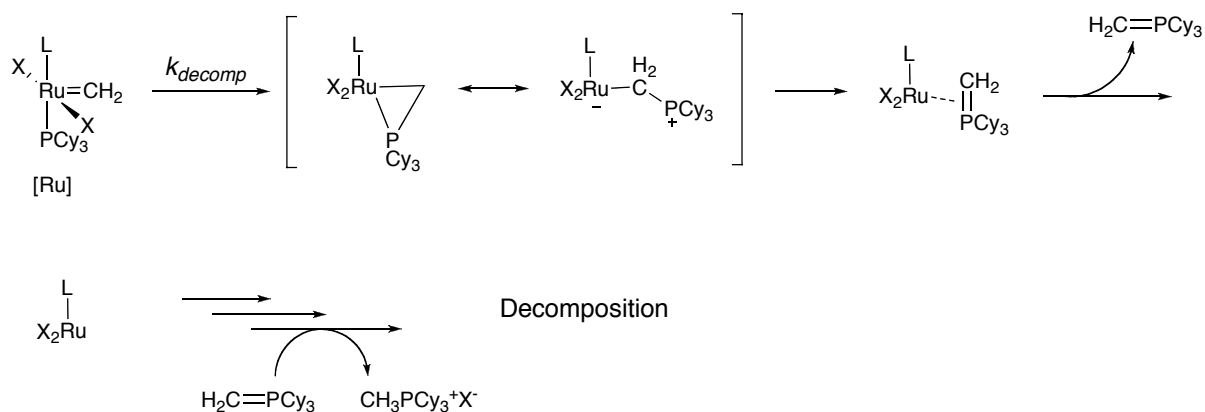
Scheme 3. Phosphine dissociation and attack mechanism.



Complexes bearing H₂IPr ligands, such as **17**, are known to initiate very quickly in olefin metathesis reactions because of the steric bulk of the *N*-heterocyclic carbene ligand.^{10,11} However, methylidene complex **17** is much less stable than the H₂IMes derivatives **5** and **16** (entries 3 and 4). The phosphine ligand of **17** dissociates faster than the phosphine of **5** or **16**, which increases the concentration of free phosphine and thus

accelerates phosphine attack on the methyldene carbon.¹² This result indicates that a mechanism involving phosphine dissociation and attack (Scheme 3) is more reasonable than a mechanism involving the internal attack of phosphine (Scheme 4).

Scheme 4. Internal phosphine attack mechanism.



$$\text{rate of decomposition} = k_{decomp}[\text{Ru}] \quad (2)$$

It was difficult to experimentally distinguish these two possible mechanisms, as both kinetic expressions are identical and consistent with the lack of rate dependence on phosphine concentration and the first-order kinetic behavior that was observed (equation 1¹³ for the mechanism in Scheme 3 and equation 2 for the mechanism in Scheme 4). Experiments, such as the addition of more nucleophilic phosphines like trimethylphosphine, were unsuccessful presumably due to the phosphine-exchange nature of ruthenium methyldenes.¹⁴ However, if decomposition occurs via the internal attack of phosphine onto the methyldene carbon, the decomposition rates of complex **5**, **16**, and **17** should not be so much different considering similar electronic properties between H₂IMes and H₂IPr

ligands.¹⁵ Because it is not, we favor the mechanism involving the nucleophilic attack of free phosphine for the decomposition of ruthenium methylene complexes (Scheme 3). The nucleophilic attack of phosphines on the carbene carbon of ruthenium alkylidenes has also been reported by Hofmann and co-workers.¹⁶

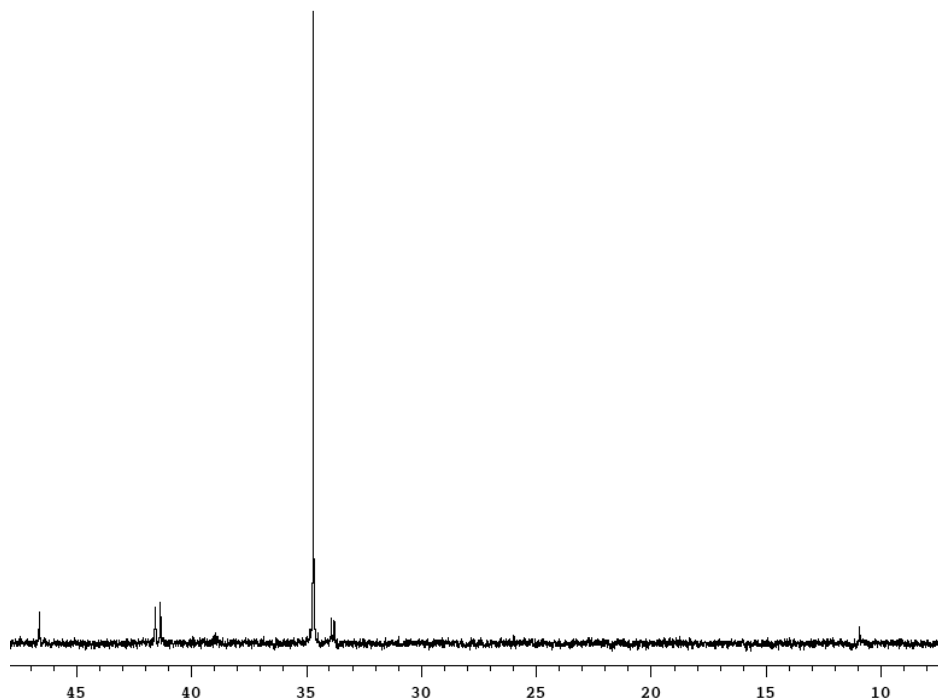


Figure 1. ³¹P NMR spectrum of the decomposition of **13** in the presence of ethylene.

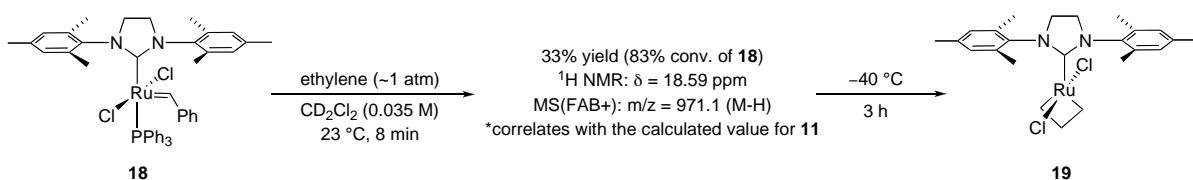
Decomposition in the presence of ethylene. Van Rensburg and co-workers have reported the substrate-induced decomposition of **5** and **13** using ethylene as a model substrate.¹⁷ Based on theoretical and experimental results, they proposed that decomposition of **5** in the presence of ethylene could occur via a ruthenium allyl species formed by β -hydrogen abstraction from the corresponding ruthenacyclobutane intermediate. Reductive elimination then yields propene as the major olefinic compound. However, they were not

able to characterize the major phosphine decomposition product. We have reexamined this reaction and found that ^{31}P NMR spectra of decomposed samples reveal a major phosphine complex at 34.6 ppm after decomposition of both **5** and **13** (Figure 1), which corresponds to $\text{CH}_3\text{PCy}_3^+\text{Cl}^-$. The identity of this species was confirmed by spectroscopic methods. The ^{13}C NMR spectra which shows a characteristic doublet for the phosphonium salt's methyl protons at 1.5 ppm, was particularly revealing.⁵ From this evidence, we believe that phosphine attack on the methyldiene carbon is also a major pathway in the decomposition of **5** and **13** in the presence of ethylene.

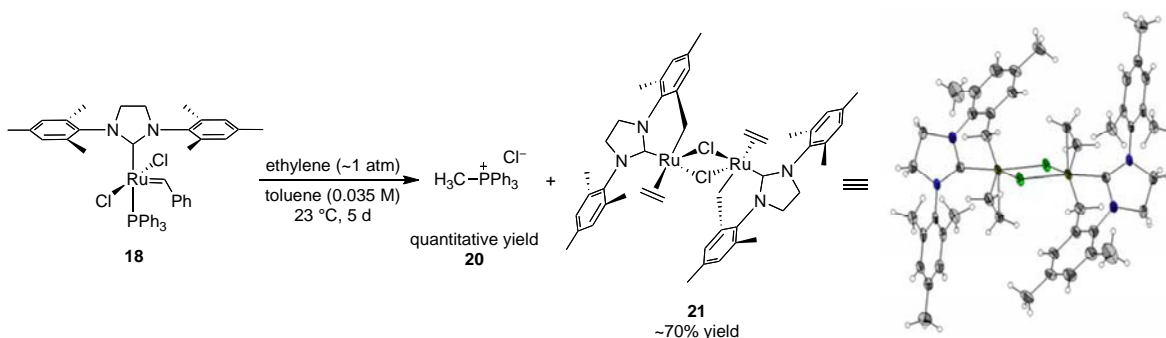
Further evidence for catalyst decomposition by phosphine attack on the methyldiene carbon and the subsequent generation of complex **11** (Scheme 2) was found in conducting a series of experiments on catalyst **18**,¹⁸ the triphenylphosphine analog of **2**, in the presence of ethylene (Scheme 5).¹⁹ Rapid conversion to a new alkylidene species at 18.59 ppm was observed by ^1H NMR upon the exposure of a 0.035 M solution of **18** in dichloromethane- d_2 to an atmosphere of ethylene at 23 °C. However, in contrast to reactions conducted using catalyst **2**, where methyldiene **5** was initially observed,⁷ this new alkylidene species was found not to be the triphenylphosphine-ligated methyldiene, which was present in only trace amounts (<2%). Attempts to characterize the new alkylidene species were hampered by its instability—the use of an internal standard indicated that the maximum conversion to this unidentified complex was approximately 33% after 8 minutes (83% conversion of **18**), which rapidly decreased to ~2% after 120 minutes.²⁰ Interestingly, the only product visible by ^{31}P NMR spectroscopy upon the complete consumption of alkylidene was methyltriphenylphosphonium chloride (23.0 ppm), indicating that no phosphine remained bound to the ruthenium and that a decomposition process similar to that of catalyst **5** might

be in effect. However, complex **6** was not observed in the reaction mixture, suggesting a divergent mechanistic pathway. Mass spectrometric analysis (FAB+) of the reaction mixture at 8 minutes identified a ruthenium species with a m/z of 971.1, supporting the identity of the intermediate alkylidene to be complex **11**, a species that had originally been proposed in the decomposition of **5** but not observed (Scheme 2).⁵ This intermediate appears to be capable of reverting back to a 14-electron methylidene species, based on the observation that decreasing the temperature of a reaction mixture containing **11** to -40 °C in the presence of ethylene was found to generate metallacycle **19**.²¹⁻²³ It is important to note that catalyst **18** does not react with ethylene at this temperature.

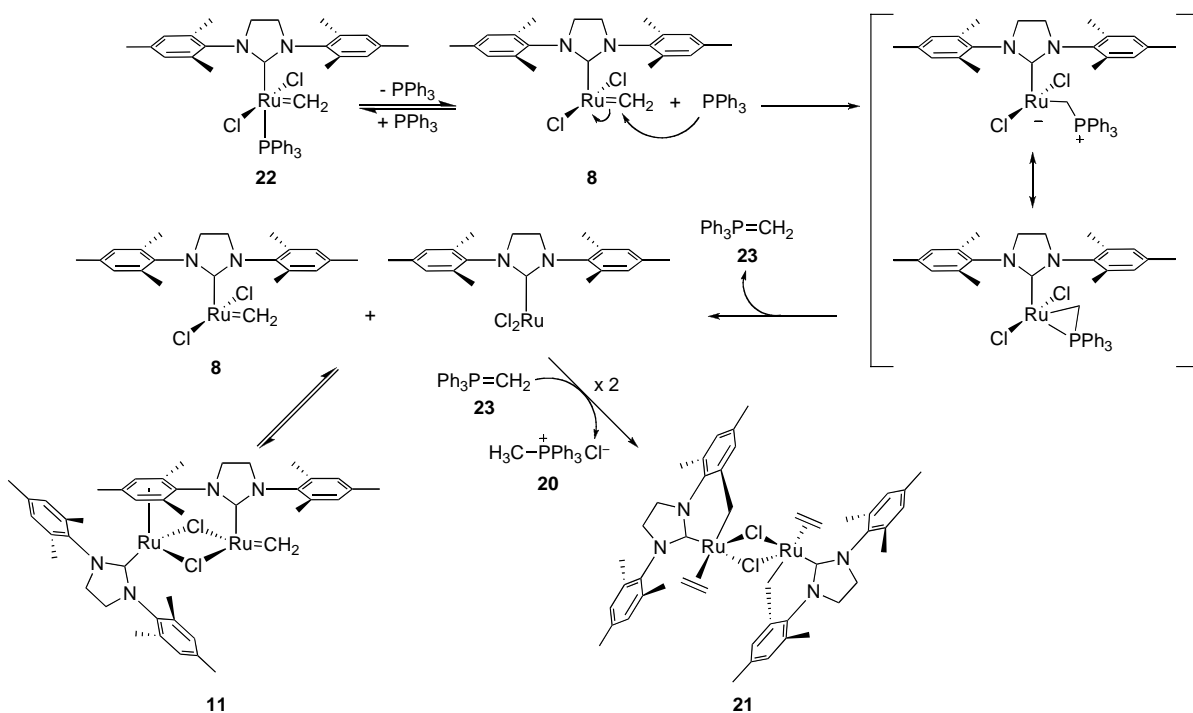
Scheme 5. Reaction of catalyst **18** with ethylene.



Scheme 6. Isolation of the major decomposition product in the reaction of **18** with ethylene.



Scheme 7. Proposed mechanistic pathway for the decomposition of the methylidene of **18** with ethylene.



The major decomposition product of **18** with ethylene ultimately was identified by running the reaction in Scheme 5 on a 77 μ mol scale in toluene. After 5 days at 23 °C, methyltriphenylphosphonium chloride was isolated in quantitative yield, in addition to 52 mg of a red-brown, crystalline solid that was found to be unstable in solution in the absence of ethylene. X-ray analysis determined the crystal structure to be that of the *C*₂-symmetric complex **21** (Scheme 6), which was presumably derived from the *ortho*-methyl C-H activation of two ruthenium-coordinated NHC ligands in the presence of two equivalents of methylenetriphenylphosphine (**23**) as a base.

A summary of the proposed decomposition pathway for catalyst **18** is depicted in Scheme 7. Although the methylidene **22** readily forms upon the exposure of **18** to ethylene, it

appears to be more vulnerable to phosphine attack and subsequent decomposition relative to **5**, resulting in the minimal population (<2%) of **22** that had been observed during the course of the reaction. Differences in this decomposition route compared to that proposed for catalyst **5** potentially can be attributed to the weaker basicity and less steric hindrance of triphenylphosphine relative to tricyclohexylphosphine^{24,25} as well as the presence of ethylene in the reaction mixture.

Other decomposition products observed during synthesis of complex 5. During the synthesis of methylidene **5** in the atmosphere of 1–1.5 atm of ethylene gas, the ruthenium dimer complex **24** was observed (Scheme 8). As shown by X-ray crystallography (Figure 2), this complex has a Ru—Ru single bond (2.7021(5) Å) and two bridging chlorides along with bridging methylene.²⁶ Formation of complex **24** can be also explained as the dimerization between complex **8** and **10** generated by phosphine-involved decomposition.

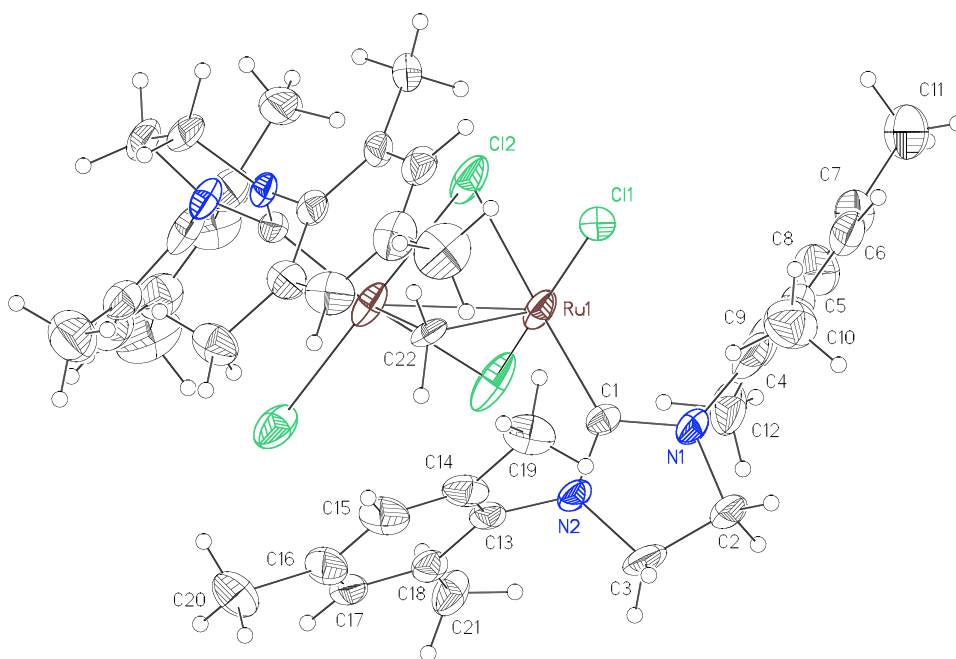
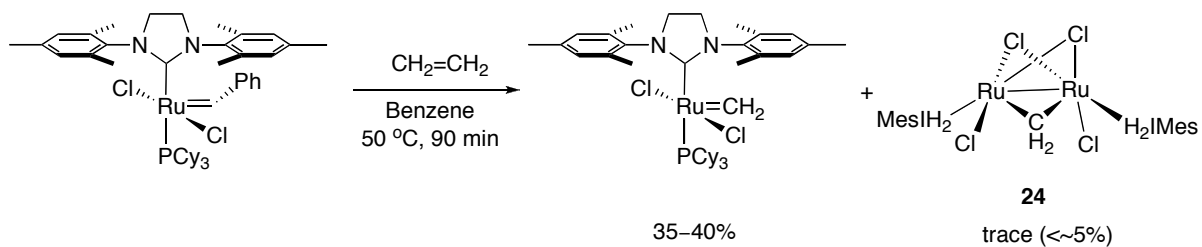


Figure 2. ORTEP drawing of **24** with thermal ellipsoids at 50 % probability.

Scheme 8



Scheme 9

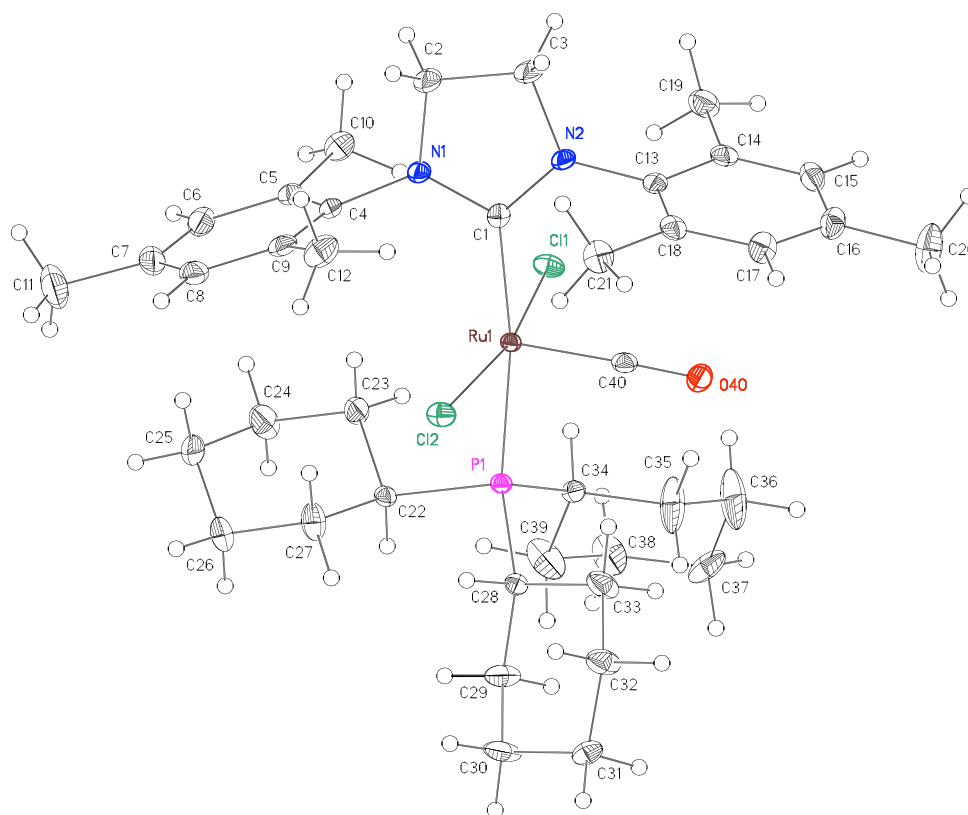
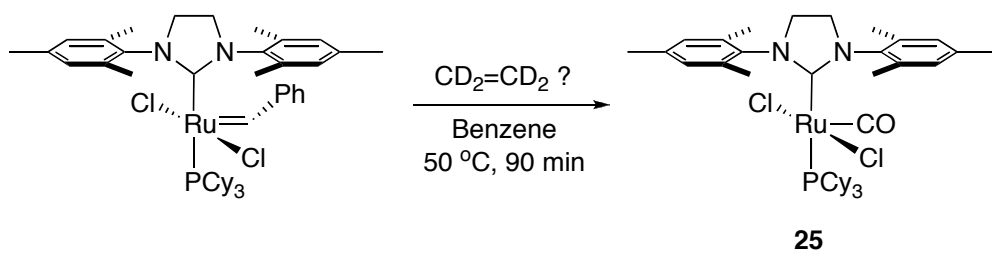
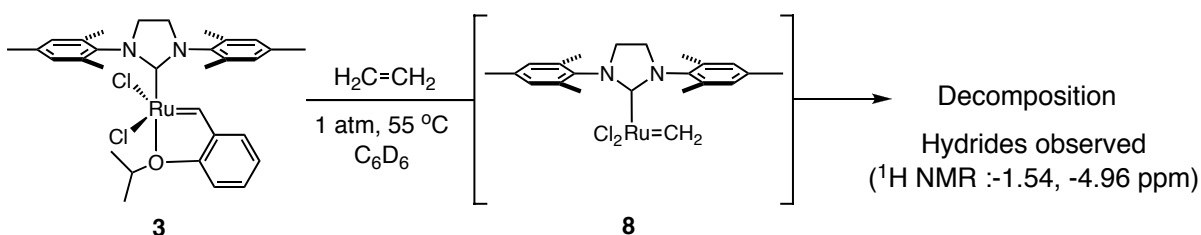


Figure 3. X-ray crystal structure of **25**.

Another decomposition product **25** was characterized by X-ray crystallography during an attempt to synthesize deuteriated methylene using $\text{CD}_2=\text{CD}_2$ and catalyst **2** (Scheme 9 and Figure 3). However, the formation of **25** was not reproducible in other attempts. The purity of the used ethylene- d_4 gas is suspected.²⁷

Decomposition of phosphine-free catalysts. Catalyst **3** is known as a more stable catalyst than **2** under air and water due to the chelation of its isopropoxy ligand.^{28,29} However, as with the phosphine-containing catalysts, a comparison of stability between initiators is not particularly meaningful.^{5,6} Both catalyst **2** and **3** are thermally stable—their half-lives at 55 °C in benzene are over a month. Because the methylene derivative of **3** cannot be isolated, its decomposition was examined directly in the presence of ethylene (Scheme 10). After one day, unidentified ruthenium hydride species were observed by ^1H NMR at -1.54 and -4.96 ppm. Attempts to isolate these species were unsuccessful. These species could be responsible for the olefin-isomerization reactions known to be catalyzed by **3**.^{30,31} This result suggests that other decomposition modes, which are only slightly slower than the phosphine-involved decomposition, are also available when a phosphine is not present.

Scheme 10. Catalyst **3** with ethylene.



Bispyridine-based catalysts, such as **4**, have proven to be useful for the synthesis of polymers due to their fast-initiation rates.^{18,32} However, the lower stabilities of these catalysts limit their application. We tried to synthesize $(\text{H}_2\text{IMes})(\text{py})_2(\text{Cl})_2\text{Ru}=\text{CH}_2$ (**26**) to compare with other methylenes complexes; however, any synthetic attempts were unsuccessful due to its instability. Even *in situ*, the methylene protons of complex **26** were never observed by ^1H NMR.

Interestingly, complex **27** and methyltricyclohexylphosphonium chloride were formed from the reaction of **5** with an excess of pyridine (Scheme 11).³³ The structure of **27** was determined by X-ray crystallography (Figure 4). All bond distances and angles in this structure are typical, but the mesityl groups are twisted by $\sim 25^\circ$ with respect to each other, which contrasts with their usual orientation perpendicular to the imidazolidine ring.

The formation of **27** was also observed during the reaction of **4** with ethylene in the absence of a PCy_3 ligand. Complex **27** also has been observed from the synthetic trials of a bulky chelating alkylidene from **4**.³⁴ Sponser and co-workers reported a similar product from the decomposition of $(\text{H}_2\text{IMes})(3\text{-bromopyridine})_2(\text{Cl})_2\text{Ru}=\text{CHR}$ ($\text{R} = \text{Me}, \text{Et}, n\text{Pr}$).³⁵ Although they did not determine the structure of this decomposition product, their ^1H NMR data match those of **27**. These observations indicate that complexes similar to **27** typically form during the decomposition of pyridine-containing ruthenium olefin metathesis catalysts regardless of the presence of phosphines. The fate of the methylene carbon is not clear in these or other cases where the $[\text{Ru}]=\text{CH}_2$ is generated in the presence of pyridines.³⁶

Scheme 11. Formation of $(\text{H}_2\text{IMes})(\text{py})_3(\text{Cl})_2\text{Ru}$ (**27**).

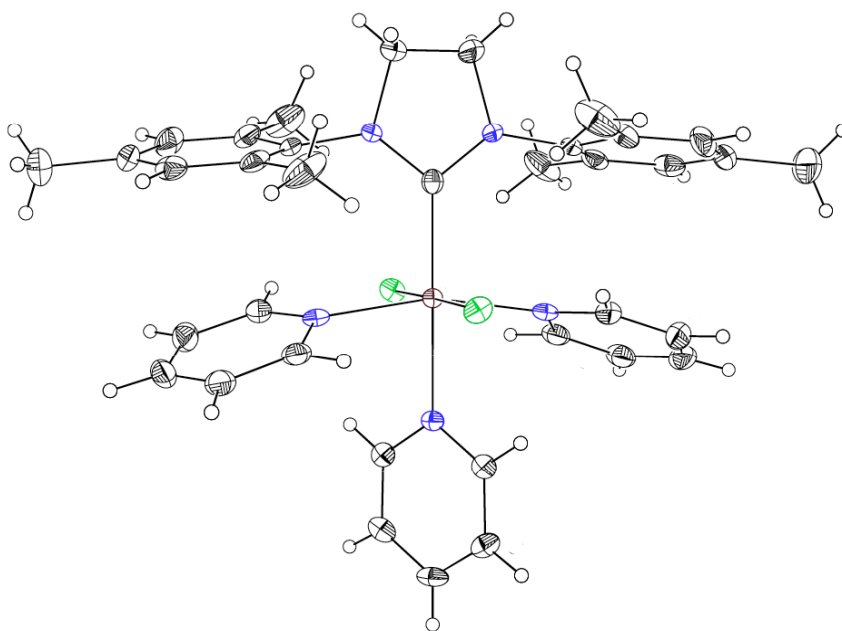
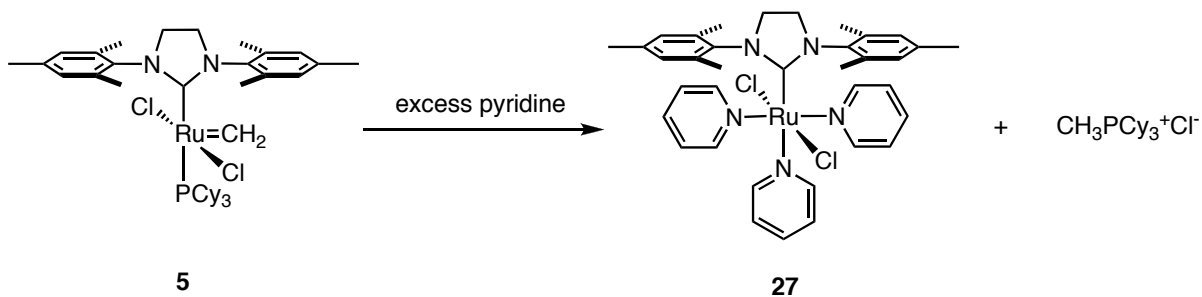


Figure 4. Crystal structure of $(\text{H}_2\text{IMes})(\text{py})_3(\text{Cl})_2\text{Ru}$ (**27**).

Conclusion

We have examined the decomposition of a series of ruthenium metathesis catalysts. Ruthenium methyldene complexes, the most common yet least stable isolable intermediate during olefin metathesis, have been chosen as model complexes. All of the phosphine-containing methyldene complexes we examined decomposed following first-order kinetics

to generate methylphosphonium salts. The observed kinetic behavior suggests that the major decomposition pathway involves attack of the dissociated phosphine on the methyldiene carbon. Such a mechanism also explains the decomposition observed in the presence of ethylene as a model olefin substrate. The novel ruthenium ethylene complex **21** was observed from the decomposition of the catalyst **18** under ethylene. The decomposition of phosphine-free catalyst **3** generated unidentified ruthenium hydride species under an atmosphere of ethylene. Attempts to synthesize a pyridine-coordinated analog of methyldiene **4** were unsuccessful presumably due to rapid decomposition. Instead, we observed the tris(pyridine) complex **27** as a decomposition product. This decomposition study will provide rational basis to design and synthesize more efficient ruthenium olefin metathesis catalysts.

Experimental

General considerations. Manipulation of organometallic compounds was performed using standard Schlenk techniques under an atmosphere of dry argon or in a nitrogen-filled Vacuum Atmospheres dry box ($O_2 < 2.5$ ppm). NMR spectra were recorded on a Varian Inova (499.85 MHz for 1H ; 202.34 MHz for ^{31}P ; 125.69 MHz for ^{13}C) or on a Varian Mercury 300 (299.817 MHz for 1H ; 121.39 MHz for ^{31}P ; 74.45 MHz for ^{13}C). ^{31}P NMR spectra were referenced using H_3PO_4 ($\delta = 0$ ppm) as an external standard. Elemental analyses were performed at Desert Analytics (Tucson, AZ). Mass spectra were recorded on JEOL JMS 600H spectrophotometer. Silica gel used for purification of organometallic complexes was obtained from TSI Scientific, Cambridge, MA (60 Å, pH 6.5–7.0). Benzene, benzene- d_6 , pentane, diethyl ether, THF, and methylene chloride were dried by passage through solvent purification columns. CD_2Cl_2 was dried by vacuum transfer from CaH_2 . All solvents are

degassed by either a generous Ar sparge or three freeze-pump-thaw cycles. Catalysts **1**, **2**, and **3** were obtained from Materia and used as received. Ruthenium complexes **4**,¹⁸ **5**,⁷ **13**,³⁷ **18**,⁷ and $(\text{H}_2\text{IMes})(\text{PCy}_3)(\text{Br})_2\text{Ru}=\text{CHPh}$ ⁷ were prepared according to literature procedures. Methyltriphenylphosphonium chloride was purchased from Aldrich.

(PCy₃)₂(Br)₂Ru=CH₂ (9). A solution of **1** (166 mg, 0.182 mmol) in CH₂Cl₂ (3 mL) was stirred under an atmosphere of ethylene for 30 min at room temperature. The solvent was removed under vacuum, and the residue was repeatedly washed with cold pentane (5 mL) and dried under vacuum. A burgundy microcrystalline solid (146 mg, 0.175 mmol, 96%) was obtained. ¹H NMR (C₆D₆): δ 19.38 (s, 2H), 3.00-2.80 (m, 6H), 1.95-1.20 (all m, 60H). ¹³C{¹H} NMR (CD₂Cl₂): δ 297.3 (t, J_{CP} = 8.2 Hz), 31.6 (t, J_{CP} = 10.1Hz), 29.7 (s), 28.0 (t, J_{CP} = 5.1 Hz), 26.8(s). ³¹P{¹H} NMR (C₆D₆): δ 44.51 (s). HRMS analysis (FAB) m/z: Calcd for C₃₇H₆₈Br₂P₂Ru [M⁺]: 836.2199, found: 836.2174.

(H₂IMes)(PCy₃)(Br)₂Ru=CH₂ (10). A solution of $(\text{H}_2\text{IMes})(\text{PCy}_3)(\text{Br})_2\text{Ru}=\text{CHPh}$ (300 mg, 0.320 mmol) in C₆D₆ (5 mL) was stirred under an atmosphere of ethylene for 90 min at 50 °C. The brown solution was cooled to room temperature, and the product was purified by column chromatography (gradient elution: 100% pentane to 8:1 pentane/diethyl ether) to afford an orange-yellow solid (95 mg, 0.110 mmol, 34%). ¹H NMR (C₆D₆): δ 18.53 (s, 2H), 6.89 (s, 2H), 6.73 (s, 2H), 3.26 (m, 4H), 2.80 (s, 6H), 2.65-2.47 (m, 3H), 2.63 (s, 6H), 2.17 (s, 3H), 2.09 (s, 3H), 1.80-1.00 (m, 30H). ¹³C{¹H} NMR (C₆D₆): δ 296.7 (d, J_{CP} = 10 Hz), 221.8 (d, J_{CP} = 74.8 Hz), 138.8, 138.4, 138.0, 137.6, 137.1, 134.9, 130.7, 130.1, 129.8, 129.6, 128.4, 127.8, 51.7 (d, J_{CP} = 3.5 Hz), 31.3, 31.0, 30.8, 29.3, 27.9, 27.8, 26.5,

21.0 (d, $J_{CP} = 2.6$ Hz), 20.9, 19.7. $^{31}\text{P}\{^1\text{H}\}$ NMR (C_6D_6): δ 38.02 (s). Anal. Calcd for $\text{C}_{40}\text{H}_{61}\text{N}_2\text{Br}_2\text{PRu}$: C, 55.75; H, 7.13; N, 3.25. Found: C, 56.04; H, 7.13; N, 3.25.

(H₂IPr)(PCy₃)(Cl)₂Ru=CH₂ (11). A solution of (H₂IPr)(PCy₃)(Cl)₂Ru=CHPh (300 mg, 0.321 mmol) in C_6D_6 (5 mL) was stirred under an atmosphere of ethylene for 30 min at 45 °C. The brown solution was cooled to room temperature, and the product was purified by column chromatography (gradient elution: 100% pentane to 12:1 pentane/diethyl ether) to afford an orange-yellow solid (95 mg, 0.110 mmol, 34%). This product was very air-sensitive, and even slowly decomposed in the dry box. Further study was done immediately after the synthesis. ^1H NMR (C_6D_6): δ 18.22 (s, 2H), 7.22-7.09 (m, 11H), 4.10 (m, 2H), 3.74-3.60 (m, 6H), 2.37-2.20 (m, 3H), 1.70-0.96 (m, 54H). $^{13}\text{C}\{^1\text{H}\}$ NMR (C_6D_6): δ 294.8 (d, $J_{CP} = 8.3$ Hz), 224.2 (d, $J_{CP} = 75.7\text{Hz}$), 150.1, 148.7, 137.9, 136.2, 130.9, 130.0, 128.9, 128.7, 128.5, 128.3, 125.1, 124.9, 55.2, 53.6, 31.2, 31.0, 29.6, 29.5, 28.8, 28.3, 28.3, 27.6, 27.0, 25.2, 24.3. $^{31}\text{P}\{^1\text{H}\}$ NMR (C_6D_6): δ 38.83 (s). HRMS analysis (FAB) m/z : Calcd for $\text{C}_{46}\text{H}_{73}\text{N}_2\text{Cl}_2\text{RuP} [M^+]$: 856.3932, found: 856.3917.

Complex 24. Crystal data for **24**: $\text{C}_{43}\text{H}_{54}\text{N}_4\text{Cl}_4\text{Ru}_2 \cdot \frac{1}{2}\text{C}_6\text{H}_6$, $M=1009.90$, tetragonal, space group $P-42_1c$, $a = 15.4853(5)$ Å, $c = 19.7050(8)$ Å, $V=4725.2(3)$ Å³, $T = 100(2)$ K, $Z = 4$, $\mu(\text{Mo-K}\alpha) = 0.900$ mm⁻¹, 76914 measured reflections, 8346 unique, 5377 reflections with $I > 2 \sigma(I)$, final $RI = 0.0515$, $wR2 = 0.0797$. CCDC reference number 231270.

Complex 25. Crystal data for **25**: $\text{C}_{40}\text{H}_{59}\text{N}_2\text{OPCl}_2\text{Ru} \cdot \text{C}_6\text{H}_6$, $M=864.94$, monoclinic, space group $P2_1/n$, $a = 11.7511(4)$ Å, $b = 21.3379(6)$ Å, $c = 17.5327(6)$ Å, $\beta = 95.1430(10)^\circ$,

$V=4378.5(2) \text{ \AA}^3$, $T = 100(2) \text{ K}$, $Z = 4$, $\mu(\text{Mo-K}\alpha) = 0.552 \text{ mm}^{-1}$, 80614 measured reflections, 21479 unique, 13014 reflections with $I > 2 \sigma(I)$, final $RI = 0.0463$, $wR2 = 0.0692$. CCDC reference number 231269. $^1\text{H NMR}$ (C_6D_6): δ 6.69 (s, 4H), 3.22 (m, 4H), 2.61 (s, 6H), 2.55 (s, 6H), 2.50 (m, 3H), 2.05 (s, 3H), 2.02 (s, 3H), 1.99 – 1.00 (m, 30H). $^{31}\text{P}\{^1\text{H}\}$ NMR (C_6D_6): δ 32.91.

(H₂IMes)(py)₃(Cl)₂Ru (27). A solution of **5** (150 mg, 0.195 mmol), excess pyridine (0.25 mL), and 1.0 mL of toluene was stirred at room temperature for 30 min. 20 mL of hexanes were added, and the solution was allowed to sit without stirring for 3 min. The red solution was decanted away from the pale yellow precipitate and cooled to 0 °C. The resulting red precipitate was collected and redissolved in a minimum amount of toluene. Again, 20 mL of hexanes were added, the solution cooled, and the red precipitate collected. This procedure was repeated three more times. Finally, the precipitate was dried under vacuum to provide 0.041 g (mmol, 29%) of **27** as a red-orange solid. $^1\text{H NMR}$ (CD_2Cl_2): δ 9.00 (d, $J = 5.5 \text{ Hz}$, 4H), 8.70 (d, $J = 5.5$, 2H), 7.30 (t, $J = 7.5 \text{ Hz}$, 1H), 6.98 (t, $J = 7.5 \text{ Hz}$, 2H), 6.76 (t, $J = 7.0 \text{ Hz}$, 2H), 6.34 (s, 4H), 6.33 (t, $J = 7.0$, 4H), 3.98 (s, 4H), 2.47 (s, 12H), 2.02 (s, 6H). $^{13}\text{C}\{^1\text{H}\}$ NMR (C_6D_6): δ 198.2, 142.2, 138.5, 128.4, 125.6, 125.0, 123.1, 120.3, 118.4, 113.1, 118.9, 54.1, 25.7, 24.5. HRMS analysis (FAB) m/z : Calcd for $\text{C}_{36}\text{H}_{41}\text{N}_5\text{Cl}_2\text{Ru}$ [M^+]: 715.1783, found: 715.2783.

Procedure for a typical decomposition measurement. 0.0161 mmol of methyldiene and ~0.00561 mmol of anthracene were weighed into a 1-dram vial. 0.700 mL of benzene- d_6 was used to transfer the sample to a screw-cap NMR tube. A screw-cap was

used to seal the NMR tube, and this seal was reinforced with parafilm. The sample was placed into the spectrometer and allowed to equilibrate at the probe temperature for 10 min. Complex decomposition was following by monitoring the diminution of the methylenic protons through collection of a time-delayed array of ^1H NMR spectra (referred to as a preacquisition delay, PAD, by Varian software). Plots of [methylenic] vs. time and ^{31}P spectra of the decompositions are shown in Charts 1–4 and Figures 5–9.

Decomposition of 18 with ethylene.³⁴ In a N_2 -filled glovebox, a J-Young tube was charged with complex **18** (17.5 mg, 0.021 mmol, 1.0 equiv) and 600 mL of a stock solution containing 0.014 M anthracene (1.5 mg, 0.0084 mmol) in CD_2Cl_2 , yielding a homogeneous brown solution. The tube was sealed with a Teflon stopper, removed from the box, and attached to a Schlenk line. The tube was cooled to $-78\text{ }^\circ\text{C}$, placed under vacuum (100 mTorr) and then backfilled with an atmosphere of ethylene. The tube was sealed, shaken and allowed to warm to $23\text{ }^\circ\text{C}$. Reaction progress was monitored by ^1H NMR(300 MHz) at $23\text{ }^\circ\text{C}$, observing the disappearance of **18** ($\delta = 19.21$ ppm, $\text{Ru}=\text{CHPh}$) and the appearance of complex **11** ($\delta = 18.59$, $\text{Ru}=\text{CH}_2$). These results are depicted in Chart 5.³⁸

Chart 1. Decomposition of 5.

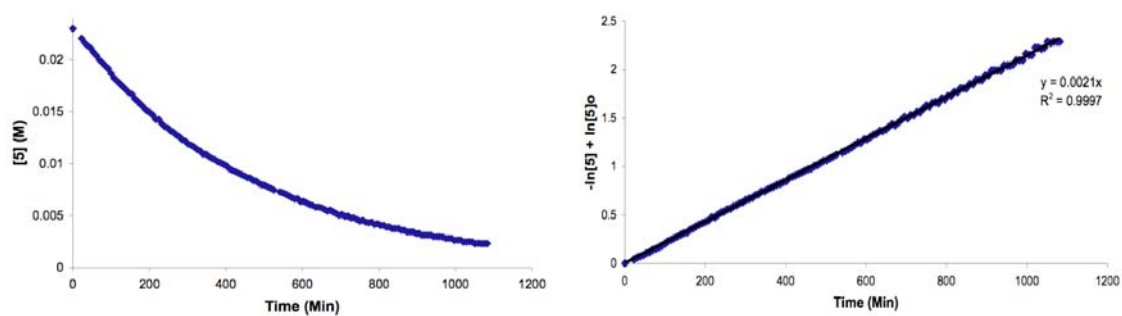


Chart 2. Decomposition of 14.

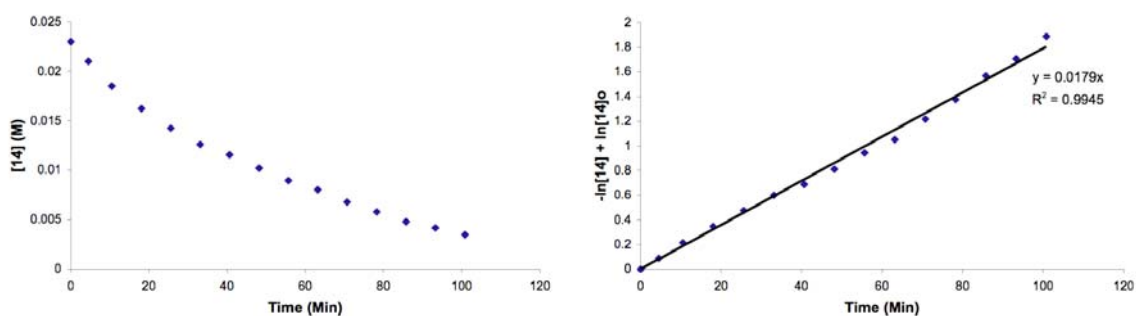


Chart 3. Decomposition of 16.

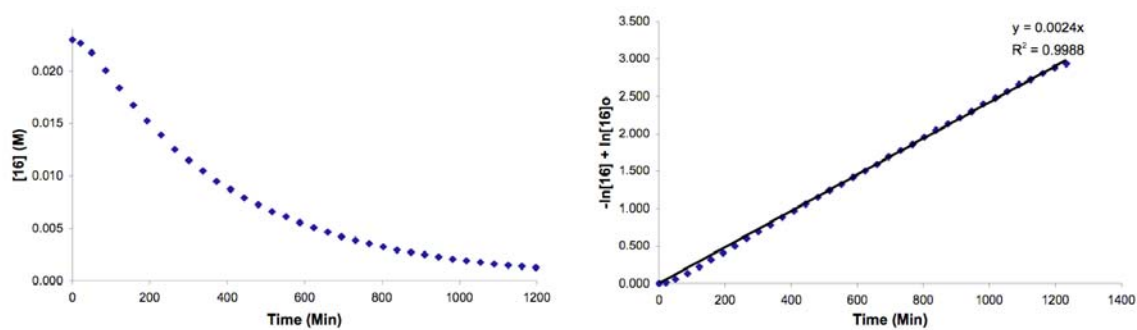
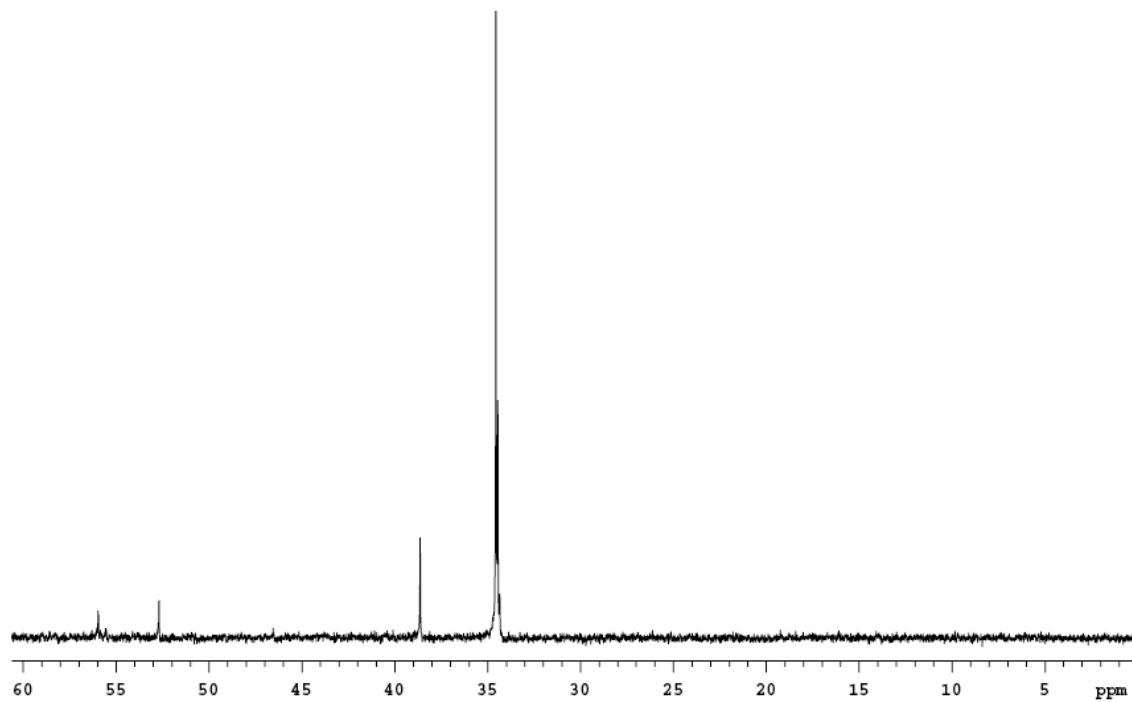
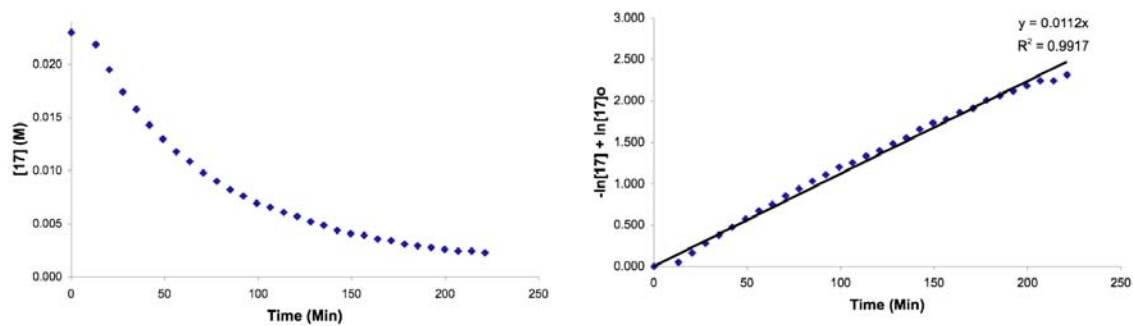


Chart 4. Decomposition of 17.

Figure 5. ^{31}P NMR spectrum after decomposition of 5.

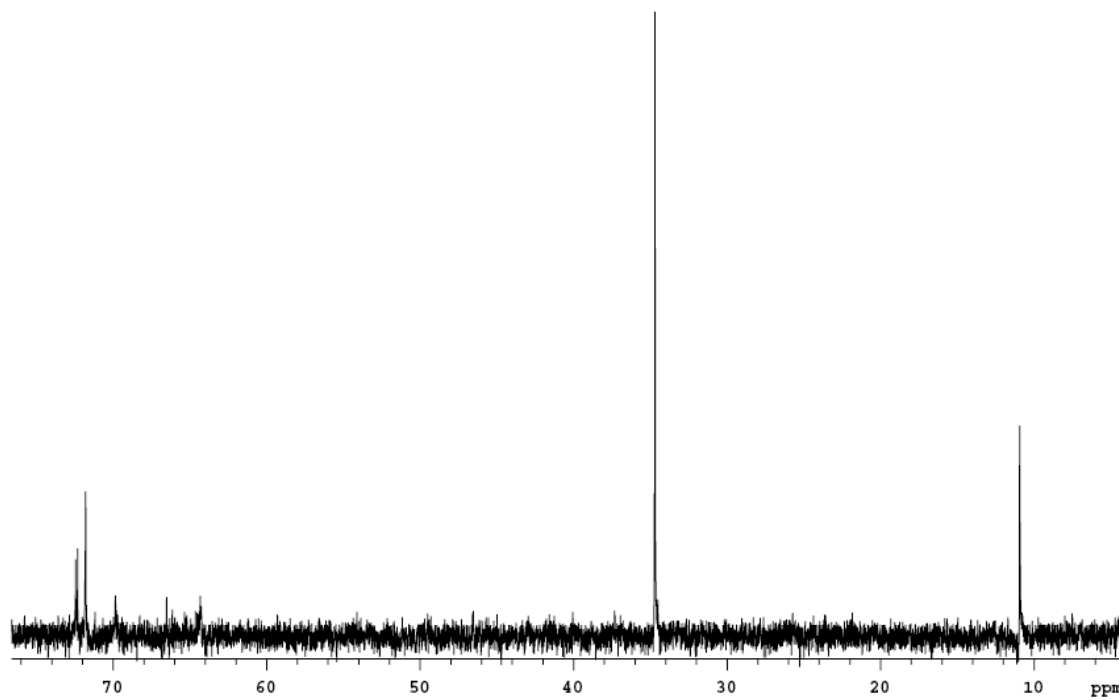


Figure 6. ^{31}P NMR spectrum after decomposition of **13**.

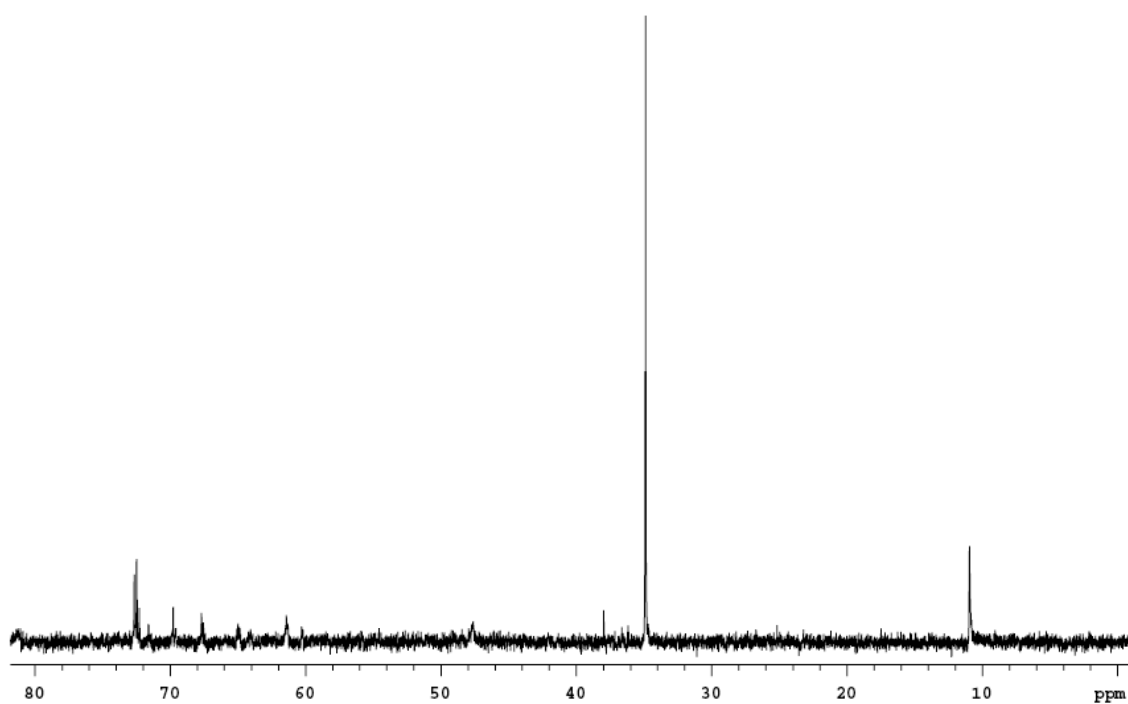


Figure 7. ^{31}P NMR spectrum after decomposition of **14**.

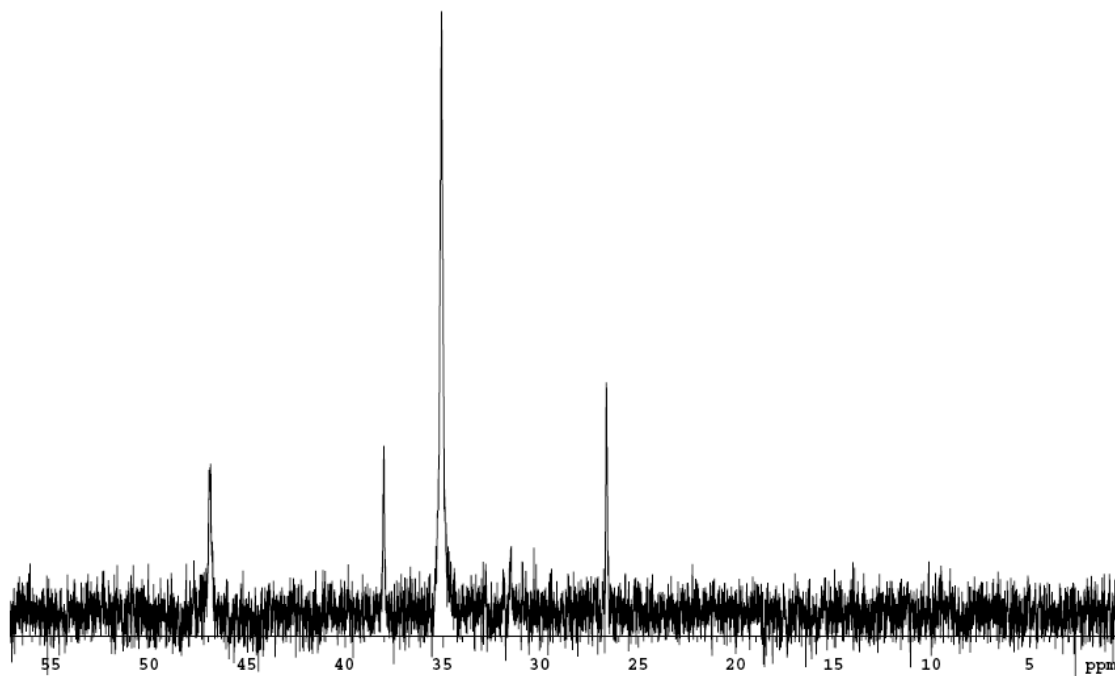


Figure 8. ^{31}P NMR spectrum after decomposition of **16**.

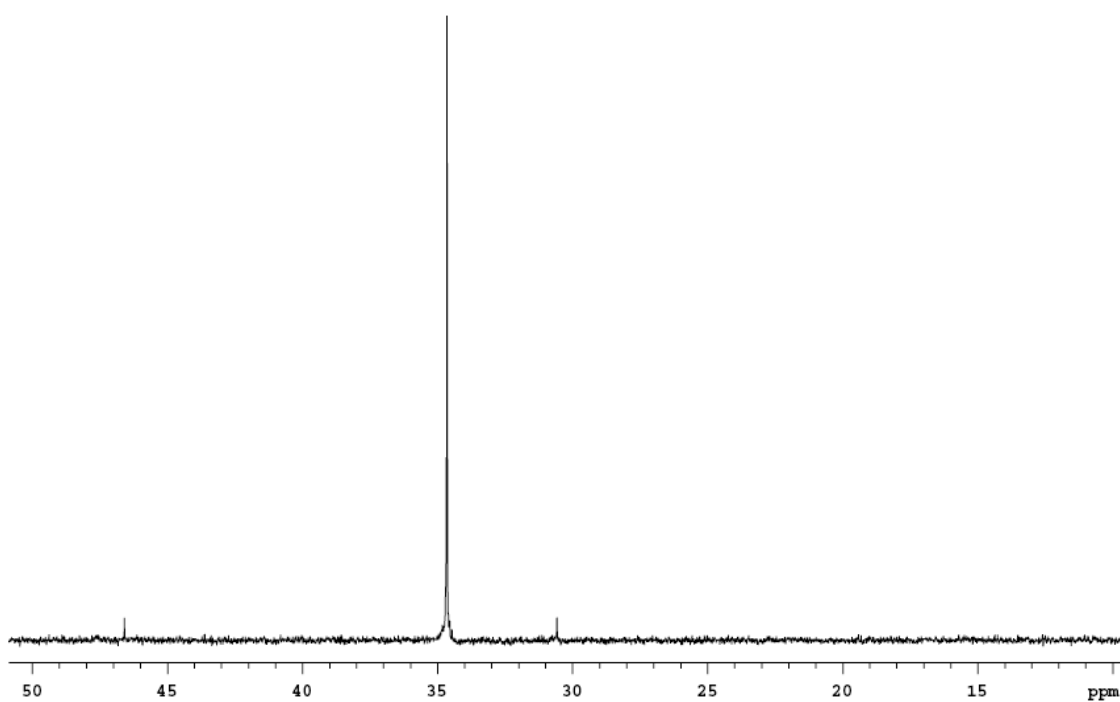
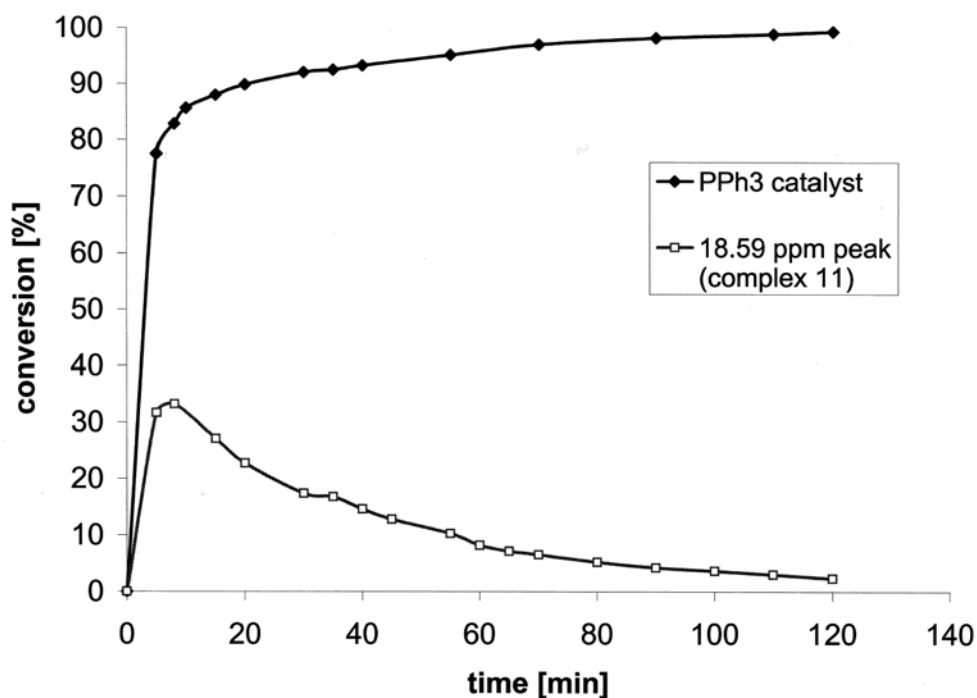


Figure 9. ^{31}P NMR spectrum after decomposition of **17**.

Chart 5. Decomposition reaction of **18** with ethylene.

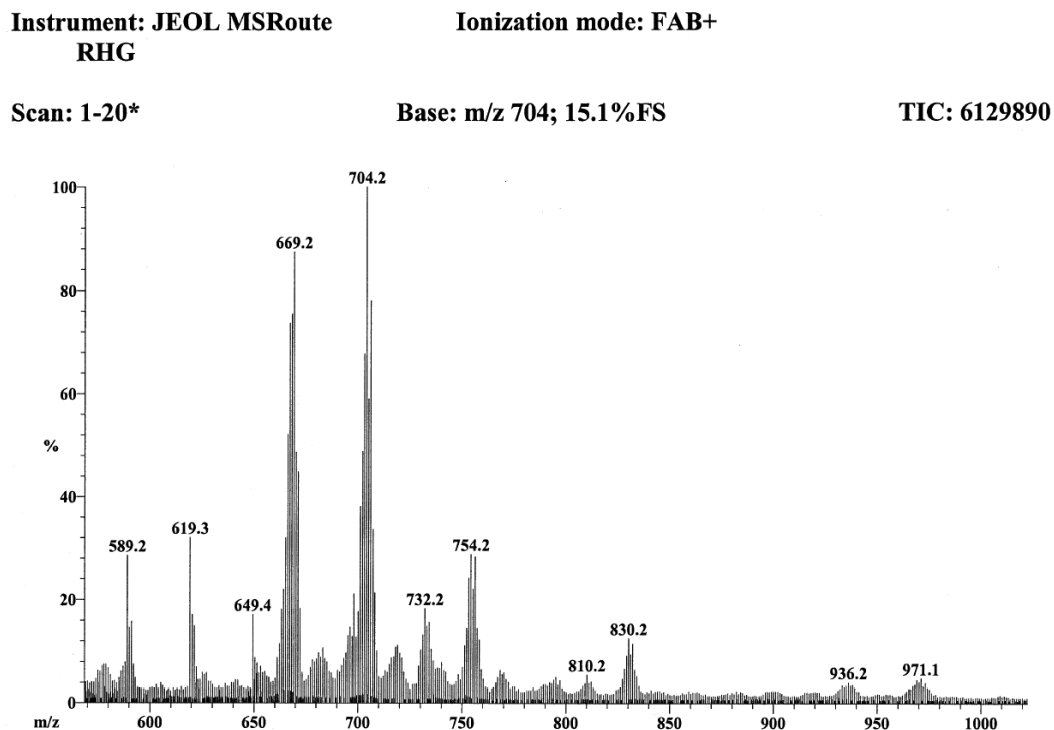


Mass spectrometric analysis of the decomposition reaction of 18 with ethylene.

To an NMR tube equipped with a Teflon screw cap in the glove box: complex **18** (17.5 mg, 0.021 mmol, 1.0 equiv) was dissolved in 600 μL of CD_2Cl_2 , forming a homogeneous brown solution. The tube was sealed, removed from the box, and attached to a Schlenk line. The tube was then cooled to $-78\text{ }^\circ\text{C}$, placed under vacuum (100 mTorr), and backfilled with an atmosphere of ethylene. The NMR tube was removed from the Schlenk line, shaken, and allowed to warm to $23\text{ }^\circ\text{C}$. Mass spectrometric analysis at 8 minutes revealed the presence of a ruthenium complex possessing the same calculated mass as **11** (Figure 6): (FAB+) m/z 971.1 (M-H):³⁹ Analysis of the reaction mixture after 24 h via ^1H NMR, ^{31}P NMR, and

HRMS confirmed the presence of methyltriphenylphosphonium chloride (**20**) via correlation to authentic material.

Figure 6. Mass spectrum of the reaction of **18** with ethylene after 8 min at 23 °C.



Reaction of **18 with ethylene to generate metallacyclobutane **19**.**³⁴ To a J-Young tube in the glove box, complex **18** (17.5 mg, 0.021 mmol, 1.0 equiv.) was dissolved in 600 μL of a stock solution containing 0.014 M anthracene (1.5 mg, 0.0084 mmol) in CD_2Cl_2 , forming a homogeneous brown solution. The tube was sealed with a Teflon stopper, removed from the box, and attached to a Schlenk line. The tube was then cooled to $-78\text{ }^\circ\text{C}$, placed under vacuum (100 mTorr), and backfilled with an atmosphere of ethylene. The tube was sealed, shaken, and allowed to warm to $23\text{ }^\circ\text{C}$. The reaction was monitored via ^1H NMR (500 MHz) at $23\text{ }^\circ\text{C}$ for 20 min, at which time complex **18** was over 90% consumed and **11** was

the predominant alkylidene species (~44% yield relative to Ru). The reaction was then cooled to $-40\text{ }^{\circ}\text{C}$. After 3 h at $-40\text{ }^{\circ}\text{C}$, the peak at 18.59 ppm (corresponding to complex **11**), had completely diminished and two new peaks at 6.64 ppm (4H) and $-2.63(2\text{H})$ were clearly visible, corresponding to the literature values for the α - and β -hydrogens of ruthenium metallacycle **19**.^{21,22}

Decomposition products of 18.³⁴ To a 10 mL Schlenk tube in the glove box, complex **18** (56 mg, 0.077 mmol, 1.0 equiv) was dissolved in 2.2 mL of toluene, forming a homogeneous brown solution. The tube was sealed with a Teflon stopper, removed from the box, and attached to a Schlenk line. The tube was then cooled to $-78\text{ }^{\circ}\text{C}$, placed under vacuum (100 mTorr), and backfilled with an atmosphere of ethylene. The tube was sealed, shaken, and allowed to warm to $23\text{ }^{\circ}\text{C}$. The reaction was allowed to stand for 5 d at $23\text{ }^{\circ}\text{C}$. During this time, a white solid (methyltriphenylphosphonium chloride, **20**) was observed to precipitate out of solution in addition to the formation of red-brown crystals. The Schlenk line was opened in the glove box and the toluene was carefully transferred out via syringe. The crystals were then washed with two 500 μL portions of a 50:50 toluene/pentane mixture. 52 mg of the red-brown crystals were isolated and analyzed via X-ray crystallography and found to be complex **21**. Further spectroscopic analysis of **21** proved problematic, due to its instability in solution. ^{31}P NMR analysis of both the white precipitate and mother liquor revealed the only phosphorous-containing product to be methyltriphenylphosphonium chloride (**20**).

X-ray crystallographic data collection and refinement.⁴⁰ For compounds **7**, **21** and **25** each crystal was mounted on a glass fiber using Paratone and placed in the cold stream of an Oxford Cryostream. Intensity data were collected on a Bruker SMART1000 diffractometer. The data were integrated using the Bruker SAINT (v6.45) program. Each crystal structure was solved by direct methods and then refined by full-matrix least squares using Bruker SHELXTL. All nonhydrogen atoms were refined with anisotropic displacement parameters. Hydrogen atoms were located in the difference Fourier and refined isotropically without restraint except for the hydrogen atoms on water in compound **7**, which were restrained as riding atoms. The crystallographic data are summarized in Table 2.

Table 2. Summary of crystallographic data for **7**, **21** and **27**

	7	21	27
formula	[C ₁₉ H ₃₆ P] ⁺ Cl 3(H ₂ O)	C ₄₆ H ₅₈ N ₄ Cl ₂ Ru ₂	C ₃₆ H ₄₁ N ₅ Cl ₂ Ru
<i>M_r</i>	384.95	940.00	715.71
crystal color	colorless	red/brown	orange
crystal size (mm)	0.30 × 0.23 × 0.18	0.21 × 0.18 × 0.07	0.33 × 0.28 × 0.08
crystal system	triclinic	triclinic	orthorhombic
space group	P-1	P-1	Pbcn
<i>a</i> (Å)	9.8774(4)	9.8735(6)	11.3376(7)
<i>b</i> (Å)	10.0035(5)	10.7053(7)	13.3755(8)
<i>c</i> (Å)	12.7700(6)	11.8315(7)	21.4203(14)
<i>α</i> (deg)	85.1580(10)	100.828(2)	90
<i>β</i> (deg)	74.3040(10)	98.018(2)	90
<i>γ</i> (deg)	63.5350(10)	116.4470(10)	90
<i>V</i> (Å ³)	1086.48(9)	1063.77(11)	3248.3(4)
<i>Z</i>	2	1	4
<i>D</i> _{calcd} (g cm ⁻³)	1.177	1.467	1.463
<i>T</i> (K)	100(2)	100(2)	98(2)
<i>λ</i> (Å)	0.71073	0.71073	0.71073
<i>μ</i> (mm ⁻¹)	0.263	0.872	0.681
<i>R</i> ₁ ^a (all data)	0.0618	0.0724	0.0481
<i>wR</i> ₂ ^b (all data)	0.0772	0.0714	0.0509
GOF	1.307	1.146	1.716

^a $R_1 = S||F_o| - |F_c||/S|F_o|$. ^b $wR_2 = [Sw(F_o^2 - F_c^2)^2/Sw(F_o^2)^2]^{1/2}$

References and Notes

- (1) *Handbook of Metathesis*; Grubbs, R. H., Ed.; Wiley-VCH: Weinheim, Germany, 2003; Vol. 1-3.
- (2) Connon, S. J.; Blechert, S. *Angew. Chem., Int. Ed.* **2003**, *42*, 1900-1923.
- (3) Trnka, T. M.; Grubbs, R. H. *Acc. Chem. Res.* **2001**, *34*, 18-29.
- (4) Grubbs, R. H.; Chang, S. *Tetrahedron* **1998**, *54*, 4413-4450.
- (5) Hong, S. H.; Day, M. W.; Grubbs, R. H. *J. Am. Chem. Soc.* **2004**, *126*, 7414-7415.
- (6) Ulman, M.; Grubbs, R. H. *J. Org. Chem.* **1999**, *64*, 7202-7207.
- (7) Sanford, M. S.; Love, J. A.; Grubbs, R. H. *J. Am. Chem. Soc.* **2001**, *123*, 6543-6554.
- (8) Ulman, M. *PhD Thesis*, California Institute of Technology, 2000.
- (9) Huang, J. K.; Schanz, H. J.; Stevens, E. D.; Nolan, S. P. *Organometallics* **1999**, *18*, 5375-5380.
- (10) Fürstner, A.; Ackermann, L.; Gabor, B.; Goddard, R.; Lehmann, C. W.; Mynott, R.; Stelzer, F.; Thiel, O. R. *Chem. Eur. J.* **2001**, *7*, 3236-3253.
- (11) Dinger, M. B.; Mol, J. C. *Adv. Synth. Catal.* **2002**, *344*, 671-677.
- (12) Courchay, F. C.; Sworen, J. C.; Wagener, K. B. *Macromolecules* **2003**, *36*, 8231-8239.
- (13) Steady-state approximation was applied to equation (1).
- (14) Several unidentified phosphorus peaks were observed in ^{31}P NMR spectra from the reaction between **5** and PMe_3 .
- (15) We think that the internal attack of PCy_3 will be less affected by the steric hindrance of H^2IPr ligands and the geometry is not favorable for the internal attack. For the electronic properties of *N*-heterocyclic carbene ligands, see Dorta, R.; Stevens, E. D.;

- Scott, N. M.; Costabile, C.; Cavallo, L.; Hoff, C. D.; Nolan, S. P. *J. Am. Chem. Soc.* **2005**, *127*, 2485-2495.
- (16) Hansen, S. M.; Rominger, F.; Metz, M.; Hofmann, P. *Chem. Eur. J.* **1999**, *5*, 557-566.
- (17) van Rensburg, W. J.; Steynberg, P. J.; Meyer, W. H.; Kirk, M. M.; Forman, G. S. *J. Am. Chem. Soc.* **2004**, *126*, 14332-14333.
- (18) Sanford, M. S.; Love, J. A.; Grubbs, R. H. *Organometallics* **2001**, *20*, 5314-5318.
- (19) This part of decomposition study of catalyst **18** was done and written by Dr. Anna G. Wenzel.
- (20) Values correspond to NMR yields utilizing anthracene (0.014 M) as an internal reaction standard. Alkylidene assumed to be methylidene-derived (2H); conversion based on Ru is 66% if it is assumed that the complex is the bis-ruthenium complex **11**.
- (21) Romero, P. E.; Piers, W. E. *J. Am. Chem. Soc.* **2005**, *127*, 5032-5033.
- (22) Wenzel, A. G.; Grubbs, R. H. *J. Am. Chem. Soc.* **2006**, *128*, 16048-16049.
- (23) Romero, P. E.; Piers, W. E. *J. Am. Chem. Soc.* **2007**, *129*, 1698-1704.
- (24) Zhang, X. M.; Bordwell, F. G. *J. Am. Chem. Soc.* **1994**, *116*, 968-972.
- (25) Streitwieser, A.; McKeown, A. E.; Hasanayn, F.; Davis, N. R. *Org. Lett.* **2005**, *7*, 1259-1262.
- (26) For diruthenium μ -methylene complexes see : Gao, Y.; Jennings, M. C.; Puddephatt, R. J. *Organometallics* **2001**, *20*, 1882.
- (27) The gas used at the synthesis was purchased at Aldrich. In another trial using other gas cylinders, the deuteriated methylidene was synthesized without formation of **25**.

- (28) Garber, S. B.; Kingsbury, J. S.; Gray, B. L.; Hoveyda, A. H. *J. Am. Chem. Soc.* **2000**, *122*, 8168-8179.
- (29) Hong, S. H.; Grubbs, R. H. *J. Am. Chem. Soc.* **2006**, *128*, 3508-3509.
- (30) Hong, S. H.; Sanders, D. P.; Lee, C. W.; Grubbs, R. H. *J. Am. Chem. Soc.* **2005**, *127*, 17160-17161.
- (31) Courchay, F. C.; Sworen, J. C.; Ghiviriga, I.; Abboud, K. A.; Wagener, K. B. *Organometallics* **2006**, *25*, 6074-6086.
- (32) Love, J. A.; Morgan, J. P.; Trnka, T. M.; Grubbs, R. H. *Angew. Chem., Int. Ed.* **2002**, *41*, 4035-4037.
- (33) The reaction in Scheme 9 and characterization of complex **25** were carried out by Dr. Tina T. Salguero.
- (34) Hejl, A.; Grubbs, R. H. Unpublished results.
- (35) Williams, J. E.; Harner, M. J.; Sponsler, M. B. *Organometallics* **2005**, *24*, 2013-2015.
- (36) Methylpyridium salt was not observed in the reaction of **4** in the presence of ethylene. Werner and co-workers have reported that a similar reaction between the ruthenium methyldiene complex $(\text{PPri}_2\text{Ph})_2(\text{CO})(\text{Cl})(\text{H})\text{Ru}=\text{CH}_2$ and pyridine yields $(\text{PPri}_2\text{Ph})_2(\text{py})(\text{CO})(\text{Cl})(\text{H})\text{Ru}$. See: Werner, H.; Stuer, W.; Weberndorfer, B.; Wolf, J. *Eur. J. Inorg. Chem.* **1999**, 1707-1713.
- (37) Schwab, P.; Grubbs, R. H.; Ziller, J. W. *J. Am. Chem. Soc.* **1996**, *118*, 100-110.
- (38) The alkylidene was assumed to be methyldiene-derived (2H); values should be doubled when calculating conversion to **11** relative to ruthenium because it is a bimetallic species.

- (39) The presence of **11** has also been observed via mass spectrometry in the reaction of the bispyridyl catalyst **4** with ethylene.
- (40) X-ray crystallographic data collection and refinement was carried out by Lawrence M. Henling and Dr. Michael W. Day.

Chapter 4

Double C–H Activation of an N-Heterocyclic Carbene Ligand in a Ruthenium Olefin Metathesis Catalyst

Abstract

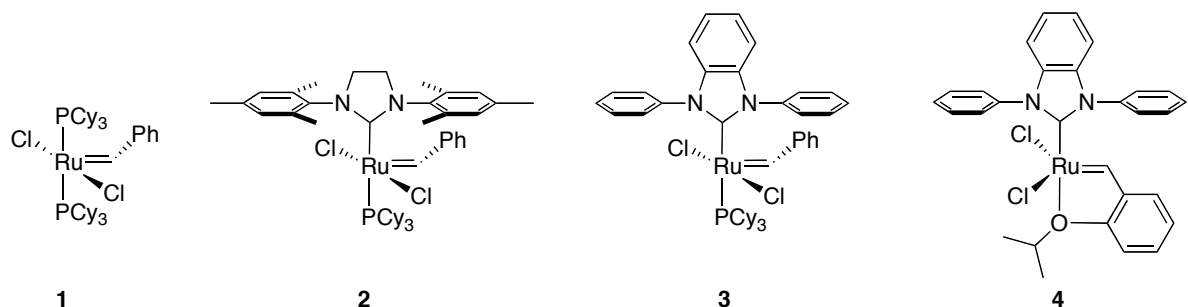
Decomposition of $(\text{BIPh})(\text{PCy}_3)(\text{Cl})_2\text{Ru}=\text{(H)Ph}$ (BIPh = *N,N'*-diphenylbenzimidazol-2-ylidene) results in the benzylidene insertion into an ortho C–H bond of a BIPh *N*-phenyl group. Ruthenium further inserts into another ortho C–H of the other BIPh *N*-phenyl ring to give a new Ru–C bond as a part of a five-membered metallacycle.

Introduction

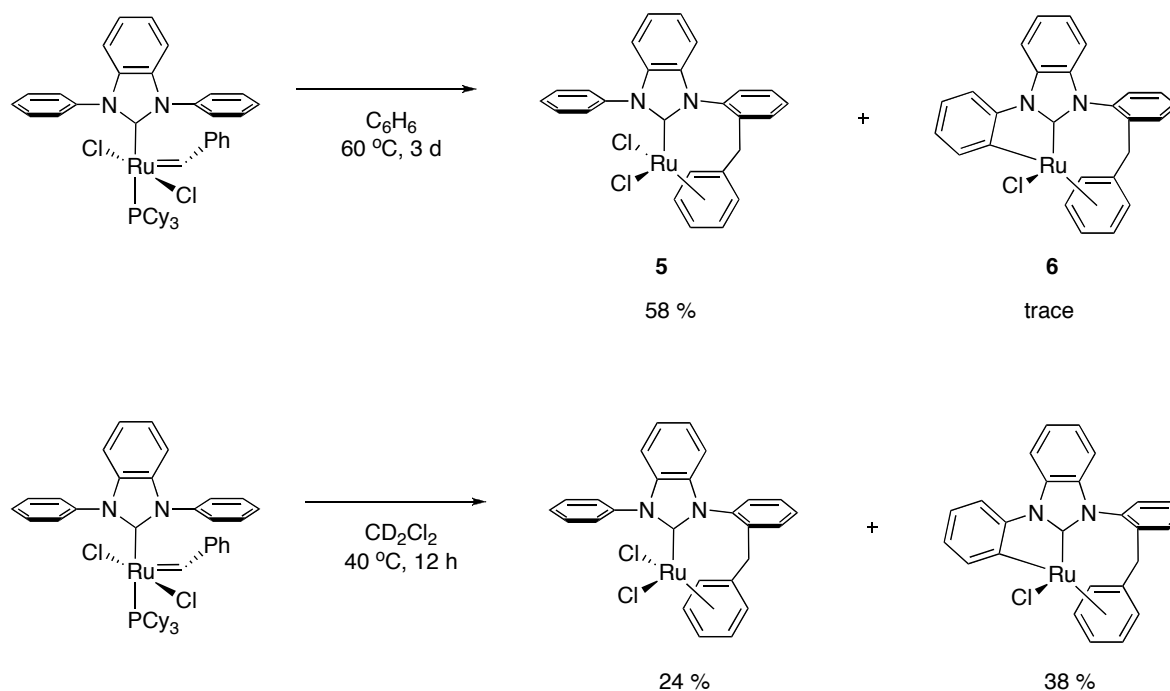
N-heterocyclic carbene (NHC) ligands have been widely used for transition metal catalysts in a role analogous to that of phosphines and other neutral two-electron donors due to their distinctive high σ -basicity and low π -acidity.¹⁻³ However, it has been demonstrated that NHCs occasionally participate in unanticipated side reactions, such as C–C and C–H activation^{4,5} and sometimes enter into abnormal binding modes.^{6,7} Because these reactions can be detrimental to catalyst function, understanding them is of fundamental importance to the design of stable transition-metal catalysts with NHC ligands.⁸ In this chapter, novel double C–H activation of an NHC in an olefin metathesis catalyst is described.

Results and Discussion

NHC-based olefin metathesis catalyst **4** shows high activity in ring-closing metathesis (RCM) reactions to form tetrasubstituted olefins.⁹ Although catalyst **3**, a phosphine analog of **4**, is also active in the RCM reactions,¹⁰ it has been found to decompose much faster having a shorter half-life than both catalysts **1** and **2** (30 min for **3** vs. 8 d for **1** and ~38 d for **2** at 55 °C in 0.023M C₆D₆ solution).^{11,12} Although it is well documented that NHC-based ruthenium olefin metathesis catalysts are generally more stable than bisphosphine-based catalysts,¹³ complex **3** is even much less stable than **1**. This abnormal instability of **3** led us to study the structural feature of the *N,N'*-diphenylbenzimidazol-2-ylidene (BIPh) ligand that lead to the decomposition of **3**.

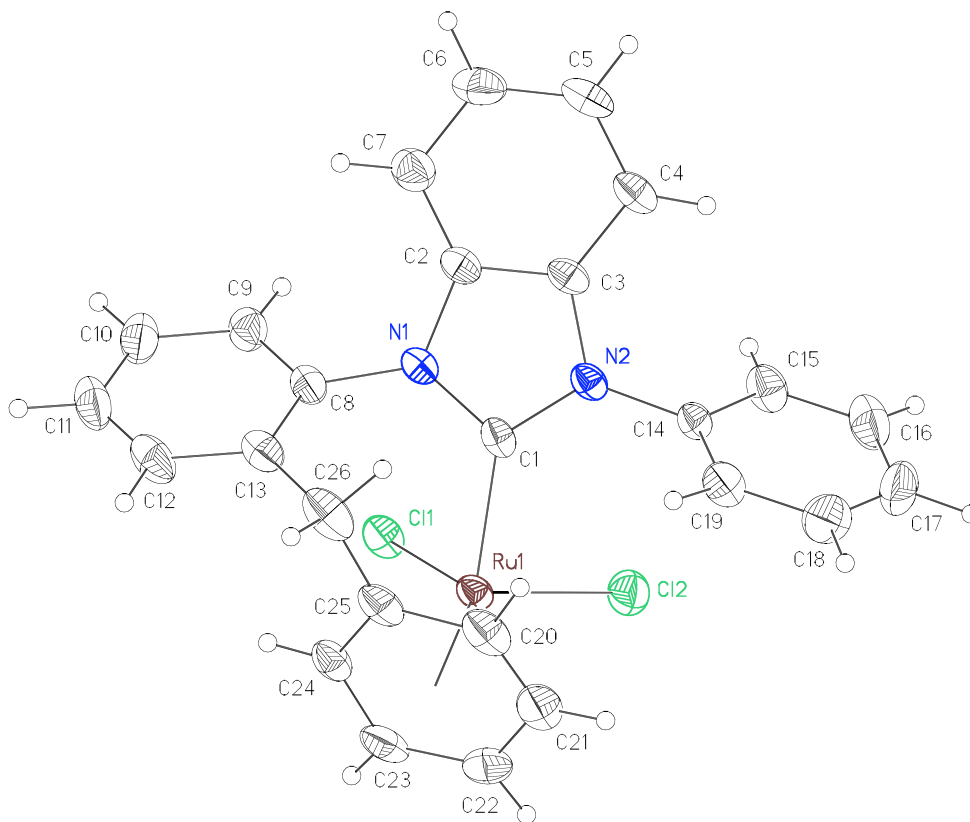


When we investigated the thermal stability of complex **3** in benzene solutions at 60 °C under inert conditions, the decomposition product **5** precipitated with an isolated yield of 58% after 3 days (Scheme 1). Complex **6** was also observed in traces (<2%). Interestingly, complex **6** was the major decomposition product along with **5** after 12 hours in CD₂Cl₂ at 40 °C (Scheme 1).

Scheme 1. Thermal decomposition of complex **3**.

The structures of **5** and **6** were elucidated by X-ray crystallography (Figures 1 and 2, respectively). The X-ray crystal structure of **5** showed that the benzylidene carbon of **3** was inserted into the ortho C–H bond of one of the *N*-phenyl rings of BIPh. Moreover, η^6 -binding of ruthenium to the phenyl group of the benzylidene ligand was observed along with complete loss of the phosphine ligand. The protons of the η^6 -bound phenyl group have characteristic upfield ^1H NMR chemical shifts at 4.5–6.0 ppm. Recently, Diver and co-workers have reported the carbon monoxide promotes benzylidene insertion into the aromatic C–C bond of a mesityl group of the NHC in complex **2**, resulting in formation of a 7-membered ring.¹⁴ Here, the benzylidene is inserted into an ortho C–H bond of a phenyl group with concomitant η^6 -coordination to ruthenium atom without the assistance of any external ligands.

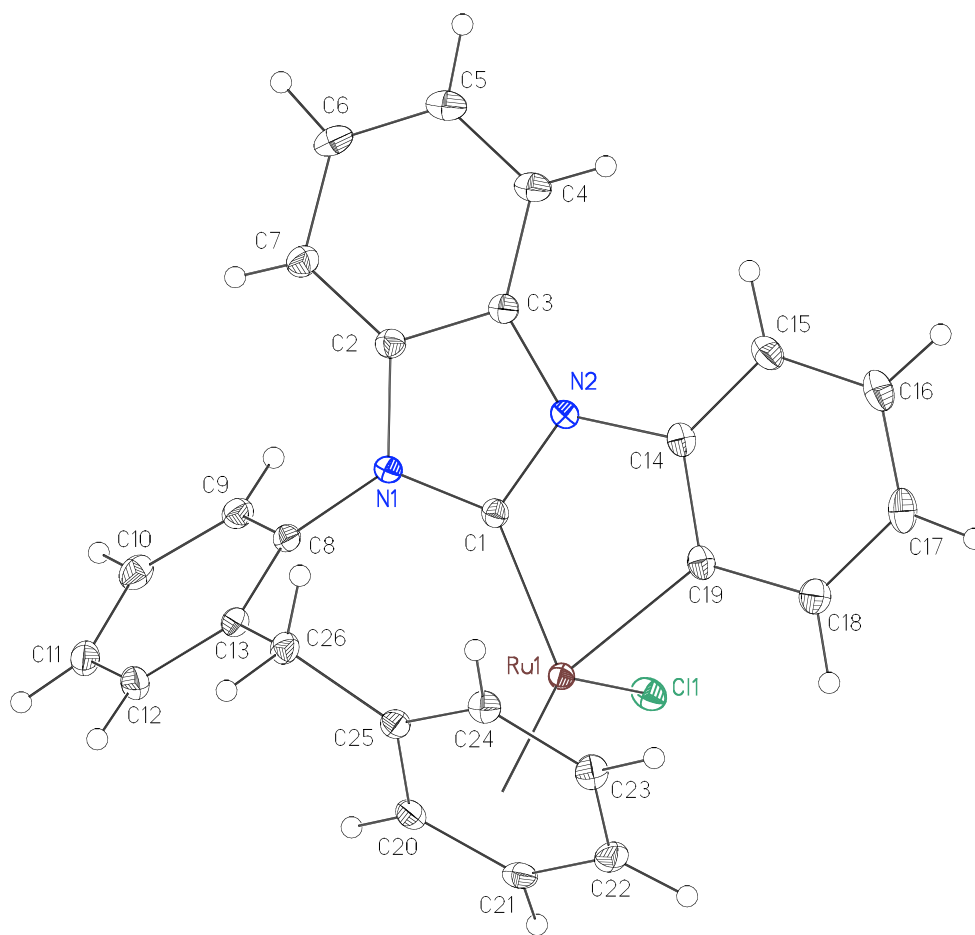
Figure 1. ORTEP drawing of **5**. Atoms are represented by ellipsoids at the 50% probability level. Hydrogen atoms have been omitted for clarity. Selected bond lengths (Å) and angles (deg): Ru–C(1), 2.042(2); Ru–Cl(1), 2.4108(5); Ru–PhCenter, 1.69; C(1)–Ru–PhCenter, 127.8; Cl(1)–Ru(1)–PhCenter, 126.0; C(1)–Ru–Cl(1), 86.55(5); Cl(1)–Ru–Cl(2), 85.280(18).



In complex **6**, ruthenium has inserted into another ortho C–H, of the other phenyl ring of BIPh, to give a new Ru–C bond (2.0693(17) Å) forming a five-membered metallacycle. This type of C–H or C–C activation of the ortho methyl groups of H₂IMes (H₂IMes = 1,3-dimesityl-4,5-dihydroimidazol-2-ylidene) and IMes (IMes = 1,3-dimesitylimidazol-2-ylidene) ligands have been reported in some ruthenium olefin metathesis catalysts^{12,15} and

other ruthenium complexes.^{4,16,17} The planes of phenyl rings of BIPh become approximately perpendicular to allow the formation of the five-membered metallacycle.

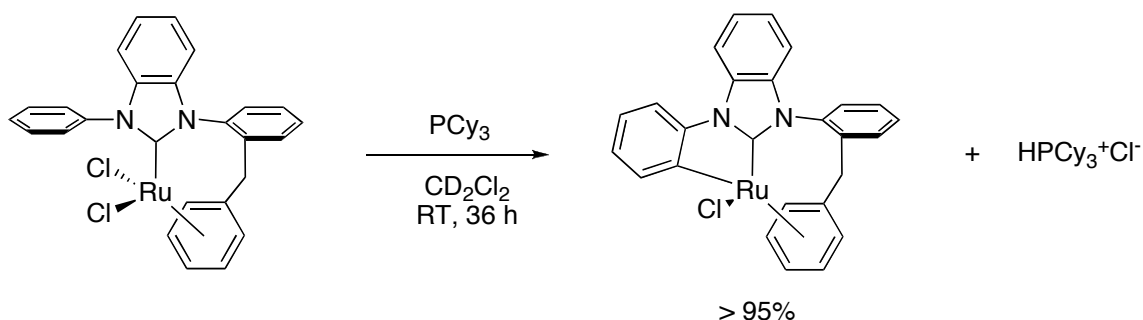
Figure 2. ORTEP drawing of **6**. Atoms are represented by ellipsoids at the 50% probability level. Hydrogen atoms have been omitted for clarity. Selected bond lengths (Å) and angles (deg): Ru–C(1), 2.0142(17); Ru–Cl(1), 2.4212(4); Ru–PhCenter, 1.730; Ru–C(19), 2.0693(17); C(1)–Ru–PhCenter, 129.9; C(19)–Ru–PhCenter, 129.7; Cl(1)–Ru(1)–PhCenter, 126.1; C(1)–Ru–Cl(1), 92.29(5); C(19)–Ru–Cl(1), 86.04(5).



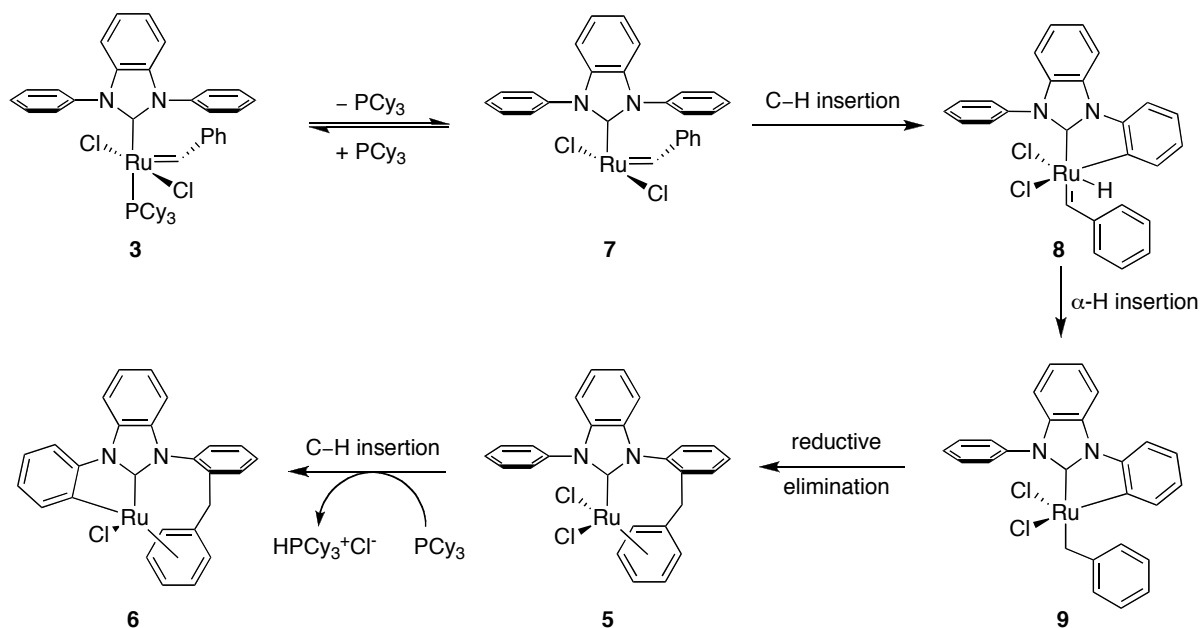
Based on their structural similarity, **5** would appear to be the precursor to **6**. This would explain the increased production of complex **6** in CD₂Cl₂, as **5** is more soluble in CD₂Cl₂ than in C₆D₆. Contrary to this hypothesis, heating a solution of complex **5** in CD₂Cl₂

for over a week at 40 °C did not yield complex **6**, as **5** is thermally stable. However, in presence of 1 equiv. of PCy₃, **5** was transformed into **6** quantitatively at room temperature after 3 days (Scheme 2). PCy₃ likely acts as a base to receive the HCl eliminated from **5** to generate HPCy₃⁺Cl⁻ which is observable by ¹H, ³¹P NMR, and HRMS.

Scheme 2. PCy₃ assisted C–H insertion.



One plausible mechanism for the decomposition of complex **3** is presented in Scheme 3. Following phosphine dissociation, which is the initiation step in ruthenium-catalyzed olefin metathesis,¹⁸ ruthenium hydride complex **8** could be formed by oxidative addition of an ortho C–H bond of a *N*-phenyl group of BIPh to ruthenium. The resulting hydride is inserted into the α -carbon of the benzylidene generating complex **9**. Formation of **5** could be explained by reductive elimination between the ortho carbon of BIPh and the α -carbon from benzyl ligand. Finally, C–H insertion with HCl elimination could generate complex **6** with the assistance of PCy₃. Intermediate complexes **7–9** are only postulated and have not been observed by spectroscopic methods most probably due to their short lifetimes.

Scheme 3. A proposed mechanism.

Conclusion

We have reported the benzylidene insertion into an ortho C–H bond of a phenyl group of an NHC ligand in an olefin metathesis catalyst **3**. Further C–H activation occurred by the assistance of the dissociated phosphine. These observations suggest that phenyl groups instead of mesityl groups of NHC-based ruthenium olefin metathesis catalysts are more vulnerable to decomposition via C–H activation. New ligand design and synthesis of olefin metathesis catalysts are currently in progress to prevent this decomposition pathway while maintaining activity for tetrasubstituted olefin synthesis.

Experimental

General considerations. Manipulation of organometallic compounds was performed using standard Schlenk techniques under an atmosphere of dry argon or in a nitrogen-filled

Vacuum Atmospheres dry box ($O_2 < 2.5$ ppm). NMR spectra were recorded on a Varian Inova (499.85 MHz for 1H ; 202.34 MHz for ^{31}P ; 125.69 MHz for ^{13}C) or on a Varian Mercury 300 (299.817 MHz for 1H ; 121.39 MHz for ^{31}P ; 74.45 MHz for ^{13}C). ^{31}P NMR spectra were referenced using H_3PO_4 ($\delta = 0$ ppm) as an external standard. Elemental analyses were performed at Desert Analytics (Tucson, AZ). Mass spectra were recorded on JEOL JMS 600H spectrophotometer. Benzene, benzene- d_6 , and methylene chloride were dried by passage through solvent purification columns. CD_2Cl_2 was dried by vacuum transfer from CaH_2 . All solvents are degassed by either a generous Ar sparge or three freeze-pump-thaw cycles. $(BIPh)(PCy_3)(Cl)_2Ru=(H)Ph$ (**2**) was prepared according to literature procedure.⁹

Procedure for a typical decomposition measurement. 13.1 mg (0.0161 mmol) of complex **3** and ~ 1.0 mg (0.00561 mmol) of anthracene were weighed into a 1-dram vial. 0.700 mL of benzene- d_6 or CD_2Cl_2 was used to transfer the sample to a screw-cap NMR tube. A screw-cap was used to seal the NMR tube, and this seal was reinforced with parafilm. The sample was placed into the spectrometer and allowed to equilibrate at the probe temperature for 10 minutes. Complex decomposition was following by monitoring the diminution of the benzylidene proton through collection of a time-delayed array of 1H NMR spectra (referred to as a preacquisition delay, PAD, by Varian software). Conversions to complex **5** and **6** were measured by monitoring characteristic 1H peaks of η^6 -bound phenyl group which show up in the region of 4.5–6.0 ppm.

Complex 5. Complex **2** (50.0 mg, 0.0616 mmol) was dissolved in benzene (5.0 mL) in a sealed tube. The reaction mixture was heated to 60 °C. Precipitation of red crystalline

solid was observed after 2 h. After 72 h, the precipitates were filtered, washed with benzene and dried under vacuum to afford complex **5** (19.0 mg, 0.0357 mmol, 58%). ^1H NMR (CD_2Cl_2): δ 7.06–7.64 (m, 13H), 5.88 (dd, $J = 6.0, 5.7$ Hz, 1H), 5.80 (dd, $J = 6.6, 5.4$ Hz), 5.30 (d, $J = 5.4$ Hz, 1H), 4.92 (dd, $J = 6.0, 5.1$ Hz), 4.64 (d, $J = 5.4$ Hz, 1H), 3.93 (d, $J = 14.5, 1\text{H}$), 3.40 (d, $J = 14.5, 1\text{H}$). $^{13}\text{C}\{^1\text{H}\}$ NMR (CD_2Cl_2): δ 189.0, 138.8, 137.8, 137.7, 136.5, 134.3, 131.7, 131.5, 131.1, 129.4, 129.3, 129.2, 129.0, 128.9, 127.3, 124.6, 124.4, 111.7, 111.6, 100.4, 97.7, 93.9, 86.1, 85.7, 81.7, 36.4. HRMS analysis (FAB) m/z : Calcd [M^+] 532.0047, found 532.0048.

Complex 6. Complex **5** (19.0 mg, 0.0357 mmol) and tricyclohexylphosphine (10.0 mg, 0.0357 mmol) were dissolved in CD_2Cl_2 (1.0 mL) in a sealed tube. The reaction was monitored by ^1H NMR spectroscopy. After 72 h, complex **5** was completely converted to complex **6**. Complete isolation of complex **6** from phosphine by-products was not facile due to air sensitivity of the compound. Yellow crystalline solids (3 mg, 0.006 mmol, 17%) are obtained by slow diffusion of benzene into CD_2Cl_2 solution and analyzed by spectroscopic methods. ^1H NMR (CD_2Cl_2): δ 8.24 (dd, $J = 7.5, 1.2$ Hz, 1H), 8.09 (d, $J = 9$ Hz, 1H), 7.77–7.82 (m, 2H), 7.65–7.72 (m, 3H), 7.41–7.47 (m, 2H), 7.33 (td, $J = 7.5$ Hz, 1.2 Hz, 1H), 7.05 (td, $J = 7.5, 1.2$ Hz, 1H), 5.98 (td, $J = 5.4, 1.2$ Hz, 1H), 5.90 (tt, $J = 5.4, 0.9$ Hz, 1H), 5.85 (td, $J = 6.0, 1.5$ Hz, 1H), 5.21 (d, $J = 6.3$ Hz, 1H), 4.13 (d, $J = 15$ Hz, 1H), 3.89 (d, $J = 5.7$ Hz, 1H), 3.35 (d, $J = 15$ Hz, 1H). $^{13}\text{C}\{^1\text{H}\}$ NMR (CD_2Cl_2): δ 202.3, 164.0, 147.3, 142.1, 137.0, 136.9, 134.1, 133.1, 131.9, 129.3, 129.1, 128.5, 124.5, 124.4, 123.4, 123.1, 113.5, 112.1, 111.7, 107.8, 102.6, 100.6, 86.6, 83.7, 69.0, 38.0. HRMS analysis (FAB) m/z : Calcd [M^+] 496.0280, found 496.0260.

Table 2. Summary of crystallographic data for **5** and **6**.

	5	6
formula	C ₂₆ H ₂₀ Cl ₂ N ₂ Ru • 2(CH ₂ Cl ₂)	C ₂₆ H ₁₉ ClN ₂ Ru • CH ₂ Cl ₂
<i>M_r</i>	702.26	580.88
crystal color	red/orange	yellow
crystal size (mm)	0.38 x 0.28 x 0.15	0.30 x 0.26 x 0.07
crystal system	monoclinic	monoclinic
space group	P2 ₁ /c	P2 ₁ /n
<i>a</i> (Å)	9.5097(3)	13.8444(5)
<i>b</i> (Å)	12.7335(4)	13.1657(5)
<i>c</i> (Å)	24.0073(8)	14.0413(5)
α (deg)	90	90
β (deg)	99.6940(10)	117.6790(10)
γ (deg)	90	90
<i>V</i> (Å ³)	2865.58(16)	2266.45(14)
<i>Z</i>	4	4
<i>D</i> _{calcd} (g cm ⁻³)	1.628	1.702
<i>T</i> (K)	200(2)	100(2)
λ (Å)	0.71073	0.71073
μ (mm ⁻¹)	1.128	1.065
<i>R</i> ₁ ^a (all data)	0.0895	0.0862
<i>wR</i> ₂ ^b (all data)	0.0798	0.0803
GOF	1.415	1.026

$$^a R_1 = \sum ||F_o| - |F_c|| / \sum |F_o|. \quad ^b wR_2 = [\sum w(F_o^2 - F_c^2)^2 / \sum w(F_o^2)^2]^{1/2}$$

References and Notes

- (1) Bourissou, D.; Guerret, O.; Gabbai, F. P.; Bertrand, G. *Chem. Rev.* **2000**, *100*, 39–91.
- (2) Crudden, C. M.; Allen, D. P. *Coord. Chem. Rev.* **2004**, *248*, 2247–2273.
- (3) Scott, N. M.; Nolan, S. P. *Eur. J. Inorg. Chem.* **2005**, 1815–1828.
- (4) Jazzar, R. F. R.; Macgregor, S. A.; Mahon, M. F.; Richards, S. P.; Whittlesey, M. K. *J. Am. Chem. Soc.* **2002**, *124*, 4944–4945.
- (5) Dorta, R.; Stevens, E. D.; Nolan, S. P. *J. Am. Chem. Soc.* **2004**, *126*, 5054–5055.
- (6) Grundemann, S.; Kovacevic, A.; Albrecht, M.; Faller, J. W.; Crabtree, R. H. *J. Am. Chem. Soc.* **2002**, *124*, 10473–10481.
- (7) Lebel, H.; Janes, M. K.; Charette, A. B.; Nolan, S. P. *J. Am. Chem. Soc.* **2004**, *126*, 5046–5047.
- (8) Waltman, A. W.; Ritter, T.; Grubbs, R. H. *Organometallics* **2006**, *25*, 4238–4239.
- (9) Berlin, J. M.; Campbell, K.; Ritter, T.; Funk, T. W.; Chlenov, A.; Grubbs, R. H. *Org. Lett.* **2007**, *9*, 1339–1342.
- (10) The conversion of the RCM of diethyl dimethallylmalonate for catalyst **3** is 76% at room temperature after 24 h (vs. >95% for catalyst **3** at 40 °C, 24 h).
- (11) Hong, S. H.; Day, M. W.; Grubbs, R. H. *J. Am. Chem. Soc.* **2004**, *126*, 7414–7415.
- (12) Hong, S. H.; Wenzel, A. G.; Salguero, T. T.; Day, M. W.; Grubbs, R. H. *J. Am. Chem. Soc.* **2007**, *129*, *in press*.
- (13) Ulman, M.; Grubbs, R. H. *J. Org. Chem.* **1999**, *64*, 7202–7207.
- (14) Galan, B. R.; Gembicky, M.; Dominiak, P. M.; Keister, J. B.; Diver, S. T. *J. Am. Chem. Soc.* **2005**, *127*, 15702–15703.

- (15) Trnka, T. M.; Morgan, J. P.; Sanford, M. S.; Wilhelm, T. E.; Scholl, M.; Choi, T. L.; Ding, S.; Day, M. W.; Grubbs, R. H. *J. Am. Chem. Soc.* **2003**, *125*, 2546–2558.
- (16) Giunta, D.; Hölscher, M.; Lehmann, C. W.; Mynott, R.; Wirtz, C.; Leitner, W. *Adv. Synth. Catal.* **2003**, *345*, 1139–1145.
- (17) Abdur-Rashid, K.; Fedorkiw, T.; Lough, A. J.; Morris, R. H. *Organometallics* **2004**, *23*, 86–94.
- (18) Sanford, M. S.; Love, J. A.; Grubbs, R. H. *J. Am. Chem. Soc.* **2001**, *123*, 6543–6554.

Chapter 5

Prevention of Undesirable Olefin Isomerization during Olefin Metathesis[†]

Abstract

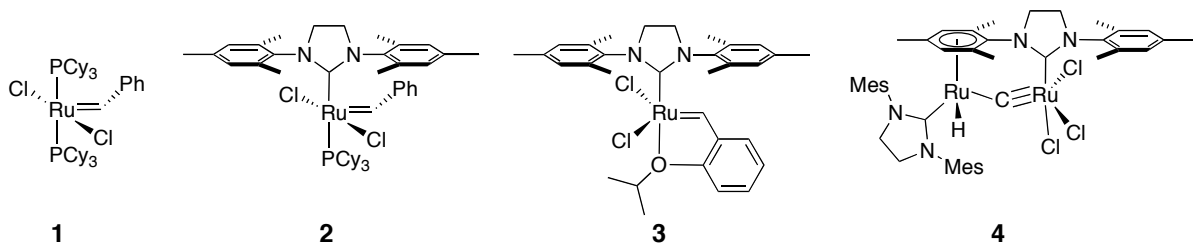
1,4-Benzoquinones have been found to prevent olefin isomerization of a number of allylic ethers and long-chain aliphatic alkenes during ruthenium-catalyzed olefin metathesis reactions. Electron-deficient benzoquinones are the most effective additives for the prevention of olefin migration. This mild, inexpensive, and effective method to block olefin isomerization increases the synthetic utility of olefin metathesis via improvement of overall product yield and purity.

Introduction

Olefin isomerization/migration is one of the side reactions in olefin metathesis that can significantly alter the product distribution and decrease the yield of the desired product, especially with ill-defined catalyst systems.¹ Additionally, the side products resulting from unwanted isomerization are frequently difficult to remove via standard purification techniques. Well-defined ruthenium-based olefin metathesis catalysts such as **1–3** are generally highly selective for olefin metathesis. However, there have been some reports of

[†] The majority of this chapter has been published: (a) Hong, S. H.; Sanders, D. P.; Lee, C. W.; Grubbs, R. H. *J. Am. Chem. Soc.* **2005**, *127*, 17160–17161. (b) Lee, C. W.; Hong, S. H.; Sanders, D. P.; Grubbs, R. H.; Pederson, R. L. *U.S. Patent* No 2005/0203324A1. September 15, 2005.

olefin isomerization as well when the catalysts are stressed by high temperatures, high dilution and forced high turnovers.²⁻⁵



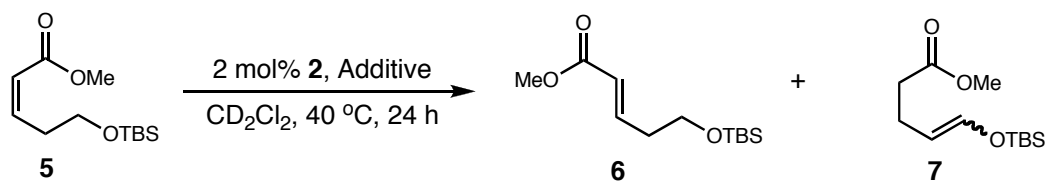
While the exact mechanism(s) responsible for this isomerization are unknown (metal-based hydride, π -allyl, or other pathways),⁶⁻⁹ recent results indicate that ruthenium hydride species such as **4** formed from the decomposition of the ruthenium metathesis catalysts can catalyze the migration of olefins under metathesis condition.¹⁰ This information has prompted us to develop a way to suppress the unwanted olefin isomerization reactions catalyzed by these metal hydrides.

Results and Discussion

Self-metathesis and isomerization of (*Z*)-5-*t*-butyldimethylsilyloxy-2-pentenoate **5** to the *E*-isomer **6** and silyl enol ether **7** served as an excellent system for initially studying the effects of additives on isomerization process.¹¹ Compounds **5**, **6**, and **7** all have clearly distinguishable ¹H NMR resonances. Through examination of the resultant *E/Z* ratio of the α , β -unsaturated carbonyl compounds (**6:5**), the effect of additives on olefin metathesis activity can be readily separated from their effect on isomerization. Upon screening additives, we found that moderate pK_a acids such as acetic acid or quinone type compounds such as 1,4-benzoquinone work well in preventing olefin migration during olefin metathesis reactions

(Table 1). Tricyclohexylphosphine oxide is an additive that has been reported to prevent isomerization of a specific substrate in a RCM reaction,⁷ however, it did not prevent the isomerization of **5** or the other substrates we tested. Acetic acid and 1,4-benzoquinone did not reduce the catalyst activity. Most metathesis reactions we tested were completed within an hour in presence of effective additives (Table 1, 2, and 3, and Scheme 2).¹² However, we elongated the reaction time to 24 h to stress the catalysts to optimize isomerization.

Table 1. Self-metathesis reaction of (*Z*)-5-*t*-butyldimethylsilyloxy-2-pentenoate



Additives	Equiv. (rel. to 5)	Product Distribution ^a	
		6+5	7^b
None	None	19% ^c	81%
2,2,2-Trifluoroethanol	1	11% ^c	89%
Hexafluoro- <i>t</i> -butyl alcohol	1	19% ^c	81%
Phenol	1	17% ^c	83%
Acetic Acid	0.1	>95% ^c	None
Tricyclohexylphosphine oxide	0.1	22% ^c	78%
Maleic anhydride	1	>95% ^d	None
1,4-Benzoquinone	0.1	>95% ^c	None

^a Determined by ¹H NMR. ^b *E/Z* ~1:1. ^c *E/Z* ~20:1. ^d *E/Z* ~1:10.

For the RCM of diallyl ether **8**, the metathesis product, 2,5-dihydrofuran **9**, was observed as the major product after 1 h. After extended reaction times, it is isomerized to 2,3-dihydrofuran **10**. This also suggests that decomposition products from the catalyst are responsible for the isomerization. Both acetic acid and 1,4-benzoquinone are also effective to prevent the isomerization of **9** to **10** (Table 2). Radical scavengers such as BHT, TEMPO, phenol and 4-methoxyphenol were, in general, not effective in preventing isomerization (Table 1 and 2). Galvinoxyl is somewhat effective to prevent the isomerization presumably due to the structural similarity with 1,4-benzoquinone (Table 2).

Table 2. Ring-closing metathesis of diallyl ether

Reaction scheme: Diallyl ether (**8**) reacts with 5 mol% of catalyst **2** and an additive in CD_2Cl_2 at $40\text{ }^\circ\text{C}$ for 24 h to yield 2,5-dihydrofuran (**9**) and 2,3-dihydrofuran (**10**).

Additive	Equiv. (rel. to 8)	Product Distribution ^a	
		9	10
None	None	< 5% ^b	>95% ^c
CH_3COOH	0.1	>95%	None
1,4-Benzoquinone	0.1	>95%	None
Galvinoxyl	0.2	80%	20%
TEMPO	0.5	7%	93%
4-Methoxyphenol	0.5	17%	83%
BHT	0.5	4%	93%

^aDetermined by ^1H NMR. ^b~80%, 1 h. ^c~20%, 1 h.

However, when applied to the metathetical isomerization of **11**, 1,4-benzoquinone is more effective in suppressing the undesirable isomerization than acetic acid (Table 3).

Table 3. Self-metathesis reaction of (Z)-1,4-bis(*t*-butyldimethylsilyloxy)-2-butene

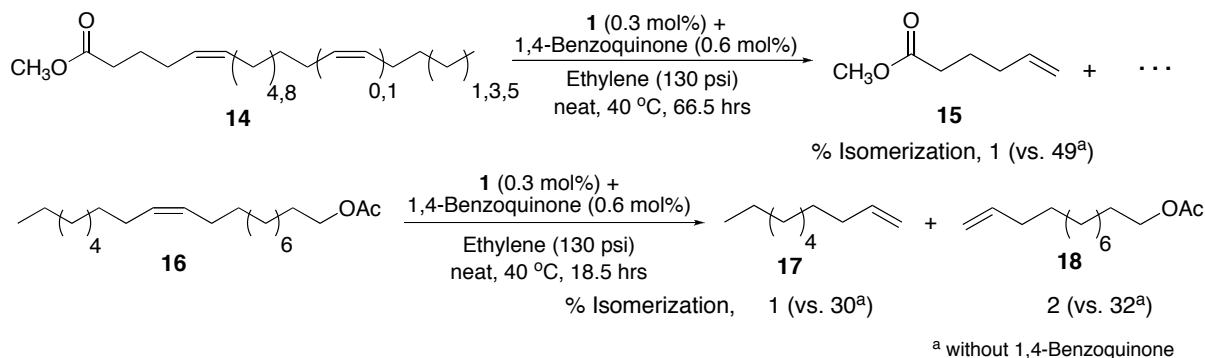


Additive	Product Distribution ^a	
	12	13^b
None	None	>95%
Acetic Acid	None	>95%
1,4-Benzoquinone	92% ^c	None

^a Determined by ¹H NMR. ^b *E/Z* ~1:1.4. ^c 8% of **11** remains due to thermodynamic equilibrium.

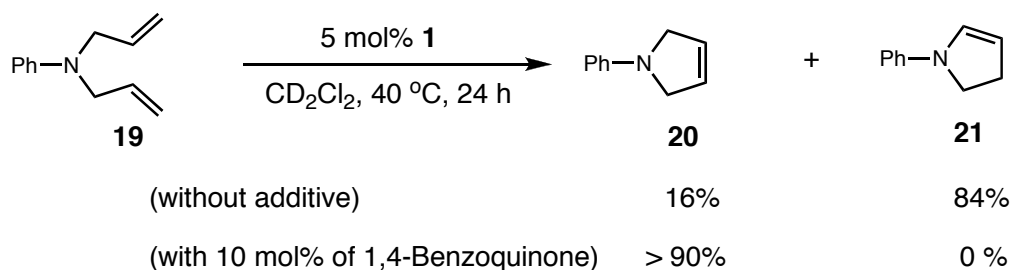
Ethenolysis, cross-metathesis of an olefinic compound with ethene, of seed oils and their fatty acid esters allows the synthesis of α -olefins which have a broad range of applications.^{13,14} However, the occurrence of olefin isomerization during this process has limited its industrial application.¹⁴ Again, 1,4-benzoquinone proved superior in suppressing olefin isomerization to other tested additives (Scheme 1), and it could be readily separated from the desired products by standard techniques.¹⁵ Further investigations on industrial applications using this mild and inexpensive additive are in progress.

Scheme 1. Ethenolysis of meadow foam oil methyl ester **14** and 11-eicosenyl acetate **16**.



It has been reported that some allylic amines such as *N,N*-diallylaniline **19** are isomerized to enamines with catalyst **1** in toluene at 110 °C.¹⁶⁻¹⁸ In RCM of **19** under normal metathesis condition, only metathesis product **20** was observed within 30 min, however, **20** was isomerized to **21** after extended reaction times. 1,4-Benzoquinone effectively prevented this isomerization and only gave the metathesis product **20** (Scheme 2). However, 1,4-benzoquinone did not prevent the isomerization of *N,N*-dibenzylallylamine and *N,N*-dimethylallylamine to enamines. *N,N*-Dialkylallylamines prevent metathesis while less basic aryl amines are active metathesis substrates.¹⁹

Scheme 2. RCM of *N,N*-diallylaniline.



To determine the optimal benzoquinone structure for prevention of olefin isomerization, several benzoquinone derivatives were screened in larger scale RCM reactions of **8** (Table 4). Electron-deficient benzoquinones are more effective in preventing isomerization (entries 7, 8, 9, and 12) than the parent 1,4-benzoquinone. Conversely, electron-rich benzoquinones are less effective (entries 2, 3, and 6) and sterically hindered benzoquinones cannot prevent isomerization to any significant extent (entries 4 and 5). Benzoquinones were also effective in preventing isomerization in reactions with the phosphine-free catalyst **3** (entries 10, 11, and 12).

To understand the role of benzoquinone in preventing isomerization, we studied the isomerization of allyl benzene catalyzed by complex **4** with and without 1,4-benzoquinone.¹⁰ As expected, allyl benzene was not isomerized with 2 mol% of **4** in presence of 10 mol% of 1,4-benzoquinone. It has been reported that quinones are reduced to the corresponding hydroquinones upon reacting with ruthenium hydrides.^{20,21} Indeed, the formation of 1,4-hydroquinone was observed by ¹H NMR in this reaction (~10%, relative to 1,4-benzoquinone). Moreover, neither the complex **4** nor any other ruthenium hydrides were observed from decomposition of (H₂IMes)(PCy₃)(Cl)₂Ru=CH₂ in benzene in the presence of 2 equiv. 1,4-benzoquinone. These results indicate that benzoquinone may prevent the formation of metal hydrides from catalyst decomposition or react rapidly with hydrides generated by decomposition. Further mechanistic investigations are necessary to fully understand the role of 1,4-benzoquinones (redox reactions,^{20,21} charge transfer complexes,²² etc.) in preventing olefin migration and to elucidate methods to prevent olefin isomerization in substrates such as allylic alcohols and some allylic amines for which 1,4-benzoquinones are not effective.

Table 4. Effect of benzoquinone structure on prevention of olefin isomerization

Entry	Additives	Catalyst	Product Distribution ^a	
			9	10
1	1,4-Benzoquinone	2	87%	13%
2	2-Methylbenzoquinone	2	62%	38%
3	2,6-Dimethyl-1,4-benzoquinone	2	16%	84%
4	2,6-Di- <i>t</i> -butyl-1,4-benzoquinone	2	<5%	>95%
5	2,5-Di- <i>t</i> -butyl-1,4-benzoquinone	2	<5%	>95%
6	2,6-Dimethoxy-1,4-benzoquinone	2	22%	78%
7	2-Chloro-1,4-benzoquinone	2	91%	9%
8	2,6-Dichloro-1,4-benzoquinone	2	>99%	None
9	Tetrafluoro-1,4-benzoquinone	2	>99%	None
10	None	3	<5%	>95%
11	1,4-Benzoquinone	3	91%	9%
12	2,6-Dichlorobenzoquinone	3	>99%	None

^aDetermined by ¹H NMR.

Conclusion

1,4-benzoquinones have been found to prevent olefin isomerization of a number of allylic ethers and long-chain aliphatic alkenes during olefin metathesis reaction with ruthenium catalysts. Electron-deficient benzoquinones are the most effective additives for the prevention of olefin migration. This mild, inexpensive, and effective method to block olefin

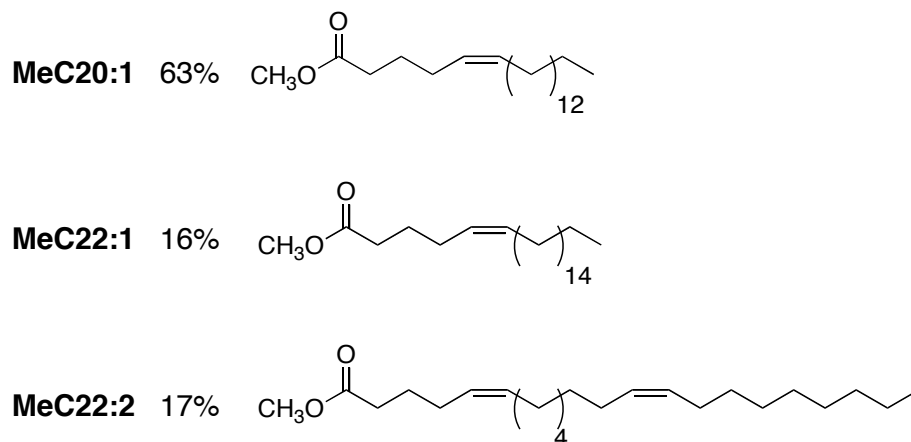
isomerization increases the synthetic utility of olefin metathesis by improving product yield and purity.

Experimental

General considerations. Manipulation of organometallic compounds was performed using standard Schlenk techniques under an atmosphere of dry argon or in a nitrogen-filled Vacuum Atmospheres dry box ($O_2 < 2.5$ ppm). NMR spectra were recorded on a Varian Mercury 300 (299.817 MHz for 1H). GC analysis were performed on Rtx-5 column (Restek, 5% diphenyl – 95% dimethyl polysiloxane) with HP 6890 GC. CD_2Cl_2 was dried by distillation from CaH_2 and degassed by three freeze-pump-thaw cycles. The catalysts **1**, **2**, and **3** were obtained from Materia and further purified by column chromatography using silica gel obtained from TSI. 1,4-Benzoquinones, allyl ether and other additives were obtained from Aldrich and used as received. *N,N*-diallylaniline **19** was purchased from Pfaltz & Bauer and used as received. The complex **4**,¹⁰ (*Z*)-5-*tert*-butyldimethylsilyloxy-2-pentenoate **5**,²³ (*Z*)-1,4-Bis(*tert*-butyldimethylsilyloxy)-2-butene **11**,²⁴ 11-eicosenyl acetate **16**² were prepared according to literature procedures. Meadowfoam oil methyl esters were produced by transesterification of Meadowfoam oil purchased from Natural Plant Products LLC, Oregon, USA.

General experimental procedure for Table 1, 2, and 3, and Scheme 2. Catalyst **2** (2 mol% or 5 mol%) and additive (0.1 – 1.0 equiv. of substrate) were dissolved in CD_2Cl_2 (0.7 mL) in a 5 mL vial in a nitrogen-filled Vacuum Atmospheres dry box. Substrate (0.16 mmol) was added to the solution, and the reaction mixture was transferred to an NMR tube fitted with a screw cap. The NMR tube was taken out of the drybox, and heated to 40 °C in

an oil bath. The reaction was monitored by ^1H NMR. The conversion was measured by ^1H NMR using 20 mol% of anthracene as an internal standard.²⁵



Meadow Foam Oil Methyl Esters

(E)-5-tert-butyltrimethylsilyloxy-2-pentenoate (6).²³ ^1H NMR (CD_2Cl_2): δ 6.96 (td, 1H, $J=7.2, 15.6$ Hz), 5.88 (td, 1H, $J=1.5, 15.6$ Hz), 3.74 (t, 2H, $J=6.5$ Hz), 3.70 (s, 3H), 2.41 (td, 2H, $J=6.5, 7.2$ Hz), 0.90 (s, 9H), 0.06 (s, 6H).

(Z) and (E) mixture of 5-tert-butyltrimethylsilyloxy-4-pentenoate (E/Z ~ 1:1) (7).²⁶ ^1H NMR (CD_2Cl_2): δ 6.30 (td, 1H, $J=1.5, 12.3$ Hz, *E*), 6.22 (dd, 1H, $J=2.4, 6.0$ Hz, *Z*), 4.95 (td, 1H, $J=7.4, 12.0$ Hz, *E*), 4.47 (dt, 1H, $J=6.0, 7.0$ Hz, *Z*), 2.40~2.15 (m, 8H, *E* and *Z*), 3.65 (s, 6H, *E* & *Z*), 0.94 (s, 9H, *Z*), 0.92 (s, 9H, *E*), 0.15 (s, 6H, *Z*), 0.13 (s, 6H, *E*).

2,5 Dihydrofuran (9). ^1H NMR (CD_2Cl_2): δ 5.91 (t, 2H, $J=0.9\text{Hz}$), 4.60 (d, 4H, $J=0.9\text{Hz}$).

2,3-Dihydrofuran (10). $^1\text{H NMR}$ (CD_2Cl_2): δ 6.32 (m, 1H), 4.95(m, 1H), 4.28 (t, 2H, $J=9.6\text{Hz}$), 2.59 (m, 2H).

(E)-1,4-Bis(tert-butyldimethylsilyloxy)-2-butene (12).²⁴ $^1\text{H NMR}$ (CD_2Cl_2): δ 5.77 (t, 2H, $J=3.0\text{Hz}$), 4.18 (d, 4H, $J=3.0\text{Hz}$), 0.92 (s, 9H), 0.08 (s, 6H).

(Z) and (E) mixture of 1,4-Bis(tert-butyldimethylsilyloxy)-1-butene (E/Z ~ 1:1.4) (13).²⁷ $^1\text{H NMR}$ (CD_2Cl_2): δ 6.29 (td, 1H, $J=1.2, 12.1$ Hz, *E*), 6.22 (td, 1H, $J=1.5, 5.7$ Hz, *Z*), 4.95 (td, 1H, $J=7.2, 12.1$ Hz, *E*), 4.49 (dt, 1H, $J=5.7, 7.2$ Hz, *Z*), 3.60 (t, 2H, $J=6.9$ Hz, *Z*), 3.57 (t, 2H, $J=6.6$ Hz, *E*), 2.30 (td, 2H, $J=6.9, 7.2$ Hz, *Z*), 2.09 (td, 2H, $J=6.6, 7.2$ Hz, *E*), 0.94 (s, 9H, *Z*), 0.91 (s, 9H, *E*), 0.15 (s, 6H, *E*), 0.07 (s, 6H, *Z*).

N-Phenyl-3-pyrroline (20).²⁸ $^1\text{H NMR}$ (CD_2Cl_2): δ 7.24 (m, 2H), 6.67 (m, 1H), 6.54 (m, 2H), 5.99 (s, 2H), 4.12 (s, 4H).

N-Phenyl-2-pyrroline (21).²⁹ $^1\text{H NMR}$ (CD_2Cl_2): δ 7.47, 7.30, and 6.56 (m, 5H aromatic), 7.13 (m, 1H), 6.35 (m, 1H), 3.30 (m, 2H), 2.02 (m, 2H).

Ethenolysis of Meadowfoam oil methyl ester 14.^{30,31} Meadowfoam oil methyl ester **14** was degassed with anhydrous argon for 10 minutes. 10 g (31.3 mmol) of **14** was added to two Fisher-Porter bottles. To one bottle was added 1,4-benzoquinone (20 mg, 0.19 mmol) followed by ruthenium catalyst **1** (77 mg, 0.094 mmol) at room temperature. To the other bottle was added only catalyst **1** (77 mg), as the control reaction. Both bottles were pressurized with ethylene (130 psi), and stirred for 66.5 h at 40 °C. The reaction mixture was

collected during the reaction, and then quenched with an excess amount of 1 M THMP solution (trihydroxymethyl phosphine in IPA), stirred at ~ 50 °C for 1 h and then analyzed by GC and GC-MS. GC and GC/MS results: t_R 1.67 min (Methyl 5-hexenoate **15**, $M^+=128$), t_R 1.73 and 1.77 min (isomerized products of **15**, $M^+=128$), t_R 2.04 min (cyclooctene, $M^+=110$), t_R 2.09 min (1-Decene, $M^+=140$), t_R 8.88 min (1-Hexadecene, $M^+=224$), t_R 16.39 min (Methyl 5-Eicosenoate, $M^+=324$), t_R 18.34 min (Methyl 5,13-Docosadienoate, $M^+=350$), t_R 18.65 min (Methyl 5-Docosenoate, $M^+=352$).

Table 5. Ethnolysis of meadowfoam oil methyl ester (reported as percent GC Area)

Time (hr)	Reaction	Methyl 5-Eicosenoate	1-Decene	Methyl 5- hexenoate 15	%Isomerized 15
0	Benzoquinone	63	0	0	0
	Control	63	0	0	0
1	Benzoquinone	31	7	10	0
	Control	39	6	8	0
3	Benzoquinone	30	8	11	0
	Control	33	7	9	1
21.3	Benzoquinone	28	7	11	1
	Control	31	7	9	3
66.5	Benzoquinone	29	7	10	1
	Control	31	4	5	49

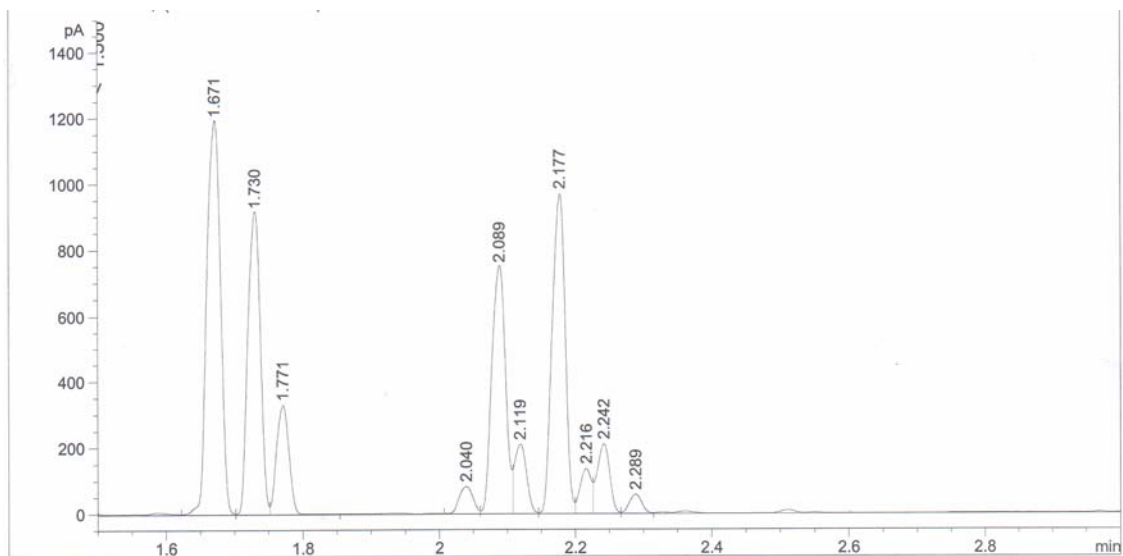


Figure 1. GC traces of ethenolysis of meadowfoam oil methyl ester **14** without 1,4-benzoquinone (control).

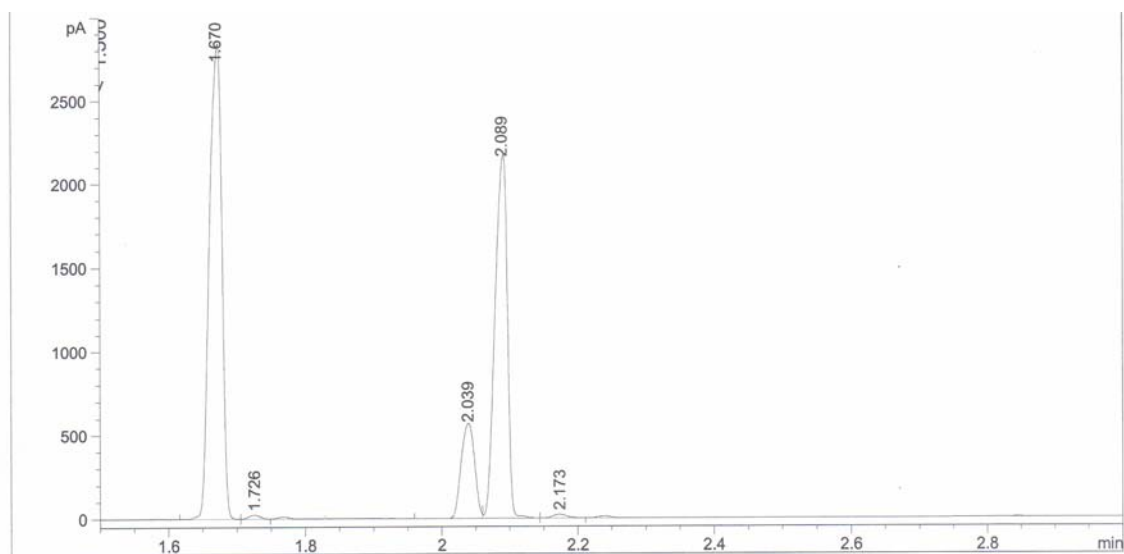


Figure 2. GC traces of ethenolysis of meadowfoam oil methyl ester **14** With 1,4-benzoquinone.

Ethenolysis of 11-eicosenyl acetate 16. 11-Eicosenyl acetate **16** was degassed with anhydrous argon for 10 minutes. 8 g (23.7 mmol) of **16** was added to two Fisher-Porter bottles. To one bottle was added 1,4-benzoquinone (15 mg, 0.14 mmol) followed by ruthenium catalyst **1** (59 mg, 0.071 mmol) at room temperature. To the other bottle was added only catalyst **1** (59 mg), as the control reaction. Both bottles were pressurized with ethylene (130 psi) and stirred for 41.5 h at 40 °C or room temperature. During the reaction, samples were collected and analyzed. The reactions were quenched with an excess amount of 1 M THMP solution (trihydroxymethyl phosphine in IPA) at ~50 °C for 1 h, then analyzed by GC and GC-MS. GC and GC/MS results: t_R 2.10 min (1-decene **17**, $M^+=140$), t_R 2.19 and 2.25 min (isomerized products of **17**, $M^+=140$), t_R 9.05 min (11-dodecenyl acetate **18**, $M^+=226$), t_R 9.18 and 9.30 min (isomerized products of **18**, $M^+=226$), t_R 10.96 and t_R 11.03 min (9-octadecene, $M^+=252$), t_R 17.27 min (11-eicosenyl acetate, $M^+=338$), t_R 30.36 and t_R 31.33 min (11-docosenyl 1,22-diacetate, $M^+=424$).

Table 6. Ethenolysis of 11-eicosenyl acetate **16** (reported as percentage GC area)

Time (min)	Reaction	11-Eicosenyl acetate	1-Decene 17	11-Dodecenyl acetate, 18	9-Octadecene	11-Docosenyl 1,22-Diacetate	%Isomerized 17 , %Isomerized 18
0	Benzoquinone	98	0	0	0	0	0, 0
	Control	98	0	0	0	0	0, 0
100	Benzoquinone	42	23	32	1	2	0, 0
	Control	27	28	39	2	3	1, 1
1110	Benzoquinone	41	22	32	2	2	0, 1
	Control	23	22	32	3	4	22, 23
2490	Benzoquinone	41	22	32	2	2	1, 2
	Control	23	20	28	3	4	30, 32

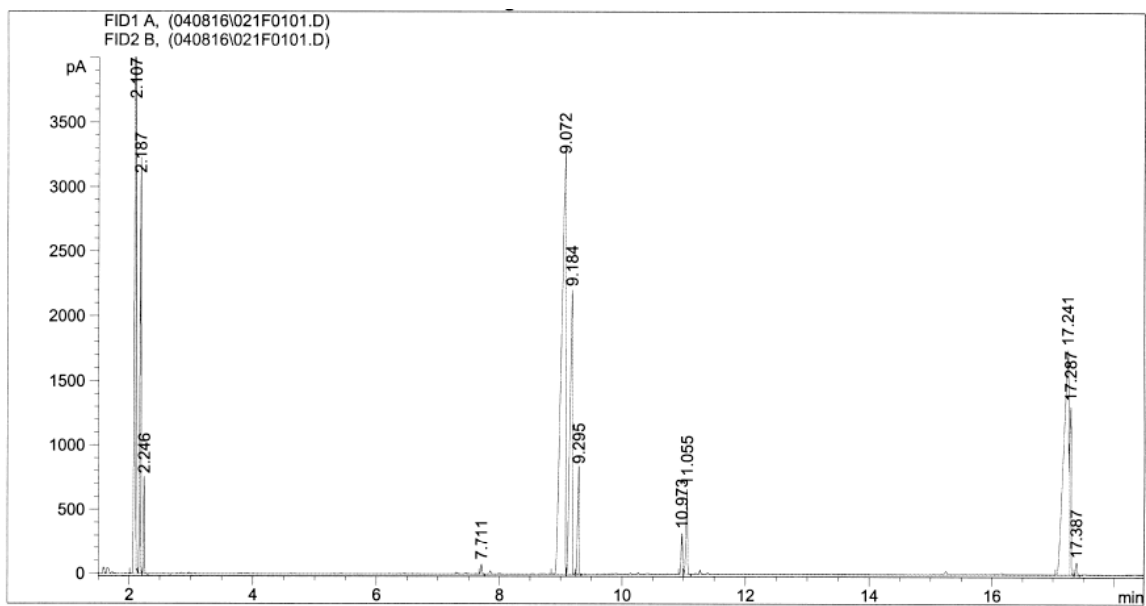
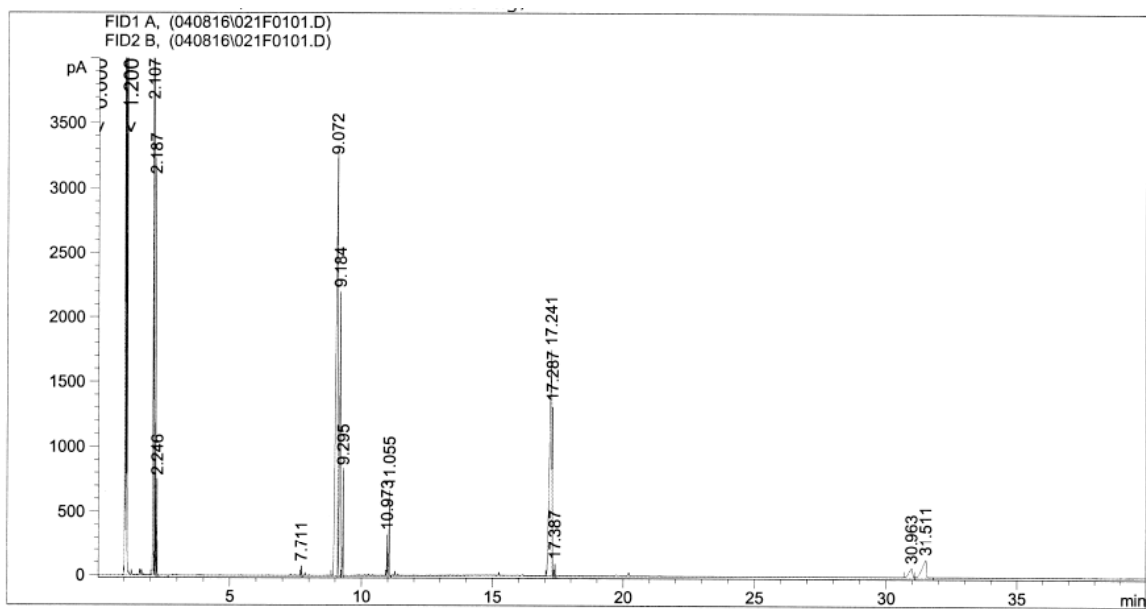


Figure 3. GC traces of ethenolysis of 11-eicosenyl acetate **16** without 1,4-benzoquinone (control).

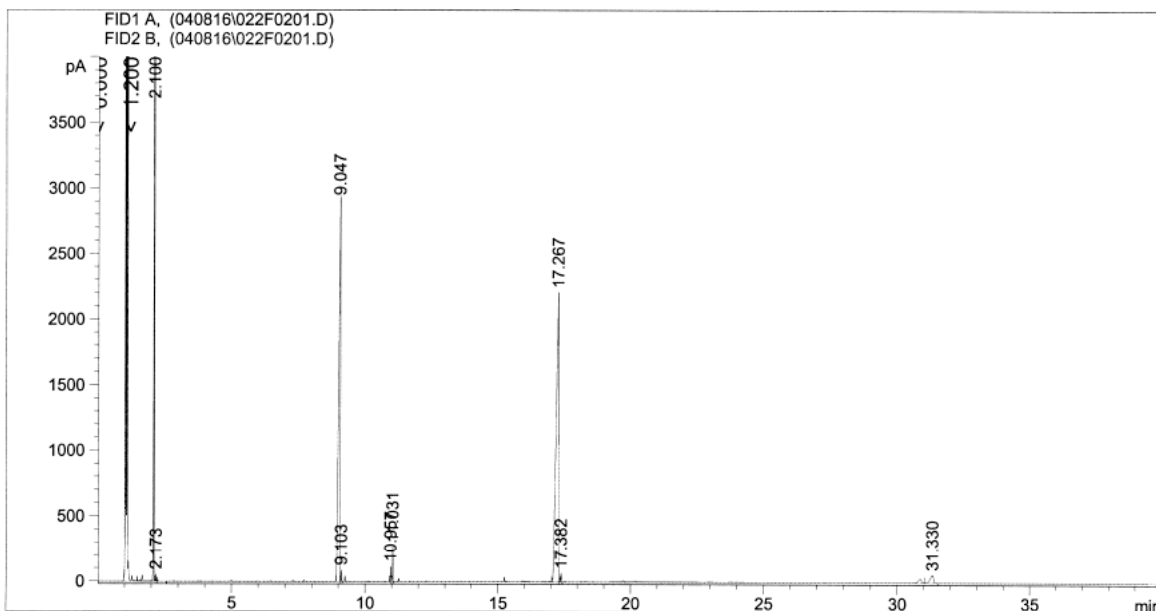


Figure 4. GC traces of ethnolysis of 11-eicosenyl acetate **16** with 1,4-benzoquinone.

Effect of benzoquinone structure on prevention of olefin isomerization. Catalyst **2** (69 mg, 5 mol%) and additive (10 mol%) were dissolved in CD_2Cl_2 (4 mL) in a 50 mL schlenk tube in a nitrogen-filled Vacuum Atmospheres dry box. The flask was removed from the drybox. Diallyl ether **8** (0.2 mL, 1.6 mmol) was added to the solution, and the reaction mixture was heated to 40 °C in an oil bath. After 24 h, conversions were determined by ^1H NMR.

References and Notes

- (1) Ivin, K. J.; Mol, J. C. *Olefin Metathesis and Metathesis Polymerization*; Academic Press: San Diego, CA, 1997.
- (2) Pederson, R. L.; Fellows, I. M.; Ung, T. A.; Ishihara, H.; Hajela, S. P. *Adv. Synth. Catal.* **2002**, *344*, 728–735.
- (3) Lehman, S. E.; Schwendeman, J. E.; O'Donnell, P. M.; Wagener, K. B. *Inorg. Chim. Acta* **2003**, *345*, 190–198.
- (4) Schmidt, B. *J. Org. Chem.* **2004**, *69*, 7672–7687.
- (5) Schmidt, B. *Eur. J. Org. Chem.* **2004**, 1865–1880.
- (6) McGrath, D. V.; Grubbs, R. H. *Organometallics* **1994**, *13*, 224–235.
- (7) Bourgeois, D.; Pancrazi, A.; Nolan, S. P.; Prunet, J. *J. Organomet. Chem.* **2002**, *643*, 247–252.
- (8) Sutton, A. E.; Seigal, B. A.; Finnegan, D. F.; Snapper, M. L. *J. Am. Chem. Soc.* **2002**, *124*, 13390–13391.
- (9) Courchay, F. C.; Sworen, J. C.; Ghiviriga, I.; Abboud, K. A.; Wagener, K. B. *Organometallics* **2006**, *25*, 6074–6086.
- (10) Hong, S. H.; Day, M. W.; Grubbs, R. H. *J. Am. Chem. Soc.* **2004**, *126*, 7414–7415.
- (11) The equilibrium *E/Z* ratio (6:5) is greater than 20:1 and the electronics of the system disfavor product redistribution during secondary metathesis.
- (12) Isomerizations also start to occur within 1 h without effective additives.
- (13) Mol, J. C.; Buffon, R. *Journal of the Brazilian Chemical Society* **1998**, *9*, 1–11.
- (14) Burdett, K. A.; Harris, L. D.; Margl, P.; Maughon, B. R.; Mokhtar-Zadeh, T.; Saucier, P. C.; Wasserman, E. P. *Organometallics* **2004**, *23*, 2027–2047.

- (15) The ethenolysis reactions were carried out by Dr. Choon Woo Lee at Materia.
- (16) Alcaide, B.; Almendros, P.; Alonso, J. M.; Aly, M. F. *Org. Lett.* **2001**, *3*, 3781–3784.
- (17) Alcaide, B.; Almendros, P. *Chem. Eur. J.* **2003**, *9*, 1259–1262.
- (18) Alcaide, B.; Almendros, P.; Alonso, J. M.; Luna, A. *Synthesis* **2005**, 668–672.
- (19) Toste, F. D.; Chatterjee, A. K.; Grubbs, R. H. *Pure Appl. Chem.* **2002**, *74*, 7–10.
- (20) Bäckvall, J. E.; Chowdhury, R. L.; Karlsson, U. *J. Chem. Soc., Chem. Commun.* **1991**, 473–475.
- (21) Csajernyik, G.; Éll, A. H.; Fadini, L.; Pugin, B.; Bäckvall, J. E. *J. Org. Chem.* **2002**, *67*, 1657–1662.
- (22) It was reported that the catalyst **1** generates radical anions on treatment with 1,4-benzoquinones, see: (a) Amir-Ebrahimi, V.; Hamilton, J. G.; Nelson, J.; Rooney, J. J.; Thompson, J. M.; Beaumont, A. J.; Rooney, A. D.; Harding, C. J. *Chem. Commun.* **1999**, 1621–1622. (b) Amir-Ebrahimi, V.; Hamilton, J. G.; Nelson, J.; Rooney, J. J.; Rooney, A. D.; Harding, C. J. *J. Organomet. Chem.* **2000**, *606*, 84–87.
- (23) Herold, P.; Mohr, P.; Tamm, C. *Helv. Chim. Acta* **1983**, *66*, 744–754.
- (24) Jones, K.; Storey, J. M. D. *Tetrahedron* **1993**, *49*, 4901–4906.
- (25) Conversions measured by ^1H NMR were identical between with and without an internal standard.
- (26) Ohba, T.; Ikeda, E.; Tsuchiya, N.; Nishimura, K.; Takei, H. *Bioorg. Med. Chem. Lett.* **1996**, *6*, 2629–2634.
- (27) Kang, K. T.; Weber, W. P. *Tetrahedron Lett.* **1985**, *26*, 5753–5754.
- (28) Martinez, V.; Blais, J. C.; Bravic, G.; Astruc, D. *Organometallics* **2004**, *23*, 861–874.
- (29) Seto, Y.; Guengerich, F. P. *J. Biol. Chem.* **1993**, *268*, 9986–9997.

- (30) Acetic acid was not as effective as 1,4-benzoquinone in ethenolysis.
- (31) Experimental details of the ethenolysis reactions were written by Dr. Choon Woo Lee at Materia.

Chapter 6

Highly Active Water-Soluble Olefin Metathesis Catalyst[†]

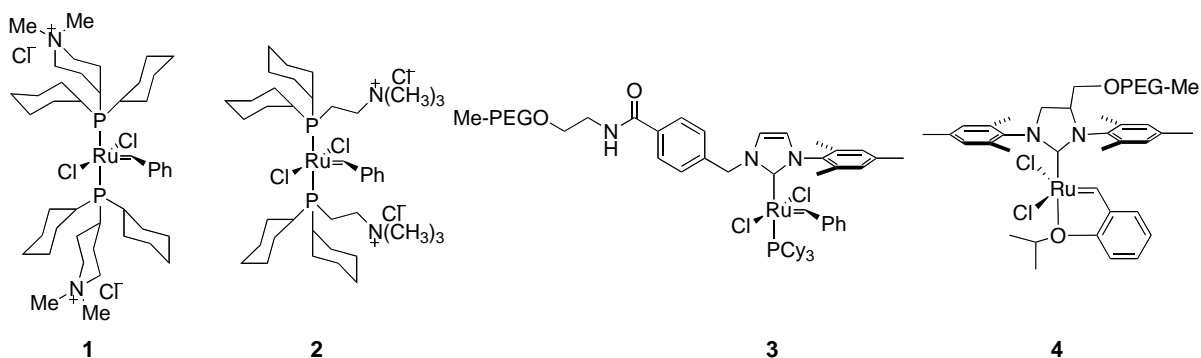
Abstract

A novel water-soluble ruthenium olefin metathesis catalyst supported by a poly(ethylene glycol) conjugated saturated 1,3-dimesityl-4,5-dihydroimidazol-2-ylidene ligand is reported. The catalyst displays improved activity in ring-opening metathesis polymerization, ring-closing metathesis, and cross-metathesis reactions in aqueous media.

Introduction

Olefin metathesis is a powerful carbon-carbon bond formation reaction in both polymer and small molecule synthesis.¹ In particular, the recent development of ruthenium olefin metathesis catalysts, which show high activity and functional group tolerance, has expanded the scope of olefin metathesis. However, performing olefin metathesis in aqueous media is still challenging due to the lack of a stable and active catalyst soluble in water. Aqueous olefin metathesis has the economic, environmental, and processing benefits of both homogeneous aqueous catalysis and aqueous two-phase catalysis.² Further, aqueous olefin metathesis is critical for some biological applications of olefin metathesis.

[†] The majority of this chapter has been published: Hong, S. H.; Grubbs, R. H. *J. Am. Chem. Soc.* **2006**, *128*, 3508–3509.

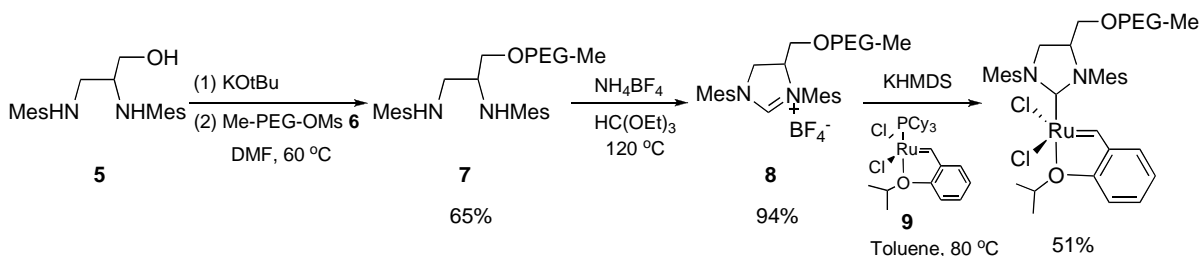


With the goal of developing a homogeneous catalyst that displays increased activity and stability, our group has reported several water-soluble catalysts such as **1**,³ **2**,³ and **3**.⁴ Catalysts **1–3** are unable to mediate the ring-closing metathesis (RCM) reaction of simple α,ω -dienes in water, and show limited RCM activity in methanol. Moreover, they do not show any activity in cross metathesis (CM) reactions in protic media. The recently developed catalyst **3** containing an *N*-heterocyclic carbene (NHC)-based ligand shows improved activity in aqueous ring-opening metathesis polymerization (ROMP) reactions.⁴ Appending poly(ethylene glycol) (PEG) to the nondissociating NHC ligand allows catalyst **3** to remain in solution throughout the entire metathesis reaction. However, having the PEG-carbamoyl-benzyl group as a pendant group of NHC limited the stability of the complex **3**. Earlier studies have shown that 1,3-diaryl group of NHCs in (NHC)(L)(Cl)₂Ru=CHPh type complexes are important for catalyst stability.⁵ As part of the ongoing effort to use PEG as a water solubilizing moiety, we have developed the novel water soluble catalyst **4** which shows improved stability and activity in water. Appending PEG on the backbone of saturated 1,3-dimesityl-4,5-dihydroimidazol-2-ylidene (H₂IMes) ligand renders catalyst **4** soluble in organic solvents such as dichloromethane and toluene as well as water, with maintaining stability and activity of well-known H₂IMes-based ruthenium metathesis catalysts.⁶

Results and Discussion

Catalyst **4** was prepared in three steps from readily available starting materials. PEG-attached diamine **7** was synthesized using an S_N2 type reaction between *N,N'*-dimesityl-2,3-diamino-1-propanol **5**⁷ and PEG mesyl methyl ether **6**. The diamine **7** was subsequently converted to the corresponding imidazolium salt **8** through condensation with triethyl orthoformate in the presence of ammonium tetrafluoroborate. Deprotonation of **8** with potassium bis(trimethylsilyl)amide (KHMDs) followed by the addition of Ru complex **9** generated the desired catalyst **4** (Scheme 1). Catalyst **4** was purified by column chromatography followed by precipitation from dichloromethane into diethyl ether. Attempts to synthesize a phosphine-containing version of this catalyst were unsuccessful.

Scheme 1. Synthesis of catalyst **4**.



Complex **4** is stable in water. In the ¹H NMR recorded in D₂O, no signal corresponding to the benzylidene proton (Ru=CHPh, δ16.4 ppm, CD₂Cl₂) was observed. Initially, this was believed to be due to either deuterium exchange of the benzylidene proton,^{3d} or from rapid decomposition of **4** in D₂O. However, upon extracting the catalyst with CD₂Cl₂ from the D₂O solution, the benzylidene peak reappeared. Even after 1 week in D₂O, the ¹H NMR spectra, after CD₂Cl₂ extraction, was not significantly altered, showing stability of this catalyst in water.⁸ This type of solvent-dependent NMR behavior has been

reported in micelle-type complexes.⁹ We believe that catalyst **4** aggregates could form a micelle-like structure in D₂O due to hydrophilic PEG chain and hydrophobic ruthenium center.¹⁰

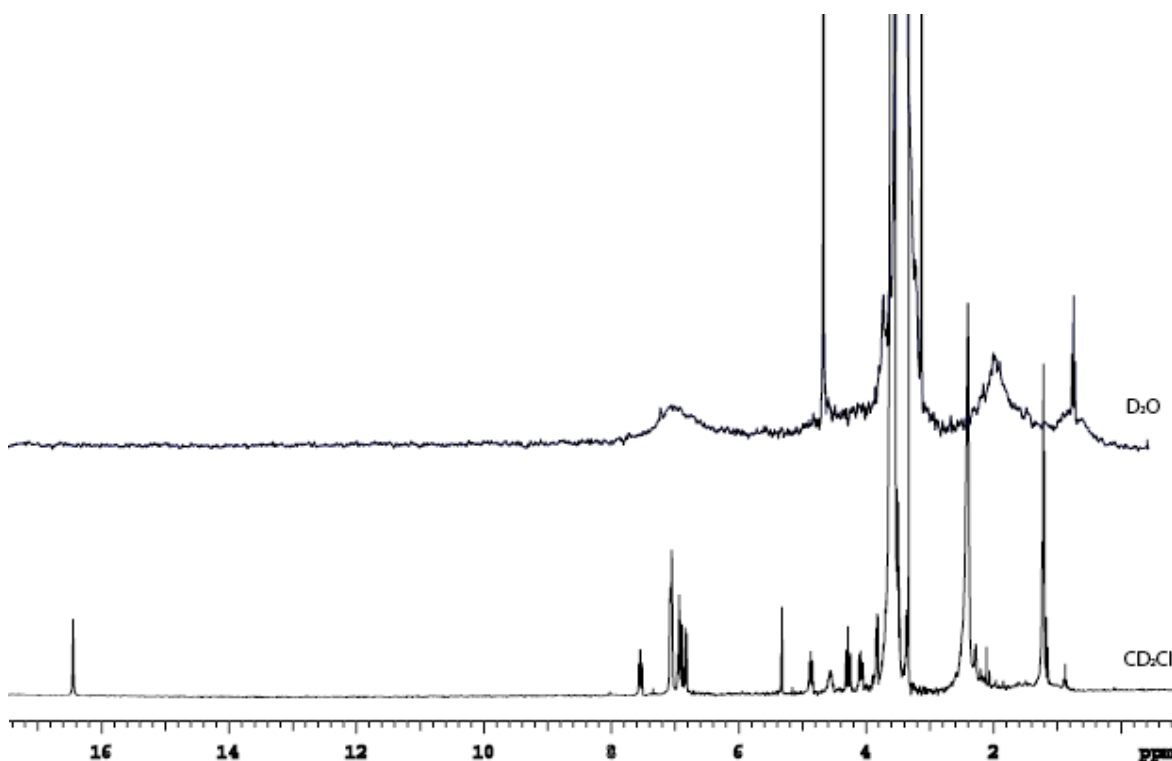


Figure 1. ¹H NMR spectra of catalyst **4** in D₂O and CD₂Cl₂.

As an activity comparison, we examined the ROMP of *endo*-norbornene monomer **10** with catalysts **2**, **3** and **4**.¹¹ As shown by Figure 2, catalyst **4** showed much improved activity when compared to other water-soluble catalysts.¹² This is consistent with past results as saturated NHC-based ruthenium olefin metathesis catalysts are known to be more active than phosphine-based and unsaturated NHC-based catalysts.^{5,6}

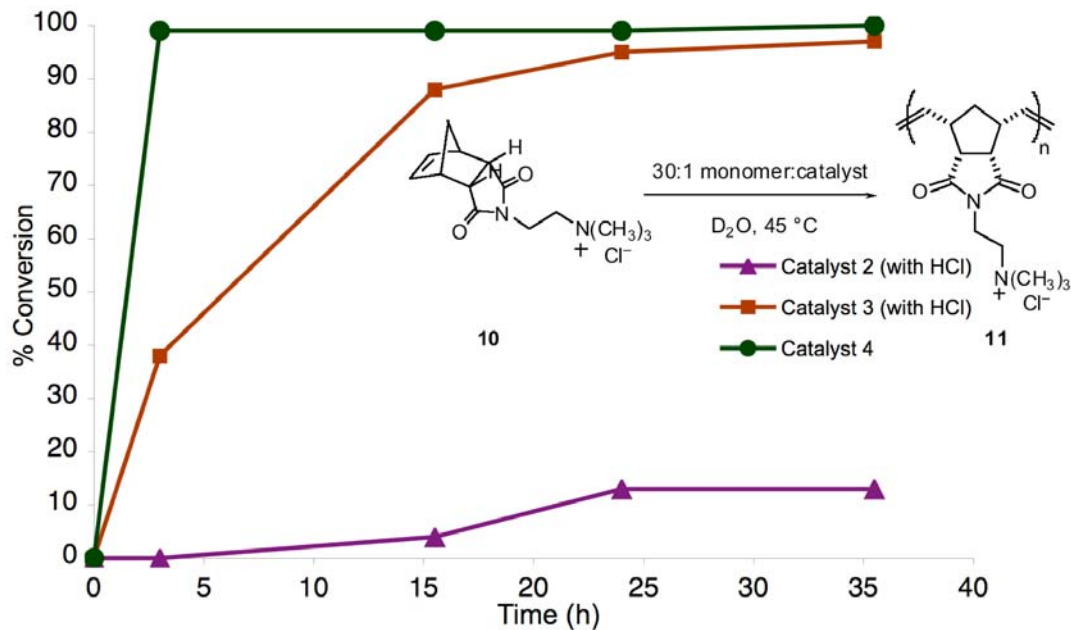
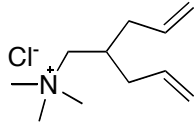
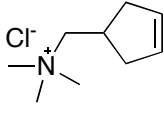
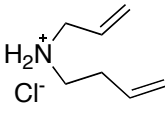
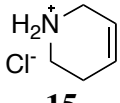
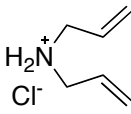
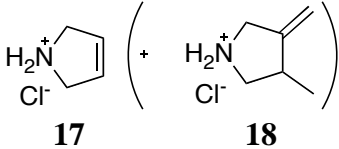
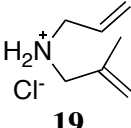
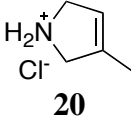
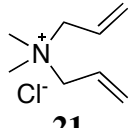
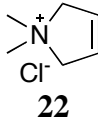
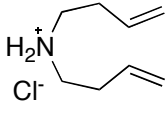
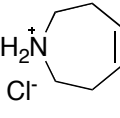
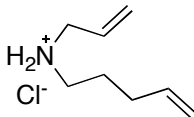
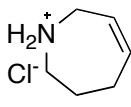


Figure 2. A comparison of the ability of water-soluble catalysts to polymerize *endo*-monomer **10** (data for catalyst **2** and **3** are obtained from reference 4).

RCM reactions of water-soluble α,ω -dienes have been highly challenging due to instability toward water of the Ru methylidene species generated after the first catalytic turnover.^{3b} There have been a few reports of RCM of α,ω -dienes in water.¹³ However, the reported reactions either involved water-insoluble substrates, or water-insoluble catalysts.¹³ The actual metathesis reactions in these systems are believed to occur in organic-friendly environments, such as inside solid supports, as a decrease in activity is observed with water-soluble α,ω -dienes. The best reported conversion of RCM of diallylamine hydrochloric acid salt **16** in water was just 11% at 45 °C.^{13b} In homogeneous systems, there has been no report of the RCM of the α,ω -dienes in aqueous media.¹⁴

Table 1. Ring-closing metathesis reactions in aqueous media^a

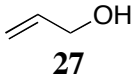
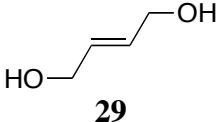
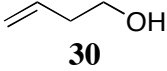
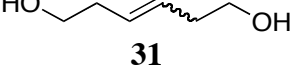
Entry	Substrate	Time	Product	Conversion
1	 12	12 h	 13	>95%
2	 14	24 h	 15	>95%
3	 16	36 h	 17 (+ 18)	67% (+28%)
4	 19	24 h	 20	42%
5	 21	24 h	 22	<5%
6	 23	24 h	 24	68%
7	 25	24 h	 26	39%

^aReactions were carried out at room temperature with 5 mol% catalyst **4** and an initial substrate concentration of 0.2 M in D₂O or H₂O. Conversions were determined by ¹H NMR spectroscopy.

Catalyst **4** showed unprecedented RCM activity with water-soluble α,ω -dienes in water yielding the corresponding 5-, 6- and 7-membered rings in good to excellent yields (Table 1). RCM of **12** and **14** produced the corresponding 5-membered and 6-membered ring compounds, **13** and **15**, quantitatively (entries 1 and 2). In RCM of **16**, cycloisomerized product **18** was observed along with the major metathesis product **17** (entry 3). This type of cycloisomerization has previously been observed during olefin metathesis, presumably by ruthenium hydrides from catalyst decomposition.^{13b,15} For the other substrates (entries 1, 2, 4–7), the corresponding cycloisomerized products were not observed. Allyl-2-methylallylamine hydrochloride **19** was cyclized to generate a tri-substituted olefin **20** with relatively lower yield (entry 4). RCM of **23** and **25** produced the corresponding 7-membered ring **24** and **26** with 68% and 39% conversion, respectively (entries 6 and 7). For reasons not yet fully understood, RCM of diallyldimethylamine chloride **21** was not successful (entry 5).

Cross-metathesis is also challenging in aqueous media. To the best of our knowledge, there have been no reports of homogeneous cross-metathesis in water. The Blechert group demonstrated homodimerization of allyl alcohol **27** in D₂O up to 80% conversion using the aforementioned heterogeneous catalyst system.^{13b} Catalyst **4** shows excellent activity in homodimerization of **27** and **30**, and the self-metathesis of *cis*-2-butene-1,4-diol **28** in water (Table 2). However, cross-metathesis reaction with catalyst **4** is highly substrate dependent. **4** is unable to homodimerize vinylacetic acid, allylamine hydrochloride, and other water-soluble olefins derived from carboxylic acid and quaternary ammonium salts. Variations of pH using DCl or NaOD solutions did not improve the cross-metathesis activity of catalyst **4**.

Table 2. Cross-metathesis reactions in aqueous media^a

Substrate	Time	Product	Conversion
 27	12 h ^b	 28	>95% ^c
 28	12 h ^b	 29	94% ^d
 30	7 h ^e	 31	83% ^f

^aReactions were carried out with 5 mol% catalyst **4** and an initial substrate concentration of 0.2 M in D₂O or H₂O. Conversions were determined by ¹H NMR spectroscopy. ^bAt 45 °C. ^c*E/Z* ~ 15:1. ^d6% of **24** remains due to thermodynamic equilibrium. ^eReaction was carried out at room temperature. Isomerization occurred at 45 °C. ^f*E/Z* ~ 8:1

Conclusion

A novel poly(ethylene glycol)-supported water-soluble catalyst which is active and stable in water has been developed. This catalyst shows unprecedented activity in ROMP, RCM, and CM in aqueous media.

Experimental

General considerations. Manipulation of organometallic compounds was performed using standard Schlenk techniques under an atmosphere of dry argon or in a nitrogen-filled Vacuum Atmospheres dry box (O₂ < 2.5 ppm). NMR spectra were recorded

on a Varian Mercury 300 (299.817 MHz for ^1H ; 75.4 MHz for ^{13}C). D_2O was purchased from Cambridge Isotope Laboratories and degassed by bubbling with Ar. Puriss water was purchased from Aldrich and degassed by bubbling with Ar. The starting materials, **5**⁷ and **6**¹⁶ were prepared according to literature procedure. Substrates **10**,¹⁷ and products **11**,¹⁷ **13**,¹⁸ **15**,¹⁹ **17**,²⁰ **18**,²¹ **20**,²⁰ and **25**²² have been previously prepared and reported. **12** was synthesized from 2-allyl-4-pentenamine²³ by treatment with MeI followed by ion exchange. **14**,²⁴ **19**,²⁵ allylamine hydrochloride were synthesized from the corresponding amines by treatment with HCl in diethyl ether. Substrate **16** was purchased from TCI and used as received. Substrate **21**, **23**, **24**, vinylacetic acid, and allylamine were purchased from Aldrich and used as received. Complex **9** was obtained from Materia and used as received.

Synthesis of poly(ethylene glycol) *N,N'*-dimesityl-2,3-diamino-1-propyl methyl ether (7). To a stirred solution of *N,N'*-dimesityl-2,3-diamino-1-propanol **5** (1.2 g, 3.6 mmol) in DMF (100 mL), KOtBu (0.40 g, 3.6 mmol) was added as a single portion. After with stirring at ambient temperature for 30 min, PEG mesyl methyl ether **6** ($M_n \sim 2078$, 2.5g, 1.2 mmol) was added. The reaction mixture was heated to 60 °C for 2 days. Upon cooling to ambient temperature, a few drops of water were added to quench the reaction. DMF was removed *in vacuo*, and dichloromethane (100 mL) was added to dissolve the product. The CH_2Cl_2 solution was passed through a pad of celite. After evaporation of volatiles, the crude mixture was eluted through a pad of silica gel using dichloromethane and methanol ($v/v = 1:1$), and the product was precipitated from dichloromethane into diethyl ether. The precipitates were collected either by vac-filtration, or by centrifuge to yield a fluffy white solid (1.80 g, 65%). ^1H NMR (CDCl_3): δ 6.75 (s, 2H), 6.74 (s, 2H), 4.12 (dd, $J = 14.0, 2.0$

Hz, 1H), 3.94 (dd, $J = 6.5, 2.0$ Hz, 1H), 3.78 – 3.43 (m, PEG), 3.32 (s, 3H), 2.25 – 2.16 (m, 18H); ^{13}C NMR (CDCl_3): δ 141.9 (br), 132.0, 130.8 (br), 130.0, 129.5 (br), 129.3, 76.1 – 66.7 (m, PEG), 65.0, 61.6, 59.0, 56.2, 51.0, 20.6, 20.5, 18.8, 18.3.

Synthesis of 1,3-bis(1-mesityl)-4-[[methoxy poly(ethylene glycol) oxy] methyl]-4,5-dihydro-1H-imidazol-3-ium tetrafluoroborate (8). Diamine **7** (0.50 g, 0.22 mmol), ammonium tetrafluoroborate (0.023 g, 0.22 mmol), and triethylorthoformate (3 mL) were heated to 120 °C for 12 h. After cooling to ambient temperature, the product was precipitated from diethyl ether. The precipitate was collected either by vac-filtration, or by centrifuge and washed several times with diethyl ether to yield a fluffy white solid (0.49 g, 94%, Mn ~ 2424). ^1H NMR (CDCl_3): δ 7.92 (s, 1H), 6.95 (s, br, 4H), 5.13 (m, 1H), 4.63 (t, $J = 12.0$ Hz, 1H), 4.43 (dd, $J = 12.0, 7.5$ Hz, 1H), 3.84 – 3.35 (m, PEG), 3.34 (s, 3H), 2.37 – 2.28 (m, 18H); ^{13}C NMR (CDCl_3): δ 158.4, 140.8, 140.5, 136.2, 135.6, 135.4, 130.6, 130.4, 130.2, 130.1, 128.4, 73.4 – 69.7 (m, PEG), 67.3, 66.7, 64.1, 59.1, 52.7, 21.2, 21.1, 18.4, 17.6, 17.5, 15.3.

Synthesis of PEG conjugated Ru catalyst (4). In a nitrogen-filled dry box, imidazolium salt **8** (0.40 g, 0.17 mmol) and potassium bis(trimethylsilyl)amide (KHMDs, 0.049 g, 0.25 mmol) were dissolved in toluene (4 mL) and added to a solution of ruthenium complex **9** (0.15 g, 0.25 mmol) in toluene (2 mL), and the solution was transferred to a schlenk flask. The flask was capped and removed from the dry box and heated to 80 °C for 3 h. The product was purified by column chromatography (Brockmann III grade neutral alumina, 50:1 CH_2Cl_2 :MeOH) followed by precipitation from dichloromethane into diethyl

ether to yield a green solid (0.22 g, 51%, $M_n \sim 2639$). ^1H NMR (CD_2Cl_2): δ 16.4 (s, 1H), 7.54 (td, $J = 9.0, 2.1$ Hz, 1H), 7.07 (s, 2H), 7.05 (s, 2H), 6.96-6.87 (m, 2H), 6.82 (d, $J = 8.1$ Hz, 1H), 4.87 (m, 1H), 4.56 (m, 1H), 4.23 (t, $J = 10.8$ Hz, 1H), 4.08 (dd, $J = 10.2, 8.4$ Hz, 1H), 3.84 – 3.36 (m, PEG), 3.33 (s, 3H), 2.40 (s, br, 18H), 1.23 – 1.90 (m, 6H); ^{13}C NMR (CD_2Cl_2): δ 296.5, 213.3, 152.4, 145.8, 145.7, 140.1, 139.3, 139.2, 130.2, 130.0, 129.9, 129.6, 122.8, 122.7, 113.4, 76.5, 75.6, 72.4, 71.7 – 68.3 (m, PEG), 63.8, 59.1, 59.0, 55.6, 21.4, 21.3, 21.3, 21.0 – 18.0 (m) (Figure 3).

General procedure for ROMP, RCM, and CM with catalyst (4). In a nitrogen filled dry box, solid substrate (if any) and catalyst were weighed onto a weighing paper and transferred into a screw-cap NMR tube. The NMR tube was sealed with a screw-cap equipped with a septum and removed from the dry-box. Liquid substrate (if any) and degassed deuterium oxide were added via airtight syringe while under a positive Ar pressure. The tube was heated in a temperature-controlled mineral oil bath, or allowed to stand at ambient temperature depending on reaction conditions. The reaction was monitored by ^1H NMR spectroscopy using a PEG peak as an internal standard.²⁶

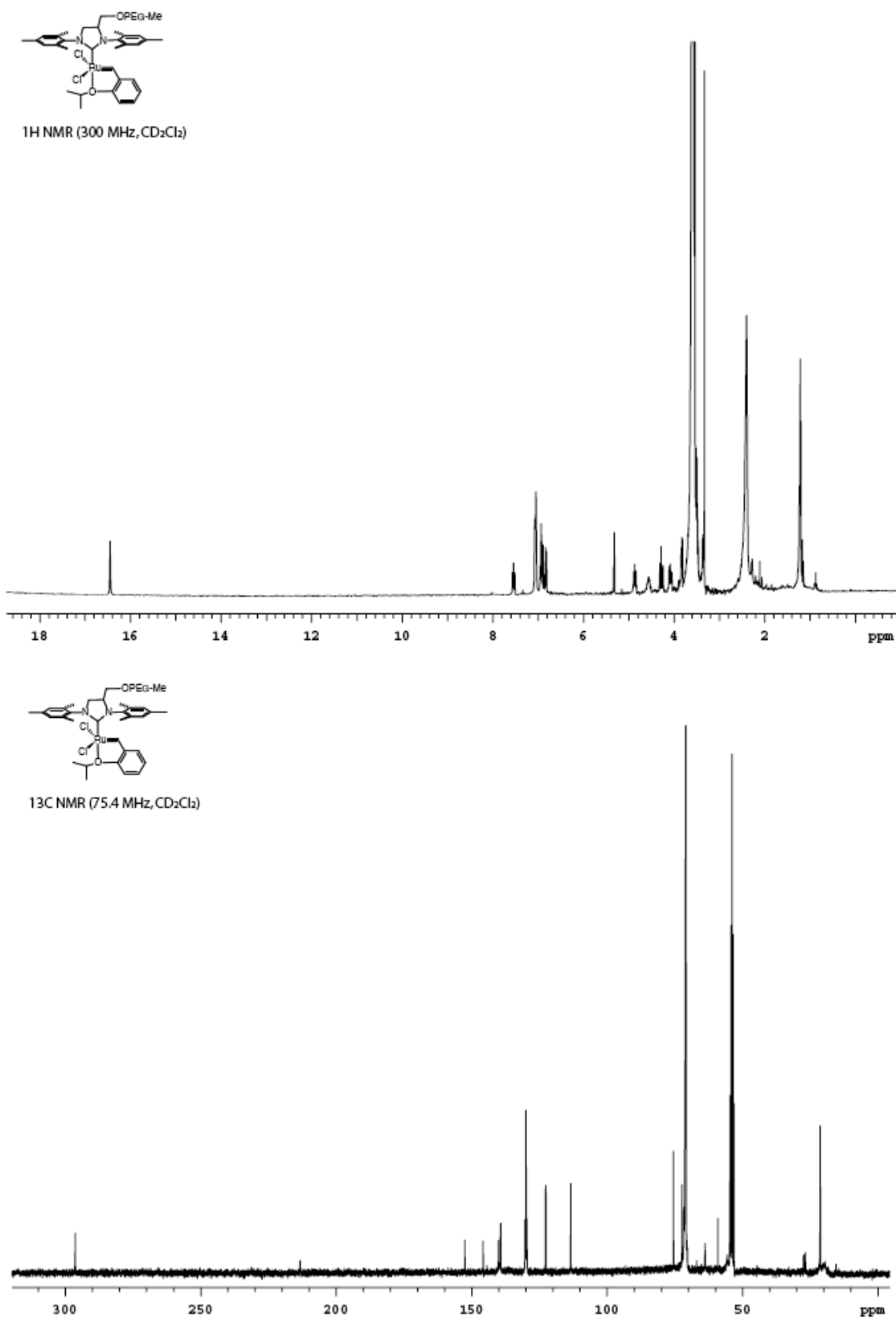


Figure 3. ¹H and ¹³C spectra of catalyst 4.

References and Notes

- (1) (a) *Handbook of Metathesis*, Grubbs, R. H., Ed.; Wiley-VCH: Weinheim, Germany, 2003. (b) Ivin, K. J.; Mol, J. C. *Olefin Metathesis and Metathesis Polymerization*; Academic Press: San Diego, CA, 1997.
- (2) *Aqueous-Phase Organometallic Catalysis*, Cornils, B., Hermann, W. A., Eds; Wiley-VCH: Weinheim, Germany, 2004.
- (3) (a) Mohr, B.; Lynn, D. M.; Grubbs, R. H. *Organometallics* **1996**, *15*, 4317-4325. (b) Kirkland, T. A.; Lynn, D. M.; Grubbs, R. H. *J. Org. Chem.* **1998**, *63*, 9904-9909. (c) Lynn, D. M.; Mohr, B.; Grubbs, R. H.; Henling L. M.; Day, M. W. *J. Am. Chem. Soc.* **2000**, *122*, 6601-6609. (d) Lynn, D. M.; Grubbs, R. H. *J. Am. Chem. Soc.* **2001**, *123*, 3187-3193.
- (4) Gallivan, J. P.; Jordan, J. P.; Grubbs, R. H. *Tetrahedron Lett.* **2005**, *46*, 2577-2580.
- (5) Trnka, T. M.; Grubbs, R. H. *Acc. Chem. Res.* **2001**, *34*, 18-29, and references therein.
- (6) (a) Scholl, M.; Ding S.; Lee, C. W.; Grubbs, R. H. *Org. Lett.* **1999**, *1*, 953-956. (b) Garber, S. B.; Kingsbury, J. S.; Gray, B. L.; Hoveyda, A. H. *J. Am. Chem. Soc.* **2000**, *122*, 8168-8179. (c) Bielawski, C.; Grubbs, R. H. *Angew. Chem. Int. Ed.* **2000**, *39*, 2903-2906.
- (7) Mayr, M.; Buchmeiser, M. R.; Wurst, K. *Adv. Synth. Catal.* **2002**, *344*, 712-719.
- (8) 71% of the catalyst **4** was recovered by evaporation of D₂O after a week.
- (9) Bütün, V.; Armes, S. P.; Billingham, N. C. *Macromolecules* **2001**, *34*, 1148-1159.
- (10) Well-ordered micelle formation of catalyst **4** aggregates in water is unlikely due to short hydrophobic chain length. For conditions of micelle formation, see: Dwars, T.; Paetzold, E.; Oehme, G. *Angew. Chem. Int. Ed.* **2005**, *44*, 7174-7199.

- (11) Earlier work demonstrated that *endo*-norbornene monomers are challenging ROMP substrates when compared to *exo*-norbornene monomers. See references 1 and 4.
- (12) Catalyst **2** and **3** require 1 equiv of HCl, relative to catalyst, as a phosphine scavenger to reach their highest conversions.
- (13) (a) Zarka, M. T.; Nuyken, O.; Weberskirch, R. *Macromol. Rapid. Commun.* **2004**, *25*, 858-862. (b) Connon S. J.; Blechert, S. *Bioorg. Med. Chem. Lett.* **2002**, *12*, 1873-1876. (c) Davis, K. J.; Sinou, D. *J. Mol. Cat. A: Chem.* **2002**, *177*, 173-178.
- (14) To avoid the methyldene intermediates, substituted dienes such as *N*-allylcinnamylamine hydrochloride salt were required. Using these substituted dienes is not an atom economical transformation since it has unnecessary substituents which require additional steps for preparation. Moreover, the yields of the RCM reactions with the substituted dienes using catalysts **1-3** in water were usually not good. See reference 3b.
- (15) (a) Terada, Y.; Arisawa, M.; Nishida, A. *Angew. Chem. Int. Ed.* **2004**, *43*, 4063-4067. (b) Hong, S. H.; Day, M. W.; Grubbs, R. H. *J. Am. Chem. Soc.* **2004**, *126*, 7414-7415. (c) Hong, S. H.; Sanders, D. P.; Lee, C. W.; Grubbs, R. H. *J. Am. Chem. Soc.* **2005**, *127*, 17160-17161. (d) Çetinkaya, B.; Demir, S.; Özdemir, I.; Toupet, L.; Sémeril, D.; Bruneau, C.; Dixneuf, P. H. *Chem. Eur. J.* **2003**, *9*, 2323-2330. (e) Sémeril, D.; Bruneau, C.; Dixneuf, P. H. *Helv. Chim. Acta* **2001**, *84*, 3335-3341. (f) Miyaki, Y.; Onishi, T.; Ogoshi, S.; Kurosawa, H. *J. Organomet. Chem.* **2000**, *616*, 135-139.
- (16) **6** was synthesized from molecular weight 2000 PEG methyl ether purchased from Aldrich. See: Zhao, X.; Janda, K. D. *Tetrahedron Lett.* **1997**, *38*, 5437-5440.

- (17) Lynn, D. M.; Mohr, B.; Grubbs, R. H. *J. Am. Chem. Soc.* **1998**, *120*, 1627-1628.
- (18) Tropsha, A. E.; Nizhinni, S. V.; Yaguzhinskii, L. S. *Bioorg. Khim.* **1985**, *11*, 1931-1941.
- (19) *Beilstein* **20**, IV, 1912.
- (20) Gajda, T.; Zwierzak, A. *Liebigs Ann. Chem.* **1986**, 992-1002.
- (21) Connon S. J.; Blechert, S. *Bioorg. Med. Chem. Lett.* **2002**, *12*, 1873-1876.
- (22) McDonald, W. S.; Verbicky, C. A.; Zercher, C. K. *J. Org. Chem.* **1997**, *62*, 1215-1222.
- (23) Paul, R.; Cottin, H. *Bull. Soc. Chim.* **1937**, *4*, 933-937.
- (24) Garst, M. E.; Bonfiglio, J. N.; Marks, J. *J. Org. Chem.* **1982**, *47*, 1494-1500.
- (25) Tiles, H. *J. Am. Chem. Soc.* **1959**, *81*, 714-727.
- (26) (a) Dickerson, T. J.; Reed, N. N.; Janda, K. D. *Chem. Rev.* **2002**, *102*, 3325-3344. (b) Annunziata, R.; Benaglia, M.; Cinquini, M.; Cozzi, F. *Chem. Eur. J.* **2000**, *6*, 133-138.

Chapter 7

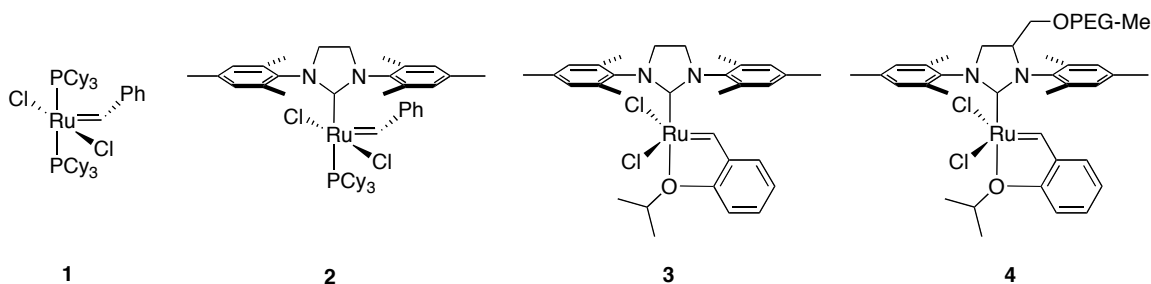
Efficient Removal of Ruthenium By-products from Olefin Metathesis Products by Simple Aqueous Extraction

Abstract

Simple aqueous extraction removed ruthenium byproducts efficiently from ring-closing metathesis reactions catalyzed by a poly(ethylene glycol)-supported *N*-heterocyclic carbene-based ruthenium complex.

Introduction

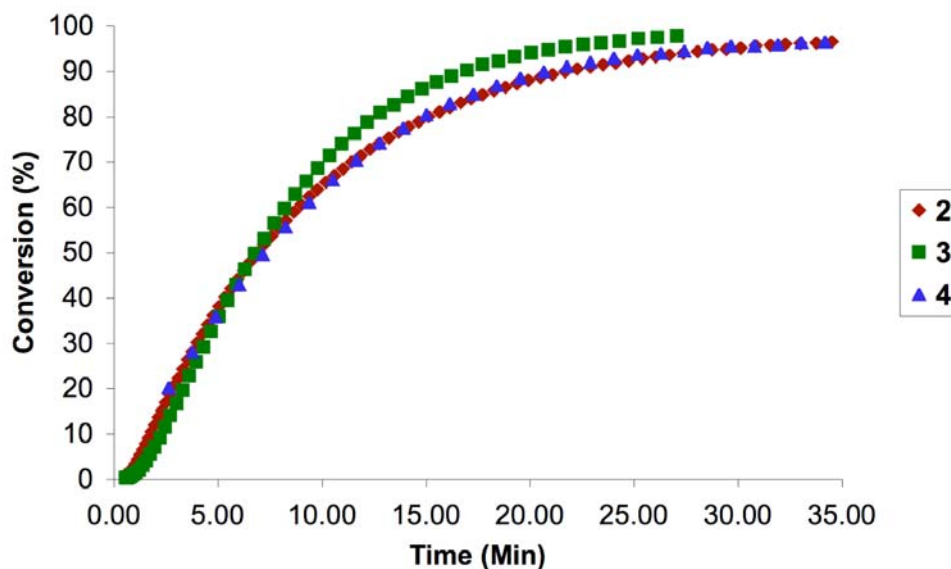
Olefin metathesis is a powerful carbon-carbon bond formation reaction in both polymer and small molecule synthesis.^{1,2} In particular, the recent development of ruthenium olefin metathesis catalysts such as **1–3**, which show high activity and functional group tolerance, has expanded the scope of this reaction.³ However, it has proved very difficult to remove the highly colored ruthenium complexes completely from the desired product even after purification by silica gel column chromatography. The residual ruthenium complexes can cause problems such as olefin isomerization,^{4–6} decomposition over time,^{7,8} and increased toxicity of the final product which is critical especially in connection with the synthesis of biologically active materials.⁹



Several protocols have been reported to remove the ruthenium by-products. The use of tris(hydroxymethyl)phosphine (THMP),⁹ $\text{Pb}(\text{OAc})_4$,¹⁰ DMSO (or $\text{Ph}_3\text{P}=\text{O}$),¹¹ activated carbon,¹² supported phosphines,¹³ supercritical fluid,¹⁴ modified catalyst,¹⁵ and mesoporous silicates¹⁶ have all been reported to reduce the ruthenium content from homogeneous olefin metathesis reactions. Although these purification methods afford low levels of residual ruthenium, they also have drawbacks, such as high loadings of expensive, toxic, or unstable ruthenium scavengers, long processing times, the requirement of silica gel column chromatography, or numerous washings and extractions, which are not practical and economical in many cases.¹⁴ Furthermore, most methods do not actually reduce the ruthenium contamination below the level of 10 ppm, which is necessary for pharmaceutical applications.^{17,18}

Results and Discussion

Recently, we reported poly(ethylene glycol) (PEG) supported catalyst **4** ($M_n \sim 2639$) which is active and stable in aqueous media.¹⁹ The unique solubility profile of PEG renders **4** soluble in some organic solvents such as dichloromethane and toluene, which are typical solvents for olefin metathesis, as well as aqueous media. The catalyst is insoluble in other organic solvents such as diethyl ether, isopropyl alcohol, and hexanes, following the

Chart 1. RCM of Diethyl diallylmalonate **4**.^a

^aConditions: 1 mol % of ruthenium catalyst, 0.1 M, CD₂Cl₂, 30 °C.²⁰

The RCM of substrate **5** by catalyst **3** followed by purification using several reported methods was undertaken to collect reference data (Table 1). Silica gel chromatography, which is not practical and efficient on an industrial scale, was avoided in all cases. Simple extraction reduced the ruthenium content by approximately half (entry 1). Treatment with DMSO treatment in the absence of silica gel chromatography, is not as effective as ruthenium removal employing THMP or activated carbon.¹¹ THMP⁹ and activated carbon¹² treatment with an aqueous workup effectively reduced the ruthenium level below 100 ppm; however, this level is still too high for practical use.

Table 1. Ruthenium level in **6** (ppm) after various purification methods.

Entry	Catalyst ^a	Purification Method	[Ru] (ppm) ^b
1	3	5 H ₂ O washes	1779
2	3	THMP (50 equiv ^c) and 5 H ₂ O washes	91
3	3	DMSO (50 equiv ^c) and 5 H ₂ O washes	786
4	3	PEG (M _n ~ 10000, 50 equiv ^c) and 5 H ₂ O washes	562
5	3	PEG (M _n ~ 550, 50 equiv ^c) and 5 H ₂ O washes	1165
6	3	5 H ₂ O washes and activated carbon ^d	82
7	4	5 H ₂ O washes	41 ^e
8	4	THMP (50 equiv ^c) and 5 H ₂ O washes	2
9	4	5 H ₂ O washes and activated carbon ^d	< 0.04

^a 1 mol%. ^b Analyzed by ICP-MS, crude [Ru] ~ 4400 ppm for both **3** and **4**. ^c Based on the ruthenium catalyst. ^d 1.3 weight equiv of the crude product **6**. ^e 3 H₂O washes do not increase the measured ruthenium level.

In contrast, simple aqueous extraction reduced the ruthenium level to 41 ppm following RCM with catalyst **4**, which is lower than the level achieved by THMP or activated carbon treatment from the reaction with catalyst **3** (entry 7).²¹ Clear diethyl ether and brown aqueous phases were observed during the extraction. Employing the aqueous extraction protocol with catalyst **4** in combination with THMP or activated carbon reduced the ruthenium level below 10 ppm, which is suitable for pharmaceutical applications (entries 8 and 9).¹⁴ The activated carbon treatment after aqueous extraction was extremely efficient reducing the ruthenium level below the detection limit of our analysis, <0.04 ppm.

PEG chains themselves were next tested for removing residual ruthenium. The tested PEG polymers (M_n ~ 10000 and M_n ~ 550) did not effectively remove the ruthenium-

containing byproducts (entries 4 and 5). These results indicate that the PEG-supported NHC ligand remains bound to the ruthenium byproducts or scavenges them after olefin metathesis reactions. The NHC-bound decomposition products isolated from reactions with catalyst **2** have been reported in both organic solvents and aqueous media.^{7,22,23}

Conclusion

In conclusion, we have demonstrated a convenient and efficient method for removing ruthenium-containing byproducts from olefin metathesis reactions by simple aqueous workup. This practical, economical and environmentally friendly method reduced the ruthenium contamination level down to the useful range for biologically active material applications.

Experimental

General considerations. Manipulation of catalysts **1–4** was performed using standard Schlenk techniques under an atmosphere of dry argon or in a nitrogen-filled Vacuum Atmospheres dry box ($O_2 < 2.5$ ppm). Ruthenium level was analyzed on an Agilent 7500c quadrupole inductively coupled plasma mass spectrometer (ICP-MS) following the literature procedure.^{9,11} CH_2Cl_2 was dried by passage through solvent purification column containing alumina and degassed by argon sparge. Diethyl ether was purchased from Fisher and used as received. Diethyl diallylmalonate **5** and activated carbon (Darco G-60, 100 mesh, powder) was purchased from Aldrich and used as received. Catalysts **1–3** were obtained from Materia and used as received. Catalyst **4** was prepared according to the literature procedure.¹⁹

Catalyst comparison was carried out in RCM of **5** according the literature procedure (Chart 1).²⁰

Procedure for RCM of 5. To a stirred solution of diethyl diallylmalonate (**5**, 120 mg, 0.5 mmol) in CH₂Cl₂ (20 mL), ruthenium catalyst (**3** or **4**, 1 mol%) was added under argon atmosphere at room temperature. The reaction mixture was stirred for 2 h, and CH₂Cl₂ was evaporated *in vacuo*. Crude 3,3-diethylester-pentene (**6**, ~100 mg, > 94%) was obtained as dark brown oil and used for further purification.

Purification of 6. Crude 3,3-diethylester-pentene (**6**, 100 mg, 0.472 mmol) in diethyl ether (~30 mL) was transferred to a separatory funnel. The diethyl ether solution was washed 3 or 5 times by water (~30 mL), dried over MgSO₄, and concentrated. Approximately 20 – 30 mg of the resulting clear oil was accurately weighed by a microbalance and digested with concentrated nitric acid overnight for ICP-MS analysis. For activated carbon purification, the activated carbon (1.3 weight equiv of the crude product **6**) was added to the diethyl ether solution after the extraction and stirred for 24 h. After the carbon was filtered, the filtrate was concentrated *in vacuo* to provide **6** as clear oil. THMP and DMSO methods were carried out following the literature procedure except avoiding silica gel treatment or column chromatography

References and Notes

- (1) Ivin, K. J.; Mol, J. C. *Olefin Metathesis and Metathesis Polymerization*; Academic Press: San Diego, CA, 1997.
- (2) *Handbook of Metathesis*; Grubbs, R. H., Ed.; Wiley-VCH: Weinheim, Germany, 2003; Vol. 1-3.
- (3) Grubbs, R. H. *Tetrahedron* **2004**, *60*, 7117-7140.
- (4) Courchay, F. C.; Sworen, J. C.; Ghiviriga, I.; Abboud, K. A.; Wagener, K. B. *Organometallics* **2006**, *25*, 6074-6086.
- (5) Hong, S. H.; Sanders, D. P.; Lee, C. W.; Grubbs, R. H. *J. Am. Chem. Soc.* **2005**, *127*, 17160-17161.
- (6) Schmidt, B. *Eur. J. Org. Chem.* **2004**, 1865-1880.
- (7) Hong, S. H.; Day, M. W.; Grubbs, R. H. *J. Am. Chem. Soc.* **2004**, *126*, 7414-7415.
- (8) Ulman, M.; Grubbs, R. H. *J. Org. Chem.* **1999**, *64*, 7202-7207.
- (9) Maynard, H. D.; Grubbs, R. H. *Tetrahedron Lett.* **1999**, *40*, 4137-4140.
- (10) Paquette, L. A.; Schloss, J. D.; Efremov, I.; Fabris, F.; Gallou, F.; Mendez-Andino, J.; Yang, J. *Org. Lett.* **2000**, *2*, 1259-1261.
- (11) Ahn, Y. M.; Yang, K.; Georg, G. I. *Org. Lett.* **2001**, *3*, 1411-1413.
- (12) Cho, J. H.; Kim, B. M. *Org. Lett.* **2003**, *5*, 531-533.
- (13) Westhus, M.; Gonthier, E.; Brohm, D.; Breinbauer, R. *Tetrahedron Lett.* **2004**, *45*, 3141-3142.
- (14) Gallou, F.; Saim, S.; Koenig, K. J.; Bochniak, D.; Horhota, S. T.; Yee, N. K.; Senanayake, C. H. *Org. Process Res. Dev.* **2006**, *10*, 937-940.

- (15) Michrowska, A.; Gulajski, L.; Kaczmarska, Z.; Mennecke, K.; Kirschning, A.; Grela, K. *Green Chemistry* **2006**, *8*, 685-688.
- (16) McEleney, K.; Allen, D. P.; Holliday, A. E.; Crudden, C. M. *Org. Lett.* **2006**, *8*, 2663-2666.
- (17) Welch, C. J.; Albaneze-Walker, J.; Leonard, W. R.; Biba, M.; DaSilva, J.; Henderson, D.; Laing, B.; Mathre, D. J.; Spencer, S.; Bu, X. D.; Wang, T. B. *Org. Process Res. Dev.* **2005**, *9*, 198-205.
- (18) Garrett, C. E.; Prasad, K. *Adv. Synth. Catal.* **2004**, *346*, 889-900.
- (19) Hong, S. H.; Grubbs, R. H. *J. Am. Chem. Soc.* **2006**, *128*, 3508-3509.
- (20) Ritter, T.; Hejl, A.; Wenzel, A. G.; Funk, T. W.; Grubbs, R. H. *Organometallics* **2006**, *25*, 5740-5745.
- (21) A typical purification procedure is as follows: Crude 3,3-diethylester-pentene (**6**, 100 mg, 0.472 mmol) in diethyl ether (~30 mL) was transferred to a separatory funnel. The diethyl ether solution was washed 3 or 5 times by water (~30 mL), dried over MgSO₄, and concentrated. Approximately 20 – 30 mg of the resulting clear oil was accurately weighed by a microbalance and digested with concentrated nitric acid overnight for ICP-MS analysis. For activated carbon purification, the activated carbon (1.3 weight equiv of the crude product **6**) was added to the diethyl ether solution after the extraction and stirred for 24 h. After the carbon was filtered, the filtrate was concentrated *in vacuo* to provide **6** as clear oil. THMP and DMSO methods were carried out following the literature procedures except avoiding silica gel treatment or column chromatography.
- (22) Dinger, M. B.; Mol, J. C. *Eur. J. Inorg. Chem.* **2003**, 2827-2833.

- (23) Trnka, T. M.; Morgan, J. P.; Sanford, M. S.; Wilhelm, T. E.; Scholl, M.; Choi, T. L.; Ding, S.; Day, M. W.; Grubbs, R. H. *J. Am. Chem. Soc.* **2003**, *125*, 2546-2558.